FAILURE INVESTIGATION AND PERFORMANCE ANALYSIS OF THE COMBUSTION AND EMISSION CHARACTERISTICS OF AN INDUSTRIAL DUAL FIRED STEAM BOILER

By

IBRAHIM, AKEEM OSAMWONYI
PG/ENG2110350

H.N.D. Mechanical Engineering (Auchi), MBA (Lasu), B.Tech. Mechanical Engineering (South Africa), M.Sc. Mechanical Engineering (Lasu) R. Engr. (COREN), MNSE, MNIMechE

DEPARTMENT OF MECHANICAL ENGINEERING
FACULTY OF ENGINEERING
UNIVERSITY OF BENIN
BENIN CITY, NIGERIA

MARCH 2026

FAILURE INVESTIGATION AND PERFORMANCE ANALYSIS OF THE COMBUSTION AND EMISSION CHARACTERISTICS OF AN INDUSTRIAL DUAL FIRED STEAM BOILER

By

IBRAHIM, AKEEM OSAMWONYI
PG/ENG2110350

H.N.D. Mechanical Engineering (Auchi), MBA (Lasu), B.Tech. Mechanical Engineering (South Africa), M.Sc. Mechanical Engineering (Lasu) R. Engr. (COREN), MNSE, MNIMechE

A THESIS SUBMITTED TO THE DEPARTMENT OF MECHANICAL ENGINEERING, FACULTY OF ENGINEERING IN PARTIAL FULFILMENT OF THE REQUIREMENTS FOR THE AWARD OF A DOCTOR OF PHILOSOPHY (Ph.D) DEGREE IN MECHANICAL ENGINEERING (THERMAL POWER ENGINEERING) AT THE UNIVERSITY OF BENIN

MARCH 2026

CERTIFICATION

This is to confirm that this study was conducted and compiled by **IBRAHIM, AKEEM OSAMWONYI (PG/ENG2110350)** of the Department of Mechanical Engineering, Faculty of Engineering, University of Benin, in partial fulfillment of the requirements for the award of the Doctor of Philosophy (Ph.D.) degree. The study represents original research and has not been submitted for any other degree or diploma elsewhere.

____________________________ ____________________

Prof O.O. Ighodaro **Date**
Supervisor

____________________________ ____________________

Prof M.A. Waheed **Date**
Co-Supervisor

____________________________ ____________________

Dr. Efe Orumwense **Date**
Co-Supervisor

____________________________ ____________________

Prof O.O Ighodaro **Date**
Head of Department

CERTIFICATION OF THESIS/ DISSERTATION ON PLAGIARISM

We the undersigned attest and declare that the thesis of **IBRAHIM, AKEEM OSAMWONYI** titled "Failure Investigation and Performance Analysis of the Combustion and Emission Characteristics of a Dual Fired Industrial Steam Boiler" has successfully passed the anti-plagiarism test and does not violate any copyright regulations.

______________________________ ____________________

Prof O.O. Ighodaro **Date**
Supervisor

______________________________ ____________________

Prof M.A. Waheed **Date**
Co-Supervisor

______________________________ ____________________

Dr. Efe Orumwense **Date**
Co-Supervisor

______________________________ ____________________

Prof O.O Ighodaro **Date**
Head of Department

Intellectual Property & Technology Transfer Office
UNIVERSITY OF BENIN, BENIN CITY, NIGERIA
Tel: [redacted] E-mail: iptto@uniben.edu, [redacted]
Website://www.iptto.uniben.edu

MEMO

From: Director **Ref:** UB/IPTTO/APTR

To: HOD, Dept of Mechanical Engineering **Date:** 29th May, 2026

SUBMISSION OF ANTI-PLAGIARISM TEST RESULT

TITLE: Failure Investigation and the Performance Modeling of the Combustion and Emission Characteristics of a Dual Fried Bole

Having conducted anti-plagiarism test on the work submitted by your student, with the above stated title, I hereby submit to you the result of your student as follows:

S/ No	Name	Department/Faculty	Degree	Result	Remark
1	**AKEEM, Osamwonyi Ibrahim**	Dept of Mechanical Engineering Faculty of Engineering	PhD ≤15	09%	Passed

Thank you.

29/05/2026

PROFESSOR S.E. OMONIGHO

Professor Solomon Esharegoma OMONIGHO PhD
Director, IPTTO

DEDICATION

This work is dedicated to God Almighty for granting me grace, wisdom, and strength throughout the course of this research. I also dedicate it to my family for their unwavering love and support, and to all those who played a part in the successful completion of this study.

ACKNOWLEDGEMENT

I am profoundly thankful to God for His guidance and strength throughout the course of this research.

I wish to extend my heartfelt appreciation to my supervisor, Prof. Osarobo O. Ighodaro, and co-supervisors, Prof M.A Waheed and Dr E. Orunmense whose valuable expertise, mentorship, and thoughtful feedback were instrumental in shaping both the direction and quality of this thesis.

My sincere thanks also go to the entire staff of the Department of Mechanical Engineering for their academic and administrative support. I am equally grateful to my colleagues and friends for their encouragement and insightful contributions during this journey.

Above all, I remain deeply indebted to my wife and family for their unwavering love, patience, and sacrifices throughout my academic pursuit.

ABSTRACT

This study presented a comprehensive investigation into the failure mechanism and performance modelling of the combustion and emission characteristics of an industrial dual-fired steam boiler operating on natural gas and diesel. The study was driven by the reoccurring failure on the third pass, operational inefficiencies and concerns over the environmental performance observed in the boiler system of a bottling company in Nigeria

The failure investigation component of the study involved a systematic diagnostic assessment of the third-pass tubes including visual inspection, chemical composition analysis, micro-structural analysis and water chemistry analysis. For performance evaluation, the study employed experimental measurements and computational fluid dynamics (CFD) simulations using ANSYS Fluent to model combustion dynamics, temperature distribution, pollutant formation, and flue gas flow behaviour under various operating loads and fuel combinations. The models were validated against plant data, Furthermore, parametric studies were conducted to optimize key operational boiler control parameters such as air flow, load, variable frequency drive (VFD) and fuel flow rate using Taguchi methodology. Failure investigation results revealed key degradation phenomena due to due to thermal stresses, corrosive water chemistry, tube fouling, scaling, fouling-induced heat transfer impairment. Also, micro-structural examination showed thermal degradation, including decarburization, grain growth, and oxidation, alongside pitting corrosion, indicating high-temperature exposure and scale deposition weakened the metal.

The water chemistry analysis revealed elevated levels of total dissolved solids, P-alkalinity, chloride, and silica in the boiler drum water, which contribute to scaling and localized overheating. Major failures was traced to inadequate water treatment and poor combustion control. CFD simulations revealed that scale layers significantly reduces heat transfer, leading to increased failure risk. An optimal water mass flow rate of 0.454kg/s was determined as the effective mass flow rate to attain the desired outlet steam temperature. The study revealed load as the most influential factor, leading to reduced emissions, improved combustion, operational stability and prolonged component life. The findings provide insights into enhancing boiler reliability, thermal efficiency, and environmental compliance.

TABLE OF CONTENTS

LIST OF FIGURES

LIST OF TABLES

NUMENCLATURE

Abbreviations

IEA- International Energy Agency

CO_2- Carbon Dioxide

barg- bar gauge (pressure unit)

O_2- Oxygen

CO- Carbon Monoxide

ppm- parts per million

kWh- Kilowatt-hour

OD- Outer Diameter

ID- Inner Diameter

TDS- Total Dissolved Solids

FEM- Finite Element Method

SEM- Scanning Electron Microscopy

EDAX- Energy Dispersive X-ray Spectroscopy

XRD- X-ray Diffraction

MW- Megawatt

CFD- Computational Fluid Dynamics

FEA- Finite Element Analysis

TPH- Tons Per Hour

NOx- Nitrogen Oxides

CI- Compression Ignition

ANNs- Artificial Neural Networks

MBT- Minimum spark timing for Best Torque

IMEP- Indicated Mean Effective Pressure

COV- Coefficient of Variation

THC- Total Hydrocarbons

SOx- Sulfur Oxides

GHG- Greenhouse Gases

VFDs- Variable Frequency Drives

FD- Forced Draft

CFB- Circulating Fluidized Bed

CFBB- Circulating Fluidized Bed Boiler

MMTLBO- Multi-objective Learning-based Optimization Algorithm

CEPA- Carbon Emission Pitch Analysis

BPUI- Biomass Power Utilization Index

ESG- Excess Steam Generation

PI- Proportional-Integral

M.F.O.- Medium Fuel Oil

I.C.- Internal Combustion

BSFC- Brake Specific Fuel Consumption

HC- Hydrocarbons

RANS- Reynolds-Average Navier-Stokes

PR EOS- Peng-Robinson Equation of State

NDT- Non-Destructive Testing

SCC- Stress Corrosion Cracking

OES- Optical Emission Spectroscopy

ASTM- American Society for Testing and Materials

S/N- Signal-to-Noise

PRV- Pressure Reducing Valve

T. Gas- Flue Gas Temperature

T. Air- Ambient Air Temperature

% Ex. Air- Percentage Excess Air

% Effy- Percentage Efficiency

K- Kelvin (temperature unit)

℃- Degrees Celsius (temperature unit)

Kg/s- Kilograms per second (mass flow rate)

W/mK- Watts per meter Kelvin (thermal conductivity)

J/kgK- Joules per kilogram Kelvin (specific heat)

Kg/ms- Kilograms per meter second (viscosity)

$N\cdot s/m^2$- Newton-second per square meter (dynamic viscosity)

kJ/kg-K- Kilojoules per kilogram Kelvin (specific heat capacity)

mm- Milli meters

µm- Micro meters

kPa- Kilopascals

MPa- Megapascals

CHAPTER ONE

INTRODUCTION

1.1 Background to the Study

Sustainability has become a major concern among manufacturing industries due to the prevailing energy challenges. The world is currently grappling with high energy costs and dwindling fossil fuel reserves, which are rapidly nearing exhaustion. At the same time, the energy demand required to sustain population growth and economic development is rising sharply. Extensive reliance on fossil fuels has considerably raised CO_2 and greenhouse gas emissions, contributing to global warming, environmental harm, and frequent climate-related disasters. These adverse effects seriously impact human health and survival.

Maximising energy usage is a critical factor in industrial development and cost savings for organisations. Utility operations rank among the most energy-demanding aspects of industrial activity. Utility equipment typically consumes substantial amounts of energy, leading to high costs that adversely affect an organisation's bottom line. The industrial sector utilizes energy in various ways, including process heating, which involves raising the temperature of components during manufacturing processes. A typical case is oil refining, which uses heat to isolate different distillate fractions.

Another common energy-intensive industrial process is boiler operation, where water is converted into steam or hot water. Industrial steam systems typically consume around 30% of the total energy used by the global manufacturing sector (Yang and Dixon, 2012). Although steam systems have substantial room for efficiency improvements (IEA, 2007), a large portion of that remains unexploited. Nevertheless, the steam industry is actively pursuing sustainable initiatives to mitigate its environmental impact.

At the core of industrial steam generation is the boiler system, which is a critical piece of equipment. A boiler is a cylindrical container engineered to produce steam by heating water through the combustion of fossil fuels (Chavan and Pathak (2010). The efficiency of a boiler significantly influences its energy consumption. For instance, boilers with significant scale build-up consume more fossil fuel due to the poor heat transfer surface caused by scaling. This increased energy consumption elevates the temperature within the boiler, leading to corrosion between the scale and the tube's outer diameter. Such conditions often result in boiler tube failures.

Improper tuning of a boiler increases these issues, causing high flue gas emissions of unburnt carbon that pollute the environment. Maintaining sustainable and efficient boiler performance, while minimizing environmental impacts, necessitates a robust maintenance program. This ensures that the boiler plant operates efficiently and consistently, preserving both operational reliability and the natural environment.

Nigeria is endowed with numerous food and beverages company. Rev Foods and Beverages Limited, located in Mowe Ibafo, Ogun State, is a leading player in Nigeria's juice and dairy manufacturing sector. The company faces recurrent boiler tube failures and emission-related issues, resulting in frequent production stoppages and significant financial losses. Over time, blocked tubes, incomplete combustion of flue gases, and multiple tube leakages have plagued the boiler. Additionally, the company has dealt with legal challenges arising from environmental pollution caused by boiler emissions.

The industrial dual-fired steam boiler under investigation, installed in 2017, operates 24/7 and has a capacity of 12 tons per hour. Despite its relatively short operational lifespan, it has experienced numerous failures, particularly in the third pass tubes. Between 2018 and 2021, 17 out of 170 tubes failed, leading to a 10% thermal efficiency loss and an average of three unscheduled plant stoppages per month. A critical incident occurred in October 2021, when the boiler feed water tank emptied due to a leakage. The feed pump collapsed, causing water starvation and a sudden pressure drop from 8 to 4 barg. This event led to several tube failures, with six tubes leaking in the boiler's third pass section. The repeated breakdowns emphasize the need for a thorough root-cause analysis and the formulation of effective preventive strategies.

This study seeks to address the recurring failures of boiler tubes and optimize the combustion parameters to enhance boiler performance. This study is intended to support efficient, durable boiler performance, minimize emissions, and offer sustainable remedies for Rev Foods and Beverages Limited.

1.2 Statement of the Problem

The 12-ton industrial dual-fired steam boiler under study has experienced significant operational challenges and recurring failures despite being only a few years into its operational life. Installed in 2017, the boiler is designed as a three-pass, fire-in-tube, wet-back system with water occupying the shell and flue gases passing through the smoke tubes from the combustion chamber to the stack. Heat loss to the surroundings is minimized through fiberglass lagging. Operating 24/7 at a capacity of 6,000–9,000 kg/h, the boiler is located in a well-ventilated environment with cross-airflow and roofing to ensure optimal conditions. Despite these provisions, the boiler has suffered frequent and severe failures, particularly in the third pass tubes, causing substantial disruptions to production and considerable financial losses for Rev Foods and Beverages Limited.

The initial tube failures were recorded in 2018, just one year after installation, with four tubes becoming blocked due to leaks. These failures continued to escalate, with five tubes failing in 2019 and two more in 2020. A critical incident occurred in October 2021 when the boiler feed water tank was emptied to address a leakage. This caused the feed pump to collapse, resulting in water starvation while the steam outlet valve remained open. Consequently, the boiler's steam pressure dropped sharply from 8 to 4 barg, and its firing rate was reduced to 50%. This incident led to six tube failures in the third pass, bringing the total number of failed tubes to 17 out of 170 within four years. These failures caused a 10% loss in thermal efficiency, forcing the company to burn additional fuel to meet operational demands.

All recorded failures occurred exclusively in the third pass tubes, which play an important role in heat transfer. The cumulative impact of these failures has been detrimental to the company's operations. Between 2018 and 2021, the boiler caused an average of three unscheduled plant shutdowns per month, severely disrupting manufacturing activities. Each shutdown required extensive repairs, including tube replacements, descaling, and additional startup fuel costs to restore operations. These repairs imposed substantial manpower and financial burdens on the organization.

Rev Foods and Beverages Limited, a leading player in Nigeria's juice and dairy sector, has also faced environmental and legal challenges due to emissions from the boiler. The high levels of flue gas emissions, primarily caused by incomplete combustion, have led to air pollution in the surrounding community. Between 2018 and 2021, the company faced two legal disputes related to environmental pollution caused by the boiler. These emissions also violate environmental regulations, adding to the company's operational challenges.

The recurrence of tube failures and the associated impacts align with industry findings. Atanu Saha (2016) states that over 80% of unscheduled boiler shutdowns are caused by tube failures, while Kalu *et al*. (2020) and Liu *et al*. (2017) highlight boiler tube failures as the primary cause of unplanned outages in power plants and manufacturing industries. These failures lead to emergency shutdowns, costly repairs and lost production, posing significant risks to operational efficiency and financial stability.

Moreover, the boiler's emissions have emerged as a critical concern. Urban areas like Lagos, Kano, Ogun, and Port Harcourt are particularly vulnerable to industrial pollution. Incomplete combustion in the boiler releases harmful greenhouse gases such as CO_2 and unburned carbon into the atmosphere. These emissions not only contribute to global warming but also pose significant health risks. The financial burden of managing the health and environmental impacts is immense, highlighting the urgent need for sustainable solutions.

The boiler's operational challenges can be summarized as follows:

1. Frequent Production Stoppages: The recurring tube failures caused an average of three unscheduled shutdowns per month between 2018 and 2021, disrupting manufacturing operations.
2. High Repair and Maintenance Costs: Each failure required expensive repairs, including tube replacements, descaling, and additional startup fuel costs.
3. Reduced Thermal Efficiency: The cumulative failure of 17 tubes resulted in a 10% loss in thermal efficiency, increasing fuel consumption and operational costs.
4. Environmental and Legal Challenges: High emissions levels caused by incomplete combustion led to environmental pollution, resulting in two legal disputes with the host community.

In addition to these challenges, the enforcement of strict air pollution legislation in many countries underscores the need for industrial operators to address emissions as a key performance parameter. As Rajput (2012) highlights, reducing emissions and improving combustion efficiency are essential to achieving sustainable industrial operations. Addressing these issues requires an engineering approach that focuses on:

Understanding Combustion Flue Gas Constituents: Analyzing the flue gas composition to identify the sources of emissions and their impacts.

Improving Fuel Combustion Operations: Enhancing combustion efficiency to reduce fuel consumption and minimize emissions.

Optimizing Combustion Parameters: Conducting a critical analysis of flue gases and fine-tuning combustion parameters to improve overall performance and reduce negative environmental effects.

Investigate the Causes of Tube Failures: Conduct a detailed analysis of the metallurgical and operational factors contributing to recurring failures, particularly in the third pass tubes.

Analyze and Optimize Combustion Performance: Examine flue gas emissions under varying conditions to identify inefficiencies and improve combustion efficiency.

Provide Sustainable Solutions: Develop engineering strategies to enhance the boiler's reliability, reduce emissions, and ensure compliance with environmental regulations.

This study seeks to deliver a comprehensive framework for resolving the recurring operational and environmental challenges associated with the boiler. By addressing these issues, the study aims to ensure long-lasting boiler performance, reduce operational costs, and contribute to a greener and more sustainable industrial environment.

1.3 Aim and Objectives of the Study

1.3.1 Aim

The study aims to carry out a detailed failure investigation and performance combustion analysis of the emission and combustion characteristics of an existing industrial dual fired steam boiler while also determining the optimal parametric setting required to enhance the combustion performance of the boiler.

1.3.2 Objectives

The objectives set out in this study to achieve the aim of the research are as follows:

i. To perform an in-depth metallurgical analysis to identify the recurring causes of tube failures in the 12-ton dual-fuel steam boiler.
ii. To construct a simulation model for the damaged boiler tube and replicate its failure behaviour under thermal loading conditions in order to determine thermal action on the failed boiler tube.
iii. To assess the true emission profile of the boiler by employing a flue gas analyzer under different loading conditions when fired on natural gas and diesel.
iv. To develop a model for the boiler combustion operating parameters and simulate the combustion of the boiler under natural gas and diesel combustion.
v. To prove the validity of the developed model by comparing the actual emission data obtained from flue gas analyzer with the result of the simulated combustion.
vi. To determine the optimal parametric setting required to optimize the boiler combustion performance.

1.4 Relevance of the Study

This research work is very relevant for the efficient performance and reliability of steam generation plant as it discusses and presents a life scenario on boiler tube failure and its emissions. This research offers a thorough insight into how boiler tubes fail under various operating conditions. As it exposes the impact of water chemistry as it affects life of a boiler. The study further reinforces, contributes, support and back existing knowledge base on boiler failure and its prevention. And the recommendations outlined in the study support extending the operational lifespan of the boiler equipment, while it also presents a lucid procedure for finding the root cause of boiler tube failure which can be follows to replicate similar studies. In return this will help to avoid the expensive cost of repair and maintenance of a failed boiler tube in operation. In same vain, there is limited exploration in literature regarding emissions from boilers operating on natural gas and diesel and this study provides enough information to assist in bridging that gap. Furthermore, the study exposes the possible boiler emissions to the environment when fired on diesel and natural gas. As a way to control boiler emissions, this work introduces a systematic method for adjusting boiler combustion emissions and also suggests optimal parameter settings for control to serve as a guide/base line/control point for tuning boiler combustion. This helps to achieve a proper boiler emission which will assist in making our environment a much better and greener place to live.

1.5 Scope and Limitation of the Study

This investigation is exclusively centered on an operational 12-ton/hour dual-fired boiler that has exhibited recurrent tube failures throughout its service life. The boiler system is designed to operate utilizing both natural gas and diesel as fuel sources, delivered via a singular combustion burner. The primary objective of this research is to ascertain the underlying causes of the observed recurrent tube failures and to formulate efficacious remedial strategies. Furthermore, a comprehensive simulation model will be developed to assess the boiler's operational performance and to scrutinize its behavioral characteristics under various failure conditions. Concurrently, this research encompasses the characterisation of boiler emissions and aims to facilitate soot-free boiler combustion through the systematic optimization of its combustion parameters. The combustion parameters analyzed under both diesel and natural gas firing across diverse load conditions include: oxygen concentration, carbon monoxide levels, carbon dioxide levels, total flue gas temperature, percentage of excess air, boiler combustion efficiency, and the gas pressure upstream and downstream of the pressure reducing valve within the gas train. Furthermore, the manipulation of combustion is achieved by adjusting key variables such as fuel supply, air input, auxiliary actuator settings, and variable frequency drive parameters across a range of load conditions. The Taguchi L27 orthogonal array will be employed within the experimental design (DOE) framework to ascertain the optimal parametric configuration for the boiler system.

CHAPTER TWO

LITERATURE REVIEW

2.1 Steam Boiler

Globally, industrial steam constitutes an integral component of the utilities essential for manufacturing processes and is additionally utilized within power generation facilities (Figure 2.1 portrays the industrial steam). With the increasing global steam consumption attributed to industrialization and development, the steam boiler has demonstrably established itself as a critical asset for achieving high-quality manufacturing and efficient power generation through steam turbines. Beyond its primary applications in manufacturing and power generation, steam is also employed for a diverse array of purposes, including direct and indirect heating, fuel atomization, humidification of air within duct systems, drying processes, pasteurization, sterilization, and disinfection. Consequently, steam boilers are deemed indispensable for national development, owing to the substantial reliance of both the manufacturing and power industries on steam generation.

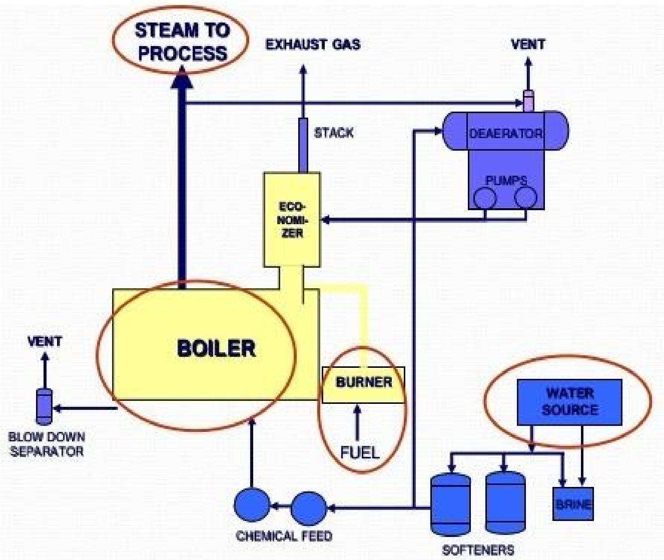

Figure 2.1: Basic Industrial Steam. (Thermax, 2015)

The considerable demand for and extensive utilization of steam are attributable to the ensuing advantages:

1. It is safe to use, as it is environmentally friendly and non-hazardous.
2. Steam energy is easily controlled because its temperature and pressure can be readily monitored.
3. It can be easily transferred due to its high heat transfer properties, requiring less transfer surface.
4. Steam offers a wide range of multiple uses, including heating, disinfection, sterilization, pasteurization, and power generation.

2.2 Classification of Boilers

Boilers are broadly categorized into six principal groups, as depicted in Figure 2.2:

1. Classification by boiler axis: vertical, horizontal, and inclined configurations.
2. Classification based on fluid passage through the boiler tubes: fire-tube boilers and water-tube boilers.
3. Classification by fabrication method: package boilers and shop-assembled boilers.
4. Classification based on the nature of fuel utilized: gas-fired boilers (employing LPG, PNG, or LNG); Oil-fired boilers (using diesel, LPFO, or furnace oil as a fuel source); Solid fuel boilers (comprising biomass-fired, wood-fired, coal-fired, briquette-fired, pet coke-fired, and rice husk-fired boilers).
5. Classification by operating pressure: boilers are delineated into low-pressure and high-pressure categories.
6. Classification by circulation method: boilers are categorized into natural circulation and forced circulation types.

Supplementary classifications comprise:

7. Classification by furnace type: single-furnace and dual-furnace boilers.

8. Classification according to boiler application: stationary and mobile boilers.

9. Classification by drum configuration: single-drum and multiple-drum boilers.

10. Classification based on draught mechanism: forced-draught and natural-draught boilers.

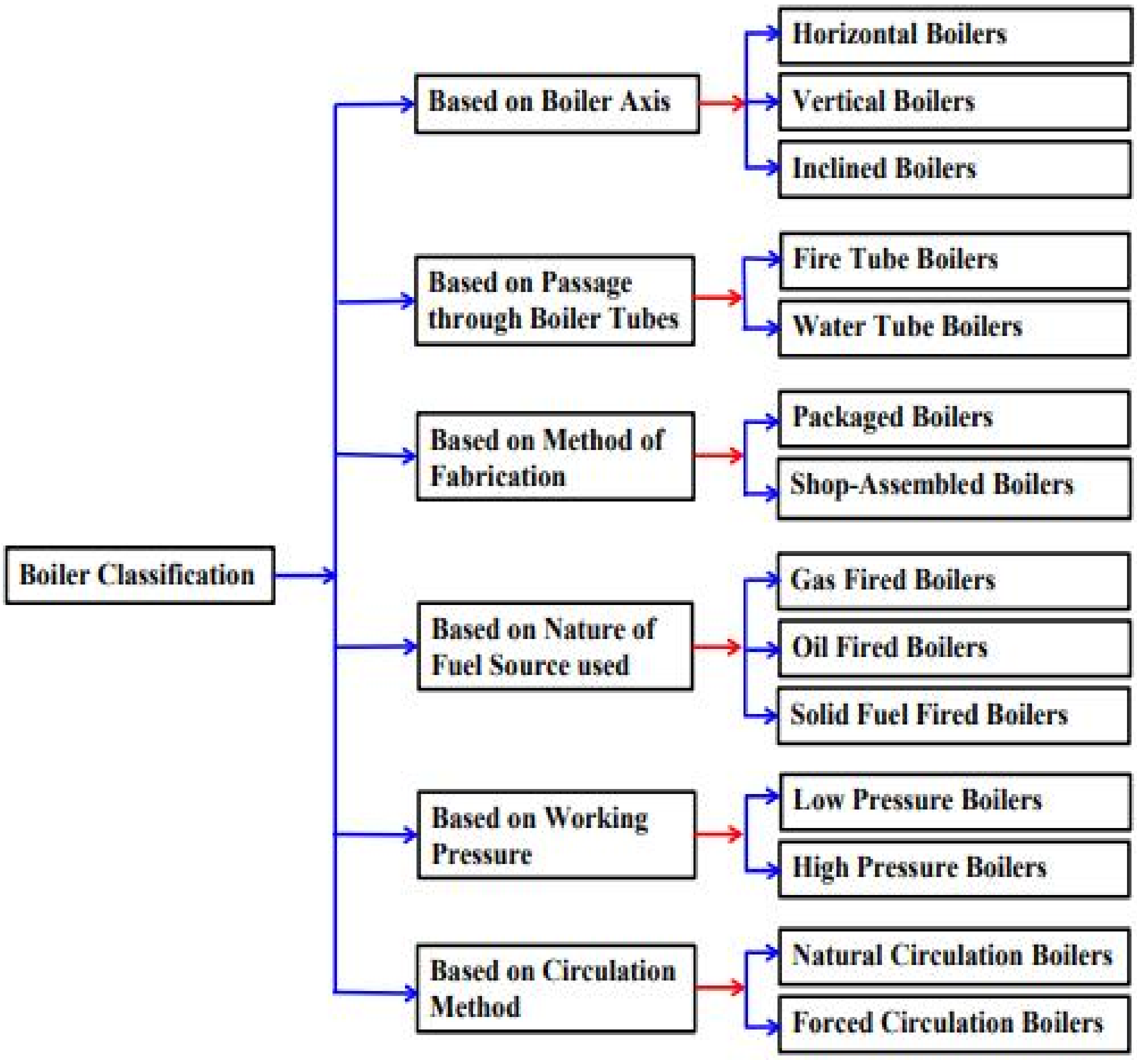

Figure 2.2: Classification of boiler (Paul and Alam , 2018)

2.3 The Uncertainties of Boiler Tube Failure

Boiler tubes are cylindrical vessels that form one of the vital parts of a boiler, used for the production of steam in power plants and industries (Kalu, 2020). As stated by Haribhakti *et al.,* a boiler is a sealed container where heat is applied to water to generate hot water, steam, superheated steam, or a combination thereof, all under pressure. They mostly provide the heat transfer surface for the energy transfer that allows the transformation of water to steam. According to Kalu (2020), steam produced in power plants is directed to turbines to produce electricity, whereas in industrial settings, it is channeled into processing tasks. As manufacturing grows, the effectiveness of combustion-based steam systems largely relies on the boiler's combustion efficiency and the integrity of its tubes. The latter affects the rate of heat transfer and boiler energy consumption. Equally, the failure of the boiler tube rupture poses serious danger to production and power generation as it cripples operations unannounced, and sometimes the boiler failure could result in a sudden catastrophic explosion.

Frequent shutdowns in power plants are often attributed to boiler tube failures, as evidenced by numerous reports in many power plants (Liu *et al*., 2017; Ahmad *et al.,* 2009; Ahmad *et al.,* 2010; Dhua, 2010). Boiler failures are either ruptures or explosions. Tube ruptures result from structural tube failure, whereas explosions may take place in the furnace or boiler chamber itself (Hewison and Christian, 1983). Industrial boiler failures can lead to severe accidents, resulting in significant damage to property and potential harm to personnel (Ahmed and Gu, 2020).

Mnizeskewi *et al.* (2004) reported a major boiler furnace explosion that occurred on Monday, February 1, 1999, at the Ford Rouge Power Plant—a facility operated by the Ford Motor Company in Dearborn, Michigan. The incident triggered a chain of secondary explosions due to the ignition of nearby flammable materials. The resulting fire tore through the plant, leading to the deaths of six individuals and injuries to 38 others, 14 of whom sustained serious injuries. The total property damage was estimated at $1 billion. The investigation revealed that the explosion was caused by the failure to close the main gas line manual valves on the second and third floors; only the first floor valve had been shut. Each main gas line supplied two burners, and gas had accumulated in the furnace through the four inactive burners left open during maintenance purging. Compounding the issue, two safety devices had been disabled due to malfunctions, leading to operational delays and ultimately contributing to the explosion.

Another typical boiler tube rupture disaster is the accident at the Chernobyl nuclear reactor that happened on April 25th and 26th, 1986, at the Chernobyl Power Station, Ukraine. The station housed four RBMK-100 reactors, each capable of producing 1.0 GW electric power (4 x 1.0 GW). This is one of the worst, most unbelievable serious accidents that has ever occurred in the nuclear power industry, as reported by the United Nations Scientific Committee on the Effects of Atomic Radiations.

Anjorin *et al*. (2019) examined a steam boiler tube rupture that occurred at the Egbin Steam Thermal Power Station in Ikorodu, Lagos State. Although there were no casualties, the report noted that during power generation, the boiler operated under extreme conditions temperatures reaching 587°C and pressures around 12,000 kPa which could lead to overheating, excessive thermal stress on the tubes, equipment malfunctions, system trips, and eventual failure. The incident was specifically identified as a boiler tube rupture. Contributing factors included the plant's operational age, sensitivity to temperature fluctuations, inconsistencies in steam quality and quantity, and issues related to water chemistry.

In some other instances, creep, corrosion fatigue, scale formation, stress corrosion, thermal cracking, pitting, oxidation, stress rupture, and erosion are many among other reasons resulting in boiler tube failure (Benac, 2009; Singh and Mahmood, 2007; Perdomo and Spry, 2005; Lee *et al*., 2009; Satyabrata, 2006; Dhua, 2010; Munda *et al*., 2016; and Ahmad *et al*., 2010). For this reason, several researchers have dwelt on finding solutions to the causes of boiler tube failures using different instruments and methodologies to analyze tube failures, with some proffering solutions to the issues.

Oxygen in boiler water is one of the major causes of corrosion and oxidation, causing a reduction in boiler tube thickness. This reduction causes the boiler tube to fail because the thinned area can no longer withstand its design pressure. Furamera (2015) investigated the causes of boiler tube failure in Harare Thermal Power Station. Liu *et al.,* (2017) conducted a study on a power plant failure caused by the rupture of a boiler tube constructed from 20G steel. Their investigation involved visual inspection, microstructural examination, and chemical analysis. The findings indicated that oxidation led to localized thinning of the tube wall on the side exposed to the flame, resulting in internal pressure surpassing the reduced strength of the tube. To prevent such failures, the study recommended maintaining proper water quality to manage oxygen levels, enhancing the operating conditions of boiler tubes, ensuring the tubes do not exceed their designated temperature and pressure limits, and performing regular cleaning and wall thickness assessments.

Corrosion fatigue is another cause of boiler tube failure. This was reported by Trojan and Turcortt (2019) in their research on failure analysis of a cracked boiler tube. Their investigation utilized visual/macroscopic examination, optical examination, and energy-dispersive spectroscopy (EDS). The optical examination did not reveal any thermal degradation but showed that cracking occurred as a result of corrosion fatigue. Further EDS analysis supported this claim, finding corroded iron oxide in all the examined cracks. It was concluded that repeated thermal cycling was responsible for forming thermal-based corrosion fatigue cracks. Corrosion fatigue occurs when cyclic thermal strains constantly crack the protective Fe_3O_4 (magnetite) oxide layer formed on the tube. Thus, thermal strains were the primary contributor to cracking, rather than issues with water chemistry.

Scaling of boiler tubes is another reason for boiler tube failure. The major sources of scale formation are calcium and magnesium salts (carbonate and s, accelerating material degradation over time. This multifaceted influence underscores the importance of maintaining optimal water chemistry to ensure the longevity and efficiency of boiler operations (Haribhakti *et al.*, 2018). Ibrahim *et al.* (2023), in their investigation of boiler tube failure in a dual-fired steam boiler at a beverage manufacturing facility, identified inadequate water chemistry as the primary factor contributing to the failure. The study also noted that when the external environment of a boiler tube is subjected to elevated levels of total dissolved solids (TDS), pH, chloride, and silica, it can result in scale and deposit buildup on the tube's outer surface.

The study highlighted that scaling within boilers significantly impairs the heat transfer process, which, in turn, leads to localized overheating on the boiler tube's heating surface. This overheating creates a high-stress environment that becomes particularly critical at elevated temperatures ranging between 450°C and 500°C, where the structural integrity of the tube is compromised, resulting in rupture. Furthermore, thermal oxidation was found to occur on the internal diameter of the tubes under these extreme conditions. The research further identified additional metallurgical changes caused by thermal oxidation, including decarburization and grain growth at the tube's internal diameter. On the outer diameter, pitting corrosion was observed, adding another layer of stress to the tube's structural integrity. Overall, the evidence indicated that pitting corrosion and thermal oxidation were the main causes of the boiler tube failures (Rajput, 2012; Ibrahim *et al.*, 2023). The key consequences of inadequate boiler water chemistry, primarily due to impurities present in the feed water are summarized as follows:

2.4.1 Scale Formation

Scale buildup inside boiler tubes is mainly caused by calcium and magnesium salts, which become less soluble as water temperature rises. This decline in solubility at elevated temperatures encourages the accumulation of these salts on the inner surfaces of the tubes, resulting in scale formation. The likelihood of scale formation grows as the feed water temperature rises because certain salts, like calcium sulfate, become less soluble with increasing temperature. For instance, calcium sulfate has a solubility of 3200 ppm at 15°C, which decreases drastically to 55 ppm at 230°C and further drops to 27 ppm at 320°C (Rajput, 2012). Calcium sulfate is identified as a major contributor to most scale formations in boiler systems. These scales primarily result from the precipitation of calcium and magnesium salts, while chlorides, being highly soluble in water, do not contribute to scale formation. Similarly, sodium salts are highly soluble and are classified as non-scale-forming salts, thus not contributing to the scaling issue in boiler tubes.

Scale causes a cemented hard mass coating by silica around boiler tubes, reducing the heat transfer rate, causing a temperature buildup, and leading to uneven temperature distribution on the heating surface of the tubes. This results in thermal oxidation, cracking, overheating (short-term and long-term), and eventual boiler tube failure or cracking of the boiler furnace. Scale formation in tubes leads to the following issues:

1. Overheating.
2. Furnace temperature rupture.
3. Increased fuel consumption.
4. Flow restriction in pipelines.
5. Malfunctioning of equipment.

2.4.2 Corrosion/Oxidation

Corrosion/Oxidation: The rate of oxidation increases significantly at higher temperatures compared to lower or room temperatures, leading to corrosion and oxidation of boiler tubes (Liu *et al.,* 2017). The iron-to-oxygen ratio significantly influences this process, playing a vital role in changing the physical structure of boiler tubes. One major consequence is the thinning of tube walls, which negatively affects key heat transfer characteristics such as steam temperature, pressure drop, mass flow rate, flue gas temperature, convection coefficient, and the temperature rise along the tube's outer surface. Collectively, these effects weaken the structural integrity of the tubes, ultimately leading to their failure (Liu *et al*., 2017; Jadhao *et al*., 2017). This highlights the importance of mitigating oxidation processes, particularly at elevated operating temperatures, to maintain the performance and longevity of boiler systems.

Dissolved oxygen in water accelerates the corrosion process. Factors like CO_2, O_2, acidic pH, and corrosive agents in water induce cracks, pits, and etching in the surfaces of metallic parts. Over time, these factors weaken the boiler shell and cause perforation, resulting in steam and condensate pipeline leakages.

Corrosion can lead to the following issues:

1. Weakening of the boiler shell.
2. Perforation of the boiler
3. Steam and condensate pipeline leakages.

2.4.3 Carry-over

Priming and foaming form boiler carryover. These terms describe the exit of dissolved solid particles from the boiler steam drum. The water level instability causes bubbles to burst violently, ejecting sludge into the steam a process called priming. Factors such as improper boiler design, improper firing methods, overloading, excessive steaming rates, fluctuating water levels, too high water levels, and sudden load variations contribute to priming.

Foaming is the bubble accumulation in the steam drum, often triggered by high levels of sodium-based alkalinity, oils, or calcium salts. Problems associated with water droplet carryover includes

1. Heat loss, as the equivalent of the carried-over water must be replaced with cooler water.
2. Reduction in the heat content of the steam
3. Entrained salts carried over lead to valve sticking.

2.4.4 Caustic Embrittlement

Caustic embrittlement is the degradation of boiler steel, marked by crack formation along crystal boundaries. This phenomenon occurs when boiler steel is subjected to prolonged exposure to a combination of mechanical stress and highly alkaline water. The interaction between stress and the chemical environment within the boiler creates conditions conducive to the formation of cracks along the grain boundaries of the steel. Over time, these intercrystalline cracks compromise the structural integrity of the boiler material, making it more susceptible to failure. To avoid caustic embrittlement, precise regulation of boiler water chemistry and system stresses is essential, as well as measures to mitigate stress within the boiler structure.

Embrittlement occurs under the following conditions:

a. The presence of free hydroxide in boiling water, alkalinity, and silica.

b. When boiler feedwater containing sodium bicarbonate breaks down into carbon dioxide (CO_2) and sodium carbonate (Na_2CO_3). The sodium carbonate partially hydrolyzes to release sodium hydroxide (NaOH), causing embrittlement as shown in the reaction:

$Na_2CO_3 + H_2O \rightarrow CO_2 + 2NaOH$.

Caustic embrittlement causes intercrystalline cracking in boiler tubes, which compromises their structural integrity and leads to failure.

2.5 Some Selected Cases of Boiler Failure Accidents

According to the Nation Newspaper on January 26, 2023, at about 10:30 am, a boiler explosion occurred at Nigerian Distilleries Limited (NDL), located in Sango-Ota, Ogun State. The explosion resulted in the tragic death of four persons and left 20 others with severe injuries. Hot water and other substances spewed out during the explosion, inflicting grave harm on the staff handling the equipment.

Similarly, On July 28, 2015, the Vanguard reported a tragic boiler explosion at the Golden Penny Flour Mill located on Eric Moore Road in Surulere. The incident resulted in the loss of two lives, highlighting the devastating consequences of boiler explosions and underscoring the critical need for stringent safety measures and maintenance protocols in industrial operations.

On September 10, 2016, the New York Times reported another catastrophic boiler explosion at a garment factory in Tongy, Bangladesh. This accident claimed the lives of 23 people, further underscoring the hazardous nature of industrial boiler systems, especially in facilities with lax safety regulations.

The infamous Chernobyl nuclear power plant disaster on April 26, 1986, remains one of the most devastating boiler-related accidents in history. While there is no official figure for the number of deaths caused by the explosion, the World Health Organization (WHO) estimates that approximately 4,000 deaths were related to illnesses caused by the disaster. This figure has been disputed, as the Soviet Union did not accept the WHO’s estimate. The long-term consequences of the explosion continue to affect lives and the environment decades later.

Another notable incident occurred on April 27, 1865, when the boiler explosion aboard the steamship SS Sultana killed over 1,800 crew members. This remains one of the deadliest maritime boiler explosions in history.

More recently, during a maintenance outage on February 17, 1999, a catastrophic explosion occurred, completely destroying the original Hawthorn Unit 5 boiler. This incident serves as a stark reminder of the importance of adhering to stringent safety protocols and maintenance procedures during boiler servicing. The event highlighted the potential dangers associated with high-pressure systems and the critical need for thorough inspections and preventive measures to avoid such devastating outcomes.

2.6 Review on Boiler Tube Failure

Steam is an essential utility required for manufacturing process operations in industries and for power operations in steam power plants, including steam turbines and other steam engines. Steam is generated from boilers, with boiler tubes forming a critical component of the system. These tubes facilitate heat transfer from the combustion system to water, thereby generating steam. Typically, boiler tubes are constructed from ferritic steels that are enhanced with various alloying elements, including Nickel, Molybdenum, Chromium, and Manganese, among others. These alloying elements play a vital role in enhancing the mechanical strength of boiler tubes, allowing them to withstand the high pressures and temperatures encountered during operation (Seng, 2013). According to Seng (2013), boiler tubes are broadly classified into two types: water tube and fire tube. In water tube boilers, water flows inside the tubes while combustion gases pass over the outer surfaces. In contrast, fire tube boilers feature combustion gases moving through the tubes, which are surrounded by water. Understanding this distinction is key to evaluating how different boiler types function under varying operating conditions. Therefore, a boiler's overall efficiency is closely linked to the condition of its tube surfaces, both internal (inner diameter) and external (outer diameter). Any degradation of these surfaces poses serious threats to the reliability of industrial operations. Boiler tube failures are often the primary reason for power failures in steam-driven power plants and result in various forms of damage, including rupture, bursts, cracks, wear, or pinholes.

The financial implications of boiler tube failures are substantial. These include production losses, wasted man-hours during repair or retubing, and the inability to generate the required steam energy needed for power generation or maintaining quality standards in processing operations. For instance, failures disrupt sterilization processes for systems and products, leading to rework that increases production costs. Studies show that over 80% of unscheduled boiler shutdowns are due to boiler tube failures, causing unplanned forced outages in power-generating units (Saha, 2006; Li *et al.*, 2017). These failures can lead to a complete halt in manufacturing operations, resulting in considerable availability loss.

The cost of boiler tube failures encompasses boiler repair or tube replacement, startup fuel (gas/diesel oil) required to restore the boiler, and the production losses incurred during the downtime. These interruptions carry significant financial consequences, making the need for continuous investigations into the root causes of boiler tube failures essential. Various investigative tools have been employed to identify the reasons for these failures and implement corrective and preventive measures to mitigate future occurrences.

To understand the causes of boiler tube failures, numerous studies have been conducted, utilizing various methodologies and tools. This literature study was undertaken to provide a comprehensive understanding of why and how boiler tube failures occur and to explore the methods used for failure analysis. Several previous works have centered on boiler tube failures, including research published in journals and projects conducted by industry professionals.

Researchers such as Kim (2017), Rahman et al., (2010), Purbolaksono et al., (2010), Srikanth *et al.,* (2003), Ranjbar (2007), Sembiring (2019), Karran (2017), Bettge (2014), Gupta and Chattopadhyaya (2017), Sanjay (2016), Kumar and Sapra (2013), Haase and Hanke (2013), Luo and Zhang (2013), Shokouhmand *et al.,*(2015), Abbasfard *et al.,* (2012), Jones (2004), Othman *et al*., (2009), Chaudhuri (2006), Dhua (2010), Liu *et al.,* (2017), Ahmad *et al*., (2010), Lee *et al*., (2009), Duarte *et al.,* (2017), Singh *et al.* (2007), Kain *et al*., (2008), Perdomo and Spry (2005), Soltanloo *et al.,* (2022), Dehnavi *et al.* (2017), Munda *et al.,* (2016), Jadhao *et al*., (2017), Himarosa *et al*., (2022), Febriyanti *et al.* (2020), Sembiring *et al.,* (2019), Hosseini and Yareiee (2019), Hu *et al*., (2014), and Javidi *et al.,* (2016) have worked extensively on failure analysis in their efforts to address boiler tube failure issues.

While some scholars have emphasized validated approaches to assessing boiler tube failures, others have concentrated on developing methodologies for performing such evaluations. Notably, Dennies (2005), Saha *et al*. (2015), Wulpi (2000), and Brooks and Choudhury (1993) have proposed detailed procedures and frameworks for conducting failure analyses. Additionally, Graham (2004) and Ryder *et al*., (1986), as cited by Gupta and Chattopadhyaya (2017), elaborated on effective strategies and recommended practices in this field. Vander Voort (2002) documented a range of failure analysis techniques, while Port and Herro (1991) compiled a specialized reference guide dedicated to boiler failure investigations.

According to Rahmana *et al*., (2010) and Xu *et al.,* (2000), approximately 35% of prevalent boiler failures are attributed to long-term overheating, leading to creep in components like superheaters, reheaters, and wall tubes, a finding also confirmed by Gupta and

Chattopadhyaya (2017). Begum *et al.,* (2012) studied terminal cracking in boiler tubes, whereas Rao and Narayanan (2012) investigated fire- and water-side damage in boiler bank tubes. They used various techniques such as optical microscopy, hardness and chemical analysis, visual checks, and SEM (Scanning Electron Microscopy) combined with EDAX (Energy Dispersive X-ray) Spectroscopy. This multifaceted investigation showed that corrosion was the main cause of damage on both internal and external tube surfaces.

Hosseini and Yareiee (2019) conducted a study on boiler tube failures in a petrochemical facility using a combination of visual inspections, thickness measurements, optical microscopy, scanning electron microscopy, hardness assessments for metallurgical evaluation, finite element analysis, X-ray diffraction (XRD), and water composition analysis of the boiler. They concluded that short-term thermal stress was the major factor behind the failure, which contradicted the earlier conclusions drawn by Rahmana *et al.,* (2010) and Xu *et al.,* (2000) regarding long-term overheating. Additionally, Hanke (2012) performed a metallurgical evaluation to determine the root cause of failure in a water wall tube from a 125 MW coal-fired boiler operating at base load within a power plant. The study used visual examination, microstructure characterization, and SEM/EDS analysis. The analysis determined hydrogen-induced damage as the main reason for the failure. According to Chaudhuri (2006), brief overheating episodes were the leading cause of final superheater tube failures. Furthermore, it has been observed that the reheater tubes that have not failed possess superior tensile properties compared to the platen superheater tubes. Purbolaksono *et al*., (2009) conducted an investigative study on failed reheater tubes utilizing finite element modeling. Internal scale deposits were found to heavily impair heat transfer, thereby causing tube failures, as it diminishes the heat transfer efficiency. Abbasfard *et al.,* (2012) conducted a case study examining superheater tube failures in a heat boiler. Similarly, Othman *et al*., (2009) and

Purbolaksono (2010) investigated superheater tube failures using the finite element method (FEM), alongside empirical calculations, visual evaluations, and metallurgical analysis.

Munda *et al.,* (2016) studied water wall tube failures in a thermal plant using visual and metallurgical inspections alongside chemical and metallurgical analyses. Their findings revealed that failures appeared as fine or micro-cracks, especially near girth weld seams. The experimental results revealed that these internal flaws grew outward through the tube walls through its thickness. To address this issue, the researchers recommended ensuring high-quality welding of tube joints and conducting thorough inspections post-welding. Additionally, they advised preventing hydrogen dissolution during welding and suggested treatments for its removal afterward to mitigate potential failures. Ahmad *et al.,* (2010) analyzed superheater tube failure, attributing it to high hoop stress. Using the Larson-Miller parameter, they also assessed the possibility of creep damage in primary superheater tubes. In a related study, Ahmad *et al.,* (2012) confirmed creep damage as a significant factor affecting superheater tubes.

Hosseini and Yareiee (2019) also conducted a failure analysis of boiler tubes in a petrochemical plant, employing methods such as microscopic examination, hardness measurements, XRD, and FEA. Their experimental results again identified short-term overheating as the root cause of failure, consistent with findings in their earlier studies. Jayaprakasam and Vino (2019) explored boiler tube failures in the superheater and economizer of a thermal power station in Chennai. Their study aimed to identify failure causes and propose remedies. Using CAESER II (ver.5.00.6) engineering software, they conducted pipe stress analyses to evaluate sustained and expansion condition stresses in the tubes. Stress under sustained load was 20,257.1 KPa, comfortably within the allowable threshold of 100,045.5 KPa. Similarly, the expansion condition stress was 891.8 KPa, compared to the allowable limit of 234,395.9 KPa. According to Clause No. 391A of the 1950 Indian Boiler Regulations (IBR), the results of the study were determined to be within acceptable limits. Similarly, various stresses, including those acting within the pipeline, were thoroughly evaluated. Additionally, forces and moments at both the boiler end and the main steam common header end were assessed against code requirements and found to comply with the established standards.

The study further emphasized identifying the different types, locations, and causes of boiler tube failures to determine their primary reasons and propose effective remedies. A significant cause of failure was attributed to flue gas stagnation in the superheater zone of the economizer and superheater tubes, which led to tube overheating. To mitigate this issue, the study recommended installing wear protection shields and girdling bands at 1.3 meters from both the top and bottom of the tubes to keep them securely fixed throughout their length, thus preventing failures.

Metallurgical assessments significantly enhanced the understanding of tube failure mechanisms. Several studies, including those by Liu *et al.,* (2017), Lee e*t al.,* (2009), Chaudhuri (2006), Dhua (2010), Ahmad and Purbolaksono (2010), Duarte et al., (2017), and Perdomo and Spry (2005), among others, have contributed extensively to understanding these failures. Numerous investigations have reported failures in superheater tubes. For example, Liu *et al.,* (2009) investigated the failure of a boiler water-wall tube using multiple diagnostic methods such as visual inspection, chemical composition analysis, optical microscopy, scanning electron microscopy (SEM), and energy-dispersive spectroscopy (EDS). The study revealed that localized wall thinning due to oxidation was the primary failure mechanism. Analyzing the failure history of equipment also provides critical insights into identifying root causes. In boiler plants where tubes share the same metallurgical composition, combining failure trend analysis with other diagnostic methods can be invaluable for pinpointing failure origins.

Duarte et al., (2017) performed an in-depth investigation into the failure of water-tube boiler wall tubes by combining historical failure data with various analytical methods, including visual inspection, chemical testing, microstructural analysis, hardness evaluation, and residual stress assessment using X-ray diffraction (XRD). The study identified stress corrosion cracking (SCC) as the primary mechanism behind the tube failures, highlighting the importance of employing diverse analytical approaches to develop effective preventive strategies. Similarly, Dehnavi *et al.,* (2017) examined the failure of secondary superheater tubes constructed from DIN-16CrMo4 steel at a steam power plant. The tubes experienced bulging and rupture after just three years in service. A thorough metallurgical investigation revealed that microstructural degradation, specifically severe external tube surface failure, was a key factor in premature boiler tube failures. Long-term overheating was identified as the primary root cause, further exacerbated by oxidation and erosion, ultimately leading to tube rupture. Sakthivel *et al.,* (2017) examined the causes of water tube boiler failures, aiming to reduce the frequency of such failures in thermal power station boiler accessories. Their study focused on three key failure mechanisms: flue gas erosion, prolonged overheating, and steam erosion. They proposed several solutions, including optimizing flue gas velocity, using materials with higher creep strength for boiler tubes, and applying protective coatings along the tube walls. Computational fluid dynamics (CFD) software, specifically Ansys Fluent, was employed to optimize flue gas velocity. The selection of boiler tube materials considered cost, creep strength, and corrosion resistance, while coatings were chosen based on operational conditions and feasibility. The study concluded that these remedies could significantly mitigate tube failures.

Himarosa *et al.* (2022) carried out a comprehensive failure analysis involving platen superheater tubes, water wall tubes, and seal pot plates. Their approach utilized several methods, including visual inspection, chemical composition analysis through optical emission spectrometry (OES), fracture surface examination using scanning electron microscopy (SEM), as well as tensile testing, hardness evaluation, and metallographic analysis. The investigation revealed average thicknesses of 6.46 mm for the platen superheater tube, 6.23 mm for the water wall tube, and 9.29 mm for the seal pot plate. However, the chemical compositions of these components were substandard and did not meet material specifications. The failure mechanism was attributed to high-velocity escaping steam, which caused leakage and subsequent damage to adjacent surfaces via steam cutting and erosion.

Chaudhuri *et al.,* (2006) focused on metallurgical assessments of boiler tubes to prevent the adverse effects of microstructural changes that compromise load-bearing capacity during prolonged operations at high temperatures and pressures. The study outlined basic principles for assessing the remaining life of service-exposed components, with case studies on reheater tubes made from 1.25Cr-0.5Mo steel, carbon steel tubes, and final superheater tubes composed of 2.25Cr-1Mo steel. The researchers also assessed the remaining creep life of exposed but intact platen superheater and reheater tubes made from 2.25Cr-1Mo steel. The findings showed that fly ash particle deposition significantly reduced effective tube wall thickness, leading to reheater tube failure. Decarburized metal with intergranular cracks at the inner surface of carbon steel tubes exhibited brittle window fractures caused by hydrogen embrittlement. The remaining creep life was estimated at over 10 years for platen superheater tubes at 50 MPa and 570°C (1058°F), while reheater tubes at 50 MPa and 580°C (1076°F) had an estimated creep life of 9 years.

Soltanloo *et al.* (2022) investigated the root cause of boiler waterwall tube failure in a 325 MW power plant. The study highlighted critical insights into failure mechanisms and emphasized the importance of addressing root causes to improve boiler performance and reliability. The researchers employed a sequential failure analysis method, incorporating multiple characterisation techniques such as macroscopic observation and micro-zone analysis. The study revealed that the damage was caused by caustic corrosion, which occurred through evaporation and led to the concentration of caustic substances in the inner grooves of the boiler tube. Lee *et al.* (2009) investigated the failure of a superheater tube in an ultra-supercritical coal-fired power plant. Their analysis involved visual inspection and scanning electron microscopy (SEM) to assess the fracture features and microstructural alterations, including grain growth and carbide coarsening. Additional microscopic examinations focused on scale exfoliation on the waterside surfaces of the tubes. The findings indicated that the failure was most likely due to creep rupture, triggered by structural softening linked to carbide coarsening. This degradation was further intensified by elevated metal temperatures, which reduced heat transfer efficiency due to the formation of voids.

Another significant cause of boiler tube failure was analyzed by Kain *et al.,* (2008), who examined superheater tubes in localized regions of an atmospheric fluidized bed combustor. Their study revealed that high oxidation in these regions led to the spalling of oxides due to elevated operating temperatures and the high velocity of alumina and silica particles in the fluidized bed. To mitigate this issue, they recommended the use of stainless steel sleeves in areas directly exposed to the fuel nozzle. In response to the increasing need to understand the underlying causes of boiler tube failures and minimize leakage-related outages, Movahedi-Rad *et al.* (2015) conducted an in-depth failure analysis of a ruptured seamless superheater tube from an oil-fired power plant boiler that had been in service for 20 years in Iran. The study involved metallurgical evaluations, including chemical composition analysis via spectroscopy and wall thickness assessments to gauge the effects of prolonged operation. Microstructural investigations using optical microscopy and scanning electron microscopy (SEM) revealed the formation of sigma-phase particles. Further characterization through energy-dispersive X-ray spectroscopy (EDS) and both transverse and longitudinal microhardness testing provided additional insight into the tube's degradation. The primary cause of failure was determined to be fire-side corrosion, which was intensified by extended overheating over time, facilitating the development of sigma-phase particles throughout the tube's lifespan.

Heyes (2012) explored oxygen pitting failure in a bagasse boiler tube. The investigation utilized optical and visual examination, along with stereo microscopy and SEM, to analyze the failure. The optical and visual analyses identified two through-cracks originating from the tube's internal surface. Pitting and transverse cracking were evident, along with magnetite scale, while many pitted areas exhibited red rusting. The fireside of the tube showed minimal deposits and little external surface deterioration. These findings highlighted the significant role of pitting in the failure mechanism. Stereo microscopy, combined with SEM, was used to further examine the morphology of the pitting, while the cracks were analyzed using SEM. The study concluded that the crack mechanism was caused by fatigue, potentially induced by cyclic stress due to pressure variations, thermal cycling, and tube vibrations. Examination at magnifications up to 65x revealed that the pitting failure occurred in areas where the breakdown of the magnetite film had led to cracks. Further electron microscopy analysis confirmed that most cracks originated from the pits due to stress concentration in those areas.

In their study, Nwachukwu and Woyengi-Ebinipre (2017) analyzed the failure of a refinery steam boiler that had exhibited dependable performance over the years, with only occasional minor leaks and damages, all of which were effectively resolved through welding.

Nevertheless, after 22 years of operation, the boiler's furnace chamber tubes were discovered to have suffered extensive perforations and punctures, indicating severe tube degradation. The investigation involved collecting background data and failure history, supported by photographic evidence. A comprehensive analysis was performed, which included visual inspection, low-magnification examination, chemical analysis, scanning electron microscopy (SEM), energy-dispersive spectroscopy (EDS), macrostructure and microstructure examinations, as well as tensile strength, hardness, and microhardness tests. The study concluded that the failures were primarily due to issues in water chemistry, which had led to localized caustic squeezing from the internal diameter (ID) of the tubes. This suggested a need for adjustments to the boiler's water chemistry, particularly the matching of phosphate pH control, to mitigate future failures. Additionally, overheating temperatures were identified as a secondary cause of the tube damage. Cvetkovski (2017) investigated the rupture of a φ45 diameter pipe in a thermal power plant boiler, which was made from 13CrMo4-5 steel. The study aimed to determine the root causes of the failure through a comprehensive set of tests, including visual inspection, chemical composition assessment, validity and mechanical testing, flattening tests, analysis of non-metallic inclusions (along with their types and distribution), microstructural evaluation, grain size measurement, and detailed metallographic examination.

The results showed no defects in the material or its processing, with the chemical composition and mechanical properties aligning with standard requirements. In fact, the mechanical properties significantly exceeded the minimum standards. The microstructural investigation revealed a clean material with minimal non-metallic inclusions and fine oxide occurrences randomly dispersed throughout the structure. The pipe exhibited a predominantly ferritic-pearlitic microstructure, consisting of about 80% ferrite with finely grained features. Notably, the microstructure remained consistent across both the edges and the central region of the pipe. No characteristic defects, such as decarburization, cracks, or corrosion, were observed during the investigation. However, the failure was attributed to overheating of the steam at 350 °C, which compromised the structural integrity of the pipe. From the reviewed studies, it was discovered that most researchers did not incorporate water chemistry analysis into their investigations. While Liu *et al.* (2017) and Dsilva *et al.* (2022) acknowledged scale formation and oxidation corrosion as primary failure mechanisms, their studies did not include detailed water chemistry analysis to validate these claims. This omission highlights a significant gap in the research.

To address this gap, the present study will conduct a thorough water chemistry analysis in conjunction with visual inspections and metallurgical evaluations. Preliminary observations of the failed tubes have already indicated traces of scale formation, which supports the hypothesis that corrosion and oxidation significantly contribute to boiler tube failures. This comprehensive approach aims to validate these findings and provide a deeper understanding of the mechanisms driving tube failures.

Recent studies have increasingly adopted computational tools such as ANSYS to analyze boiler tube failures. Deshmukh and Dhamangaonkar (2023) employed an integrated approach using Computational Fluid Dynamics (CFD) and Finite Element Analysis (FEA) to examine a bulging tube failure that occurred in the hot temperature zone of a boiler. Their study highlighted the effectiveness of computational modeling in identifying and resolving intricate failure mechanisms in boiler tubes.

Jadhao *et al.,* (2017) investigated a tube leakage failure in a 32TPH WIL boiler at a sugar factory in Maharashtra, India. Their analysis focused on the superheater tube, which is responsible for transforming wet saturated steam into superheated steam for power generation. Using static thermal analysis via ANSYS 16.0 ICEPAK, the study evaluated heat flux under three conditions: absence of scale, presence of scale, and the inclusion of shedding rings on the superheater tube. The results identified key contributors to the failure, including scale buildup on tube side bends, substandard weld joints in bend areas, and corrosion and erosion from flue gas ash accumulation. The research concluded that minimizing scale formation, enhancing material quality at bend regions, and installing shedding rings over weak welds could collectively reduce tube leakage by up to 21.34%.

Wapplied ANSYS to analyze the failure of reheater tubes located within a boiler at the Mettur thermal power station, a key contributor to electricity production in Tamil Nadu. The study examined various points along the reheater tube and evaluated performance by altering scale thickness and temperature. The analysis revealed that leakage was primarily caused by scale formation on the tubes. To mitigate these failures, the use of zirconium was recommended as a material for reducing reheater tube failures.

In a related study, Trojan and Taler (2013) developed a mathematical model to evaluate the performance of a steam superheater exchanger by investigating the effects of scale buildup on the internal surfaces of the tubes. The study aimed to understand how such deposits influence heat transfer and temperature distribution within the system. To accomplish this, the researchers assumed scale formation on the inner tube walls and applied the finite volume method to formulate a partial differential equation that correlates the temperatures of the flue gas, tube wall, and steam.

The model allowed for comprehensive predictions of temperature profiles across the steam, tube wall, and flue gas along the full length of the superheater. It also offered valuable insights into steam pressure variations along the flow path and enabled the calculation of the total heat transfer rate. The findings indicated that internal scale deposits notably reduced steam temperature and impeded effective heat transfer from the flue gas to the steam.

Furthermore, the presence of these deposits led to elevated tube wall temperatures, increasing the risk of accelerated degradation and potential tube failure due to overheating. This study highlighted the critical importance of mitigating scale formation to maintain efficient heat transfer and ensure the longevity and reliability of superheater components. CFD analysis has proven to be a valuable tool for determining, analyzing, and optimizing boiler tube failures. Researchers such as Ingale *et al.* (2012), Mohamed and Vincent (2014), and Prashant (2014) utilized CFD analysis to investigate superheater tube (SHT) failures caused by high flue gas temperatures. Similarly, Dewangan *et al.* (2017) and Sakthivel *et al.* (2017) explored the optimization of tube failure using CFD analysis, demonstrating its potential in addressing issues related to thermal and mechanical stress on boiler components.

From the foregoing review of literature on boiler tube failures, it is evident that most investigations have relied on microstructural analysis and various non-destructive testing (NDT) methods to assess boiler tube integrity. This study adopts similar methodologies, including visual examination, boiler water analysis, and CFD simulations to investigate stress-induced tube failures on the third pass. Additionally, chemical and microstructural analyses are employed to determine the root causes of the observed failures.

The common causes of boiler tube failures include creep, corrosion, pitting, stress cracking, bursting, and other degradation mechanisms. Verma and Desai (2018) noted that accurately predicting the root causes of boiler failures is critical for ensuring reliability and mitigating future breakdowns. According to their findings, thermal-hydrodynamic phenomena occur in boiler tubes as fluids flow through them, reducing performance and sometimes leading to catastrophic failures. Factors such as high temperature, pressure, corrosion, layer separation, and scale formation exacerbate these issues.

The drive to investigate and prevent boiler tube failures has led researchers to employ various advanced tools and methodologies. Arezoo *et al.* (2018) explored the window rupture failure of ASTM A213-T12 superheater boiler tubes in a natural gas liquid plant. The investigation revealed the formation of a dense iron oxide magnetite layer on the inner surfaces of the superheater tubes. This oxide layer hindered heat transfer, causing a significant rise in tube temperature and leading to metallurgical degradation. The internal oxide layer adversely affected the mechanical strength of the superheater tubes. Simulations confirmed that the operating temperatures of the tubes exceeded their design limits, corroborating the microstructural degradations observed during the analysis. Another method to understand boiler tube failures involves predicting residual stresses. Duarte et al., (2017) studied residual stress in boiler tubes caused by bending and operational loads at the point of failure. They identified tensile residual stress arising from inadequate stress relief treatment and high concentrations of dissolved oxygen in feedwater as primary contributors to premature tube failure through stress corrosion cracking. Likewise, Liu *et al.,* (2017) examined failures in boiler water-wall tubes through a combination of chemical analysis, visual inspection, optical microscopy, energy-dispersive spectroscopy (EDS), and scanning electron microscopy (SEM). Although pearlite spheroidization was not observed, the investigation identified localized wall thinning caused by oxidation as the primary cause of the failure.

Neural network modelling also provides insights into boiler behavior under various operational parameters. Rusinowski and Stanek (2007) created a neural network-based simulation model to capture the dynamic behavior of boilers. This data-driven approach established relationships between key operating variables and losses associated with flue gas and unburned fuel, presenting an innovative method for forecasting and optimizing boiler efficiency. Recent advancements emphasize the application of numerical techniques and sophisticated software like Computational Fluid Dynamics (CFD) for boiler analysis. CFD is invaluable for understanding complex phenomena, such as combustion, heat transfer, and fluid dynamics, in large-scale boilers, especially in scenarios where experimental studies are infeasible or costly. CFD simulations often solve continuity equations and Reynolds-Averaged Navier–Stokes equations (Rahimi *et al.,* 2006). Using commercial software packages, CFD can model heat and fluid flow, predict boiler performance, and enhance design and operational conditions (Tide and Kumar, 2012).

CFD applications extend to devolatilization studies in biomass and bagasse combustion. Centeno-González *et al.* (2017) assessed the performance of a sugarcane bagasse-fired boiler using a CFD model developed in Ansys Fluent, enhanced with user-defined functions coded in C. This custom programming provided detailed insights into devolatilization processes and combustion behavior occurring on the grate. Simulations indicated that devolatilization dominated the particle trajectory and was a critical factor in predicting thermal fields. This highlights the utility of CFD in uncovering nuanced processes in boiler operations, paving the way for efficiency improvements and design optimizations. CFD modeling also facilitates investigations into large-scale systems where traditional experimental approaches may not be feasible. Rahimi *et al.* (2006) applied Computational Fluid Dynamics (CFD) to model a 320 MW natural gas-fired boiler, aiming to determine the root cause of tube rupture within the system. The study focused on analyzing heat transfer to the boiler tubes and the internal temperature distribution, which required integrating combustion modeling with other transport phenomena, including continuity equations. A three-dimensional CFD simulation of the Bisotoun power plant boiler was carried out, capturing combustion behavior, fluid flow, and heat and mass transfer processes within the system. The 4889.43 m^3 boiler volume was discretized into 2,000,000 tetrahedral control volumes, with finer mesh applied around critical areas such as burners, air inlets, and tube sections to improve computational accuracy.

The study determined that the primary cause of rupture in the long tube elbows was the alteration of the tube's metal microstructure due to prolonged operation at temperatures exceeding the design specifications. Additionally, structural fatigue stresses made the final elbow of the long tube more susceptible to rupture compared to other areas. These findings were validated through photomicrographic analysis of metal samples taken from both damaged and intact sections of the tube. Numerical simulations, often used in conjunction with CFD analysis, have proven essential for studying combustion processes in boiler operations. Xu *et al.* (2000) performed a numerical simulation of the flow and combustion processes in a pulverized coal-fired 350 MW utility boiler. The boiler featured 24 swirl burners positioned along the furnace front wall. Their findings, based on comparisons between predicted results and plant data, showed significant agreement, affirming the accuracy of their simulation. Similarly, Soren and Kaer (2004) used CFD analysis to study a 33 MW straw-fired grate boiler. Their research focused on biomass combustion, emission levels, and the quantity of unburned carbon. While secondary superheater zones were explored, the heat transfer predictions closely aligned with real-world boiler data. The study concluded that elevated levels of unburned carbon in the fly ash resulted from inadequate mixing within the furnace.

Saripally *et al.*(2005) utilized CFD simulations to analyze thermal flow within an industrial boiler, aiming to resolve operational inefficiencies and determine optimal performance strategies. The results indicated that excessive heating could cause rupture in superheater tubes, potentially leading to boiler shutdowns. The simulation offered detailed insights into fluid velocity, pressure, temperature distribution, and species concentrations throughout the computational domain. In a related study, Masoud *et al.,* (2006) investigated tube damage in the superheater platen section of a 320 MW boiler at the Bisotoun power plant. Using a three-dimensional CFD model, the study concentrated on heat transfer and temperature profiles within the boiler, concluding that the observed damage was due to thermal and mechanical stresses localized in a series of elbows along the extended tube sections.

McKenty *et al.* (1995) further demonstrated the versatility of CFD by successfully simulating various industrial boilers operating with different fuel types. Their simulations were validated by comparing predicted outputs with measurements taken at multiple outlets, which showed strong alignment between observed and simulated data. These studies highlight the critical role of CFD in improving boiler efficiency, reducing emissions, and mitigating failure risks. However, several studies failed to show the interrelationship between experimental results and CFD analysis, often neglecting to validate their findings. This highlights the necessity for robust methodologies that integrate experimental and numerical data to enhance the accuracy of boiler failure investigations.

2.7 Combustion Processes, Energy Utilization, and Environmental Impact

According to Chavan and Pathak (2015), boilers have a long historical background, with initial developments traced back to the first century by Mr. Hero of Alexandria. Early boilers were primarily fire-tube types or tank boilers used for generating hot water for bathing purposes. Until the 17th century, there were no significant advancements in boiler design and manufacturing. However, in A.D. 1679, Mr. Denis Papin designed and developed the first boiler with a safety valve. Following this, in 1769, James Watt of Scotland created the practical steam engine, which further revolutionized boiler applications. As previously mentioned, a boiler is a steam generator and is described as a closed vessel in which water is heated and converted into steam. This process occurs through heat transfer obtained from the combustion of fuel (Rajput, (2007). Steam generated by boilers is widely used in industries for power generation, space heating, and process heating in manufacturing operations, such as sugar refineries, sugar mills, and beverage and juice processing (Nagpal, *et al* (2000).

Manufacturing industries consume significant amounts of steam energy to convert raw materials into finished goods.

Steam energy is achieved through the combustion of fossil fuels in boilers, a process that heats the boiler and converts water into high-enthalpy, high-pressure steam. However, this combustion process generates flue gases that contain harmful oxides and greenhouse gases. As industrialization continues to expand globally, significant energy resources such as natural gas, electricity, and steam are consumed. The combustion of fossil fuels (coal, oil, and natural gas) to meet energy demands produces large quantities of flue gases and greenhouse gases, contributing to environmental concerns.

In Nigeria, fossil fuels account for approximately 80% of the country's energy sources (WorldData.info, 2020). Globally, the unending demand for energy due to population growth and wealth creation further exacerbates the situation (Roser and Ritchie, 2020). Since the industrial revolution, fossil energy consumption has steadily increased, along with the emission of harmful by-products. This growing reliance on fossil fuels continues to pose challenges for the environment and public health.

According to the research conducted by Festus and Ogoegbulam (2015), a significant number of energy sources are composed primarily of carbon and various other compounds. These substances release gases commonly identified as greenhouse gases, which play a crucial role in trapping heat that would otherwise escape from the Earth's surface into the atmosphere. This phenomenon is known as the greenhouse effect. Conversely, many of these energy forms also produce emissions that are detrimental to the ozone layer. These harmful gases interact with and deplete the ozone layer, leading to its gradual deterioration. Festus and Ogoegbulam (2015) highlighted the seriousness of this issue, stating that the greenhouse effect and ozone layer depletion are key factors driving the rapid rise in global temperatures, commonly known as global warming. This temperature rise, significantly disrupts the overall climatic conditions on Earth. When this trend persists over an extended period, it results in substantial changes to climate patterns, culminating in what is widely recognized today as climate change. The more fossil fuel energy is harnessed, the higher the concentration of greenhouse gases (GHG) and ozone-depleting elements such as carbon and sulfur in the environment. These emissions promote global warming and climate change, making the environment increasingly less green (U.S. Environmental Protection Agency, 2016; Millelo et al., 2014).

Combustion processes used to generate energy in industrial operations primarily rely on fossil fuels burned in boilers for steam generation, as well as in generators and gas turbines for electricity production. For these processes, it is essential to properly estimate the stoichiometric air/fuel ratio, measure combustion efficiency, and conduct combustion analysis to understand combustion characteristics. Quantifying energy derived from the combustion process and optimizing the combustion system are critical to achieving competitive production while minimizing environmental impacts.

Recent studies emphasize the importance of energy optimization in manufacturing. Eltohami Abdelsalam (2019) and Ibrahim and Waheed (2020) described energy consumption as a vital factor for economic growth and highlighted the need for prudent energy use. The combustion of fossil fuels is a leading source of greenhouse gas emissions, which negatively impact the global environment and contribute to the depletion of the ozone layer. Yang et al. (2021) further emphasized that the expansion of the manufacturing sector substantially elevates carbon dioxide emissions, highlighting the pressing need for renewable energy initiatives.

To tackle these environmental challenges, it is important to assess and compare flue gas emissions across various energy sources used in manufacturing. Selecting the most efficient fuel for combustion and enhancing boiler performance are key steps toward advancing a low-carbon economy. Combustion performance optimization is a comprehensive process that requires attention, as inefficiencies in combustion can lead to hidden losses and increased energy costs. Moreover, incomplete combustion contributes to environmental degradation, affecting the host community and global climate.

This chapter aims to evaluate published and unpublished research, journals, and articles on combustion parameters of boilers to establish a foundation for this research. The U.S. Department of Energy's National Energy Technology Laboratory, in partnership with Air

Liquide and B&W (2008), articulated in their report titled "Advance Low/Zero Emission Boiler Design and Operation" that the combustion of fossil fuels stands as the primary source responsible for the increase in greenhouse gas (GHG) emissions. This assertion highlights the critical role fossil fuel combustion plays in contributing to environmental degradation. The report underscores that these emissions significantly impact climate change, necessitating urgent attention and action to mitigate their effects on global warming and overall environmental health. This assertion highlights the critical role fossil fuel combustion plays in contributing to environmental degradation. The report underscores that these emissions significantly impact climate change, necessitating urgent attention and action to mitigate their effects on global warming and overall environmental health. This is particularly relevant because fossil fuels are predominantly used in industrial boilers for steam generation, as well as in generators and gas turbines for electricity production. In this context, related studies on boiler tube failure, combustion performance optimization, and emission characteristics of dual-fired boilers are reviewed in three parts:

1. Boiler tube failure analysis.
2. Boiler emission characteristics based on fuel type.
3. Performance optimization.

These areas significantly impact boiler performance from an operational perspective. Experimental investigations into boiler tube failure causes, flue gas compositions, and combustion performance will be analyzed using commercial software (e.g., Aspen Ansys and Aspen Hysys) to verify results. Furthermore, optimizing critical combustion parameters that influence boiler performance will contribute to improved efficiency and environmental sustainability

2.8 Boiler Emission

With growing global awareness of environmental protection, the efficient performance, combustion processes, and pollution emissions from industrial boilers and furnaces have become critical concerns for achieving internationally acceptable emission standards. Understanding the mechanisms of failure, combustion dynamics, and emission patterns of these boilers is essential for optimizing their operations. Key challenges in this domain include identifying failure mechanisms, analyzing the distribution characteristics of pollutant emissions, understanding the formation mechanisms of nitrogen oxides (NOx), implementing emission reduction technologies, and ensuring optimal operation of industrial boilers. The food and beverage industry, in particular, depends greatly on the reliable and uninterrupted operation of its core equipment, with steam boilers serving as a crucial component in industrial processing activities. The performance and reliability of these boilers directly impact the production process, emphasizing the need for effective management and technological advancements to mitigate failure risks and reduce environmental impact.

The performance efficiency of boilers reduces over time due to poor combustion, tube fouling, and poor operation of the plant (James *et al.,* 1980; Higgins *et al.,* 1981). Despite these, other factors that could improve the performance of boilers, according to the Bureau of Energy Efficiency of India as described by Hasanuzzaman *et al.,* (2020) highlighted various practices in India to optimize boiler performance and mitigate issues related to combustion emissions. These measures include periodic cleaning of boilers, regular soot blowing, implementing proper water treatment programs, performing blowdowns, ensuring draft control, maintaining fuel quality, controlling excess air, managing the percentage loading of the boiler, and monitoring steam generation temperature, pressure, and boiler insulation. Globally, combustion emissions have remained a significant concern, prompting industry leaders across various nations to address this challenge proactively. For instance, in April 2002, the United

States initiated efforts by assembling a group of industry experts to draft and evaluate a combustion roadmap. This roadmap aimed to set measurable goals to assess the contribution of proposed actions toward the nation's energy objectives. Milestones were also established to enable the combustion community to track progress against the roadmap's objectives effectively.

One of the primary objectives outlined was to minimize emissions of NOx, CO, CO_2, and particulates by developing advanced methods for maintaining stable flames with low emissions across various fuel types. Furthermore, the roadmap emphasized the need for innovative burners equipped with real-time adjustable operating parameters. These advancements would enhance operational flexibility while achieving significant reductions in harmful emissions, thereby aligning with the broader goals of environmental protection and energy efficiency. The combustion efficiency of the boiler depends mostly on the performance of the combustion system and central to this is the burner unit. The performance of the burner unit is of high importance to the boiler engineer because this determines whether combustion of the air-fuel mixture will be complete or incomplete. While complete combustion is essentially required for boiler emission control and complete burning of the fuel for a green combustion. Incomplete combustion on the other hand promotes the release of greenhouse gases to the environment. Tunning the burner for an efficient combustion performance determines to a larger extent the emission characteristics of the flue gas that is released to the environment as exhaust from the chimney and the heat generated for the boiler operations. Abdallah (2017) stated that the combustion of fossil fuel (either diesel or natural gas) in the boiler combustion chamber leads to the generation of the heat required for the boiler by transferring heat to the water to produce steam, as a result, combustion by-products are expelled as flue gases from the boilers' stack. The flue gases consist of the emission of greenhouse gases which includes carbon monoxide, carbon iv oxide, excess oxygen, unburnt carbon, oxides of nitrogen and sulphur, which are harmful to the environment. Boilers are among the most essential and widely utilized components in various industrial sectors, particularly in developing economies (van der Gaast *et al.*, 2007; Shen *et al.,* 2017). Their ubiquitous application underscores their critical role in supporting industrial processes, making them indispensable for sectors reliant on consistent steam and heat generation. Hence the need to optimize the boiler's performance for efficient operation to produce steam and, at the same time, prevent the emission of greenhouse gases to the environment where it operates becomes a crucial business.

2.9 Review of Related Literature on Boiler Emission Characteristics

With increasingly stringent regulations governing combustion systems in manufacturing processes, industrial boilers have become critical components of modern production operations. The demand for research on controlling boiler combustion processes has grown significantly in recent years. This increased focus aims to enhance both combustion efficiency and overall economic performance in industrial applications (Wang *et al.,* 2006; Pan *et al.,* 2018). Fasogbon *et al.,* (2020) investigated the emission characteristics of a compression ignition (CI) engine powered by blends of tropical almond seed oil-based biodiesel. The study utilized Artificial Neural Networks (ANNs) to evaluate the effect of injection timing on the engine's emission profile. Through a series of experimental tests conducted on an engine rig, the researchers generated data to train the ANNs. The findings revealed that tropical almond oil-based biodiesel exhibited environmentally friendly emission patterns, with optimal injection timing being retarded rather than advanced.

The study concluded that ANNs are highly reliable tools for predicting both compression behavior and the emission profiles of biodiesel-fueled CI engines on a large scale. Furthermore, the results demonstrated a strong correlation between the predictions made by the ANN model and the actual experimental values for various engine emission parameters. The mean relative error values were found to be less than 10%, indicating the model's accuracy within acceptable limits for such analyses.

However, the study did not examine the effects of retarded injection timing on other greenhouse gases besides NOx and CO. Additionally, there was no information on flue gas analysis to confirm compliance with other oxide emission standards. The combustion temperature was not disclosed, leaving an important aspect of the study unexplored. Furthermore, the optimal parametric settings for the combustion process were not provided, and no guide on performance efficiency was included, which could have offered useful information to automotive designers.

Fleming and Allsup (1972) studied the emission behavior of natural gas as a low-emission fuel for automotive applications by conducting experiments on a single-cylinder engine, a multi-cylinder engine, and six vehicles. Their results indicated that lean-limit misfiring in natural gas engines occurs at air-fuel ratios ranging from 140% to 150% of the stoichiometric value. The study further showed that while nitrogen oxide (NOx) and hydrocarbon emissions are sensitive to changes in ignition timing, carbon monoxide (CO) emissions remain relatively stable. It was further suggested that emission reductions could be achieved with existing engine designs, albeit at the cost of engine performance. Additionally, temperature changes within the range of 20°F to 100°F had virtually no impact on emissions from vehicles powered by natural gas. The reactivity of natural gas exhaust, measured at 22-25%, was reported to be comparable to that of gasoline exhaust.

Lin *et al.,* (2008) examined the emissions from industrial furnaces burning diesel fuel oils of varying sulfur contents under atmospheric air containing sodium chloride (NaCl). The study assessed diesel fuels with sulfur contents of 0.3 wt.% and 1.0 wt.%, mixed with NaCl at a concentration of 1.5 ppm. Results indicated that emissions of CO, SO_2, and O_2 increased with higher sulfur content in the diesel fuel, while flue gas temperature and NOx concentration were only slightly impacted. However, the study did not evaluate the implications for boiler efficiency or the effects on boiler tubes.

Cho and He (2009) examined how different fuel injection timings during the intake stroke affect the combustion and emission behavior of a natural gas engine. Their research demonstrated that fuel injection timing significantly influences combustion characteristics. The optimal spark timing for maximizing indicated mean effective pressure (IMEP) varied based on both the injection timing and the air-fuel ratio. Delayed injection generally resulted in postponed ignition and longer combustion duration. However, when the air-fuel ratio (lambda) was held constant, injection timing had little impact on IMEP. The coefficient of variation (COV) of IMEP was affected by throttle position, air-fuel ratio, and injection timing at the MBT spark setting, with COV typically rising as lambda increased. At partial load conditions, later injection timings helped reduce COV, along with lowering engine-out emissions of carbon monoxide (CO) and total hydrocarbons (THC).

Saxena and Maurya (2020) carried out experimental studies to evaluate the performance and emission behavior, including nanoparticle emissions, of a non-road diesel engine operating on pure diesel and various butanol-diesel blends. The tests were performed under optimal engine conditions at a fixed speed of 1500 revolutions per minute. In the initial phase, diesel fuel was used to fine-tune the engine parameters in order to improve brake thermal efficiency and minimize exhaust emissions, both gaseous and particulate. To achieve this optimization, the researchers applied Taguchi's design of experiments, focusing on key factors such as compression ratio, injection pressure, and engine load.

To assess the impact of butanol-diesel blends, the researchers evaluated three volumetric ratios: 10%, 20%, and 30% under optimized engine conditions. The results showed that these blends significantly lowered emissions of carbon monoxide, nitrogen oxides, and particulates. Furthermore, a consistent decrease in the concentration of ultra-fine particles was noted under all test scenarios. The most substantial reductions in total particle number concentration were recorded at engine loads of 25 percent and 50 percent, relative to pure diesel.

Despite these extensive studies, there remains a significant gap in analyzing dual-fired boilers using diesel and natural gas. This study aims to investigate the emissions, combustion performance, and failure characteristics of dual-fired boilers operating on these fuels. This focus is particularly relevant as industrial plants are increasingly located in urban areas due to industrialization, necessitating emission verification from these areas to address environmental and societal concerns.

Korytnyi *et al.*, (2008) developed an engineering tool aimed at forecasting coal combustion behavior within coal-fired utility boilers. Their study showed that CFD models can effectively replicate the operation of full-scale pulverized-coal utility boilers under a range of configurations. However, the accuracy of these simulations relies heavily on the proper selection and validation of the model parameters applied during the analysis.

2.10 Review of Related Literature on Boiler Performance Optimization

Combustion in boilers can be categorized into two types: complete combustion and incomplete combustion. The process of burning fossil fuels in a boiler's burner generates the necessary heat for its operation. However, this process often releases large quantities of flue gases, which include greenhouse emissions such as carbon monoxide (CO), carbon dioxide (CO_2), unburnt carbon, excess oxygen, and oxides of nitrogen (NOx) and sulfur (SOx). These emissions pose significant environmental hazards. Incomplete combustion is the primary contributor to these toxic emissions, emphasizing the importance of optimizing combustion performance. Such optimization not only improves boiler efficiency but also mitigates the environmental impacts of industrial operations.

Aminmahalati *et al.*, (2021) investigated the combustion performance of a CO boiler at an oil refinery. Using CFD and a non-dominated sorting genetic algorithm II, they identified the optimal operating conditions of the boiler. Their methodology involved determining the number of mesh points via a network independence test, with numerical and experimental results confirming a 96% accuracy for validated variables. Similarly, Jiang *et al.,* (2021) optimized the operating conditions of a 550-MW tangentially fired pulverized coal boiler to achieve combustion stability and reduce NOx emissions under half-load conditions. While they succeeded in reducing gas emissions and achieving combustion stability, asymmetrical combustion caused by burner group arrangements remained a limitation.

Jagtap *et al.* (2021) conducted a performance analysis of a 500-MW thermal power plant by employing Markov simulations to model its boiler-furnace system. Their research analyzed various combinations of failure and repair rates, revealing that boiler drum failures had the most significant impact on system availability, while reheater failures had the least. Using particle swarm optimization, the study achieved a maximum system availability of 99.9845%. While their findings provided valuable insights for maintenance prioritization, the study did not account for flue gas emissions, highlighting a gap in addressing environmental concerns.
In a related study, Mirek *et al.* (2009) optimized the primary and secondary air distribution of a 225-MWe Circulating Fluidized Bed (CFB) boiler to reduce NOx emissions. By altering the internal geometry of the primary air channel and plenum chamber, they observed a 10% reduction in NOx emissions and a more uniform temperature distribution in the combustion

chamber. Despite these achievements, the study did not address other emissions such as SOx and CO_2, nor did it provide details about the optimized combustion parameters.

Zhang (2014) examined an industrial boiler system to identify opportunities for energy efficiency improvements. Their research proposed several optimization strategies, including resetting vapor pressure, installing variable frequency drives (VFDs) on forced draft (FD) fans, and optimizing feedwater systems. Specifically, optimizing the air-to-fuel ratio in a single-burner model reduced fuel consumption by up to 7% at lower loads. However, the study lacked a comprehensive flue gas analysis, limiting its insights into the environmental impact of these optimizations.

Ochoa *et al.* (2019) implemented the ISO 50001 energy management system to optimize steam boiler performance. They applied three key strategies: reducing steam generation pressure, automating boiler purges, and correcting combustion air measurements in real-time. These interventions collectively reduced natural gas consumption by 2%, improved energy performance, and minimized environmental impacts. Despite its success, the study did not disclose the total efficiency of the boiler or the operational firing rates, leaving gaps in understanding the full extent of the optimization's effectiveness.

Artificial intelligence techniques have also been applied to optimize boiler performance. Zhou (2004) utilized artificial neural networks (ANNs) to forecast NOx emissions in a large-capacity pulverized coal-fired boiler. Their study incorporated a modified genetic algorithm to identify optimal operating conditions, guiding operators to implement corrective measures for reducing emissions. Similarly, Ma (2021) employed a multi-objective learning-based optimization algorithm (MMTLBO) to enhance the combustion process of a circulating fluidized bed boiler (CFBB). Their work improved thermal efficiency and significantly reduced NOx and SO_2 emissions.

Other advancements in boiler optimization include the use of mathematical models. In 2020, researchers developed a model to optimize fractional collection efficiencies in biomass-fired boilers, focusing on electric fields within electrostatic precipitators. Oswald *et al.,* (2012, 2020) developed algorithms to improve biomass boiler combustion processes, successfully enhancing efficiency and reducing emissions. . In the same vein, Oswald *et al.,* (2020) also worked on controlled technology of various biomass boilers by developing a control algorithm that optimizes a large that was able to optimize efficiencies of large biomass-fired boilers efficiencies by controlling the combustion process and, at the same time lessen the associated emissions problem by way reduction. Gray relational analysis was used by Moran *et al.*, (2006) to study different biomass as fuel with pellets as a co-firing element to determine the performance and emission of the biomass boilers. Their study found out that co-firing of the crust of pine together with wood pellets was compatible with biomass fuel with less environmental and economic effect. Moreover, the multi-stakeholder analysis, often referred to as the Shapley-Shubik power index, has been employed to assess stakeholder contributions in transitioning biomass power plants. This analytical tool provides a systematic approach to evaluating the influence of various stakeholders during such conversions.

Tilahum *et al.* (2021) modelled a salt boiler using MATLAB, integrating it into a solar system, and optimizing it through GenOpt. Their optimization efforts successfully reduced the biomass power utilization index (BPUI) and minimized excess steam generation (ESG). A case study demonstrated these achievements, revealing a plant efficiency improvement of 31.5% and 23% under different scenarios. Furthermore, the research achieved an optimal design cost of $0.094 per kilowatt, effectively lowering generation costs.

In another vein, Stritih *et al.,* (2004) explored the performance of a boiler equipped with built-in thermal storage using TRNSYS, emphasizing energy efficiency. Recently, computational fluid dynamics (CFD) has emerged as a pivotal tool in optimizing boiler performance. CFD utilizes advanced scientific principles to simulate fluid flow, heat transfer, mass transfer, chemical reactions, and other related phenomena. By solving complex mathematical equations through numerical processes, CFD provides invaluable insights for optimizing boiler systems (Ansys, 2010).

The application of CFD modeling and simulation involves specialized software to investigate diverse aspects such as fluid dynamics, heat transfer mechanisms, aerodynamic systems, industrial designs, and combustion analysis. Several researchers have leveraged CFD to enhance combustion efficiency. For instance, Ingale *et al.,* (2012) demonstrated how CFD results could be utilized to predict the lifespan of boiler tubes, identify high-temperature zones, and implement strategies to mitigate tube erosion and minimize leakage risks.

Echi *et al.*, (2019) used CFD modeling via the ANSYS-FLUENT code to optimize the performance of a sulfuric acid production boiler. This simulation provided detailed insights into fluid and thermal dynamics, facilitating operational improvements. Similarly, Aminmahalati *et al.* (2022) used CFD to evaluate the performance of an oil refinery CO boiler. By focusing on combustion chamber optimization and determining mesh points through a network independence test, their study achieved 96% accuracy for validated variables. Moreover, the simulation revealed complete hydrocarbon combustion at the combustion chamber's onset. NO reaction rate analysis was applied to quantify environmental pollutants near the burner, and the optimal operating conditions for the CO boiler were determined using a non-dominated sorting genetic algorithm II.

Further research by Chaney *et al.* (2012) employed CFD to develop a model for a 50kW biomass boiler. Their study focused on optimizing combustion performance and reducing NOx emissions by adjusting key parameters such as the primary and secondary air supply, orientation, height, direction, and secondary inlets. These modifications significantly enhanced the boiler's efficiency while mitigating harmful emissions. However, this study only focused on NOx emission reduction while other greenhouse gases were not considered. Also, the flue gas temperature was not emphasized in this study. Bianco *et al.,* (2021) in their research to optimize the air manifold of a biomass-fired boiler using computational fluid dynamics (C.F.D.) model developed and authenticated with experimental data, and was used to improve the boiler's performance by reducing entropy generation in the system.

Oischinger *et al.* (2022) and Zinurov *et al.* (2022) conducted a comprehensive investigation into the performance of gas boilers and the enhancement of the combustion process for hydrocarbon fuels within combustion chambers. Their primary objective was to assess how the geometry of boiler chambers equipped with premix burners influences hydrocarbon combustion and to evaluate the heat load distribution on the chamber surfaces and outlet. The simulation results revealed that the heat-transfer coefficient for the external contour of materials like cast iron and sheet steel decreased significantly, by approximately 4.2 times, when the diameter expanded from 100 mm to 300 mm. Conversely, reducing the diameter of the boiler's external contour significantly heightened the heat load on the chamber surfaces, which subsequently improved heat transfer efficiency.

Similarly, Rahimi *et al.* (2006) investigated the damage mechanisms of tubes in the superheater platen section of the 320 MW Bisotoun power plant in Iran. This study employed a three-dimensional CFD model developed in-house to analyze the entire boiler, including its walls, burners, air channels, and three tube types, all modeled at real scale. The model, which used nearly 2,000,000 tetrahedral control volumes, incorporated the standard k–ε turbulence model and Rosseland radiation model to achieve accuracy. The findings revealed that the inlet saturated steam at 18.9 MPa became superheated inside the tubes and exited at a reduced pressure of 17.8 MPa. Importantly, the temperatures of the steam and tube walls were notably higher in long tubes compared to shorter and medium-sized tubes, and the mass flow rate in the longer tubes was lower.

These observations led to the conclusion that long tubes suffered from ruptures primarily due to changes in their metal microstructure caused by exposure to temperatures exceeding their design specifications. Additionally, structural fatigue tensions were identified as contributing factors, with the final elbow of the long tubes being particularly prone to rupture. These conclusions were validated through photomicrograph analyses of metal samples from both damaged and undamaged tube sections.

Chaney *et al.* (2012) approached boiler optimization by developing a CFD model for a 50-kW biomass boiler. Their work focused on optimizing combustion performance and reducing NOx emissions by modifying factors such as the primary and secondary air supply, air orientation, height, direction, and secondary inlets. While this study successfully reduced NOx emissions, it did not address other greenhouse gases, and the flue gas temperature was not emphasized.

Zhou *et al.* (2004) employed artificial neural networks (ANN) to forecast NOx emission characteristics in large-capacity pulverized coal-fired boilers. Their parametric field experiments examined NOx emissions and carbon burnout characteristics, studying variables such as over-fire-air (OFA) flow rates, coal properties, boiler load, air distribution schemes, and nozzle tilt. To enhance accuracy, the study utilized a modified genetic algorithm (GA) with a micro-GA technique to optimize the ANN model. The optimal setpoints derived from this model provided actionable insights for operators to effectively reduce NOx emissions under varying conditions.

Ma *et al.* (2021) advanced boiler optimization efforts by applying a multi-objective learning-based optimization algorithm known as MMTLBO to refine adaptive extreme learning machines (AELM). Their study focused on enhancing the combustion process in a circulating fluidized bed boiler (CFBB), and the results showed notable gains in thermal efficiency along with reduced concentrations of nitrogen oxides (NOx) and sulfur dioxide (SO_2), demonstrating the effectiveness of MMTLBO in improving boiler performance.

In a related study, Bianco *et al.* (2021) utilized a computational fluid dynamics (CFD) model validated through experimental data to optimize the air manifold of a biomass-fired boiler. This approach aimed at improving boiler efficiency by minimizing entropy generation within the system. Similarly, Oischinger *et al.*, (2020) developed a mathematical model to optimize the fractional collection efficiencies of electrostatic precipitators used in biomass boilers. Their work focused on analyzing the impact of the electric field across three stages of precipitation.

Oswald *et al.* (2012) proposed an algorithm to enhance the combustion process in biomass boilers, which led to reduced harmful emissions and improved overall efficiency. Expanding on this work, Oswald *et al.,* (2020) designed a control algorithm to regulate combustion in large-scale biomass-fired boilers. The goal was to increase thermal efficiency while simultaneously lowering emission levels.

Moran *et al.* (2006) evaluated the performance and emissions of biomass boilers using various types of biomass fuel, incorporating pellets for co-firing. They employed Gray relational analysis to assess the operational efficiency and environmental impact of these fuel combinations. The study showed that co-firing of the crust of pine together with wood pellets was compatible with biomass fuel with less environmental and economic effect.

Franke *et al.* (2003) conducted an optimization study on drum boiler startups using a simplified non-linear model derived from prior research. This model was implemented through the Modelica platform, incorporating the advanced Modelica-Media and Modelica-Fluid libraries. The study focused on three main control inputs: the flow rate of feedwater, the amount of heat input, and the position of a valve at the steam outlet. A proportional-integral (PI) controller was employed to regulate the feedwater flow, while the remaining two variables were optimized to minimize deviations in steam pressure and flow rate from their specified reference levels. These references included an amount of approximately 110 units for steam pressure and 180 units for the steam flow rate.

Optimization was conducted under specific constraints, including the fuel flow rate, valve positioning, and the firing rate, with thermal stress factored in as an output constraint. The results showed substantial performance improvements when compared to conventional control strategies, significantly reducing discrepancies between actual and reference outputs. This demonstrated the effectiveness of model-based optimization in enhancing boiler efficiency during startup, ensuring stable operation within defined limits.

Tilahum *et al,* (2021) approached boiler optimization differently by creating a model for a salt boiler using MATLAB. This model was integrated into a solar-powered system and further optimized using GenOpt. The optimization achieved notable improvements, lowering the biomass power utilization index (BPUI) and minimizing the generation of excess steam (ESG). A case study highlighted increases in plant efficiency of roughly 31% and 23%, respectively. Furthermore, the optimal design yielded a cost of approximately 0.094 monetary units per kilowatt, effectively standardizing the cost of energy generation. By combining solar energy with traditional biomass systems, the study not only enhanced operational efficiency but also demonstrated the economic feasibility of hybrid energy solutions.

However, this study intends to carry out optimization of the boiler input parameters using Taguchi experimental design and minitab-18 software to carry out the optimization of the boiler operation. Since little work on natural gas-fired boilers and diesel-fired boilers, as well as dual fired boilers, are there, this study then reviewed related combustion works on internal combustion engines on diesel, natural gas; biodiesel, and biomass-fired boilers where extensive works have been done in other to establish a firm description of the aim and objective of the present study. Najmi and Arhosazani (2006) carried out a feasibility study to replace medium fuel oil (M.F.O.) with natural gas due to cost and emission issues related to the fuel oil. However, many researches have been conducted to optimize different engineering thermal systems' performance and emission characteristics, mostly on biomass-fired boilers, internal engines, furnaces, and others. (Yessian and Varthanam (2020); Zheng *et al.,* (2008); Keskin *et al.,* (2008); Soundal *et al.,* (2017); Jagtap *et al.*, (2019); Ponnusamy *et al.*, 2011; Resitoglu et al., (2015); Pohit, and Misra,(2013); Patil and Thipse (2014); Bhuiyaa et al., (2017).

Similarly, other researchers conducted investigations into the combustion optimization of biodiesel engines and combustion systems, with the aim of mitigating the environmental impact of their emissions and concurrently enhancing their operational efficiencies.

Recently Yessian and Varthanan (2020) studied the optimization of the combustion performance and emission characteristics of catalytic coated internal combustion (I.C.) engines using biodiesel. The study employed the Taguchi method and Grey-Taguchi method for the analysis. An *et al.,* (2013) carried out an experimental study using biodiesel blend fuel obtained from waste cooking oil on a Euro IV diesel engine to determine the combustion performance optimization and emission characteristics of the biodiesel blend fuel on the internal combustion engine.

An *et al.* (2013) conducted an experimental investigation into the combustion behavior and emission characteristics of biodiesel blends derived from waste cooking oil in a Euro IV diesel engine. The study tested four engine speeds (800, 1200, 2400, and 3600 rpm) under three load conditions (25%, 50%, and 100%). Results indicated that biodiesel and its blends exhibited higher brake specific fuel consumption (BSFC) than conventional diesel, especially at lower engine speeds and partial loads. At 25% load, BSFC increased by 42% at 800 rpm and 34.4% at 1200 rpm when using biodiesel. In terms of thermal efficiency, biodiesel outperformed diesel at medium and full loads (50% and 100%) but was less efficient at 25% load.

The combustion analysis showed that biodiesel had a slightly shorter ignition delay and a lower peak heat release rate compared to diesel, suggesting improved combustion characteristics. Emission measurements revealed modest reductions in hydrocarbons (HC) and nitrogen oxides (NOx) with biodiesel use. However, at lower engine speeds, emission levels rose, underscoring the influence of low-speed operation on combustion efficiency and pollutant formation. Additional research by Elkalawy *et al.* (2019), Guedes *et al.,* (2018), and others further explored biodiesel-diesel blends with various additives, enriching the current understanding of alternative fuels and their environmental impact.

Optimization studies on boiler performance and emissions have also been widely conducted. Abroshan (2020) used computational fluid dynamics (CFD) and mathematical modeling to examine the performance of a tangentially gas-fired boiler under full-load conditions. The study analyzed the effects of varying combustion excess air levels (0–20%) and burner tilt angles (-30° to +30°) on boiler efficiency. The findings indicated that the highest boiler efficiency was attained with 10% excess air and a negative burner tilt angle. For superheated steam at 538 °C, maximum efficiency was observed either at a zero or positive tilt angle with 10 percent excess air, or with a negative tilt angle when excess air was increased to 15 percent.

Moreover, carbon monoxide (CO) emissions were lowered by optimizing burner tilt angles under low excess air conditions, while nitrogen oxide (NOx) emissions were most effectively reduced using positive burner angles across both low and high excess air levels. The importance of boiler optimization has been emphasized in earlier works by Liptak (1999) and Santoso *et al.,* (2005), who identified combustion improvement as a critical factor in reducing operating costs. Reducing excess air and oxygen levels during combustion can significantly enhance boiler performance. Recent advances in boiler combustion control systems have further supported these goals, as explored by Dukelow (2001) and Santoso *et al.*, (2005).

Ramakrishnan and Arumugam (2013) applied the Taguchi method to optimize cooling tower performance using expanded mesh packing in a counterflow setup. Similarly, Coskun *et al.,* (2011) utilized the Taguchi method to optimize operating parameters in a waste heat recovery application, achieving maximum effectiveness. Ramkumar and Ragupathy (2013) also employed the Taguchi method to assess and optimize cooling tower effectiveness. These studies underscore the utility of optimizing operating parameters as a fundamental approach to improving system performance, whether in boilers, cooling towers, or other industrial equipment.

Anam and La Ode (2019) designed and optimized the economizer of a laundry boiler using the experimental Taguchi method to improve the boiler feed water temperature. Morakinyo and Bamgboye (2017) optimized the operational parameter of a biomass-fired boiler using the Taguchi design method.

According to Fagbolagun and Oke (2020), several optimization tools are available, some of which are: memetic algorithm, self-organizing, differential evolution, particle swarm optimization, migrating algorithm, genetic algorithm, linear programming, combinatorial optimization, numerical analysis, non-linear modeling, response surface methodology, mathematical models, Grey relational analysis, artificial neural networks, case-based reasoning, linear programming, and the Taguchi method are all significant optimization techniques. In line with the findings of Fagbolagun and Oke (2020) and Morakinyo and Bamgboye (2017), this research also utilizes a combination of the Taguchi method and Minitab-18 software to optimize variables related to boiler combustion. The Taguchi method is favored in industrial applications due to the challenges associated with traditional trial-and-error approaches, which are often resource-intensive in terms of both time and finances, requiring numerous experimental runs (Jou *et al.,* 2014, Fagbolagun and Oke, 2020).

Unlike other optimization techniques, the Taguchi method efficiently identifies optimal parameter values with fewer experimental runs while minimizing variability from noise factors (Jou *et al.,* 2014; Fagbolagun and Oke (2020). This method employs a robust design framework to determine the best parameters that influence boiler combustion performance. The imperative to identify control factors that reduce variations in the combustion process while achieving optimal settings that minimize fuel consumption, enhance steam generation, and mitigate greenhouse gas emissions—has become a crucial concern for boiler operators in various industries (Li *et al.,* 2002).

Moreover, addressing issues related to poor combustion performance is essential for improving emission characteristics and reducing environmental impact. Optimizing boiler combustion performance is vital for achieving maximum combustion efficiency and minimizing greenhouse gas emissions through careful manipulation of combustion parameters. Thus, the importance of boiler optimization cannot be overstated, positioning the Taguchi method as a leading approach among various optimization strategies.

Genichi Taguchi, born in Japan in 1924, was an electrical engineer who contributed significantly to improving Japan's telephone communication system in the 1950s post-World War II. He is widely recognized as the father of the Taguchi method and robust engineering. The term "robust" refers to designs that are less sensitive to external factors while consistently performing at target values, thereby delivering desirable outcomes. To achieve design robustness, numerous researchers have implemented various optimization methods to enhance boiler performance.

For instance, Bianco *et al.,* (2021) optimized an air manifold for a biomass-fired boiler using a Computational Fluid Dynamics (CFD) model, validating their results against experimental data. This optimization primarily focused on reducing entropy generation within the system. Alvarez *et al.* (2018) examined biomass combustion in medium-sized commercial pellet boilers to establish requirements for bioclimatic buildings. They developed a miniature gaseous emission model that optimized boiler performance by manually adjusting fuel and air inlet parameters, resulting in a 20% reduction in fuel consumption and a 21% decrease in excess oxidizing air inlet. Consequently, emissions of CO, NOx, and SOx fell below 200 ppm while thermal yield improved from 78.6% to 94.9%, with chamber and flue gas temperatures rising by 160°C and 20°C respectively.

Nimmanterdwong *et al.* (2022) investigated steam production from four types of biomass using a neural network model combined with Constrained Particle Swarm Optimization (CPSO) to identify cost-effective production methods for optimized feedstock. Additionally, Mariajayaprakash and Senthilvelan (2012) utilized cause-and-effect diagrams alongside failure mode and effects analysis to further explore optimization strategies within this domain.

2.11 Research Gap

To the best of my knowledge from the review of literature, the following research gaps were identified in existing research and they are as follows

1. In the existing literature, boiler tube failure, emission characterization, and combustion performance are largely studied as separate phenomena, despite their strong interdependence are not succinctly explored in academic research.
2. Most studies focus on emissions from single-fuel boilers or internal combustion engines, the emission characteristics of dual-fired boilers, particularly under natural gas and diesel switching or mixed-fuel operation, remain largely unexplored.
3. The emission characteristics of dual-fired boilers operating on natural gas and diesel remain poorly understood, as most studies focus on single-fuel boilers or internal combustion engines; moreover, critical combustion parameters such as flue gas temperature and excess oxygen are often neglected, leaving the environmental impacts inadequately characterized.
4. Optimization techniques such as the Taguchi method and CFD modelling have been employed in some studies to enhance boiler performance. However, these tools are rarely integrated with experimental findings, particularly for dual-fired boilers.
5. This limitation reduces the practical applicability of optimization techniques in industrial settings. Furthermore, many optimization studies fail to provide detailed analyses of key combustion parameters or validate computational models with real-world data, undermining their reliability and relevance.

In terms of boiler tube failures, while many studies address the phenomenon, they often overlook the combined effects of water chemistry, operational stresses, and combustion inefficiencies. Few studies integrate metallurgical analysis with water chemistry evaluations to provide a holistic understanding of tube failure mechanisms. This lack of integration leaves critical questions unanswered regarding the factors contributing to recurring failures.

Another key gap pertains to the environmental and societal impacts of boiler operations in urban industrial settings. As manufacturing plants increasingly operate in urban areas, the need for localized emission verification and mitigation strategies becomes essential. However, this aspect is often neglected, despite its importance for ensuring sustainable industrial practices.

CHAPTER THREE

3.1 METHODOLOGY

The methodology adopted in investigating the failure mechanisms, performance modelling, and emission characteristics of the 12 tonne industrial boiler under study shown in figure 3.1 entails the employment of a combination of experimental analysis, numerical modelling, and emissions assessment to comprehensively evaluate the boiler’s operational efficiency, identify potential failure modes, and quantify pollutant emissions.

As seen from Figure 3.1, the study begins by detailing the experimental setup which includes the data collection process, instrumentation and tests carried out to investigate the boiler tube failures and its pattern. Next, the modelling approach is presented where thermodynamic and heat transfer models are developed to predict boiler efficiency and performance under varying stages of failure. Therefore, the combustion and emission characteristics of the burner are analyzed through combustion modelling and flue gas analysis. Furthermore, optimization of the combustion control parameters was carried out using Mintab-18 and Taguchi method to obtain the optimum combination of combustion control parameters.

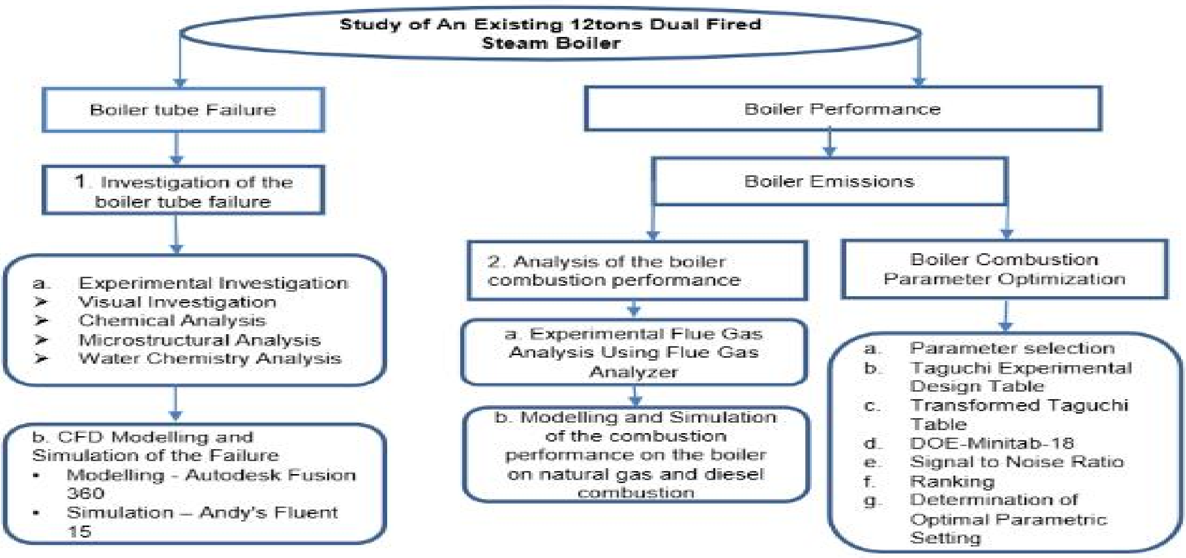

Figure 3.1: Overview of methodology for the study

3.1 Boiler Experimental Setup and Its Fuels

The dual-fired steam boiler utilized in this study was provided by Rev Foods and Beverage Limited, located in Lagos, and is illustrated in Figure 3.2. This boiler has a capacity of 12,000 kg/h and operates on both natural gas and diesel, featuring a total of 170 tubes. For the failure analysis, samples were taken specifically from the third-pass tube section. In the experimental phase, only natural gas was used to validate the results obtained from the CFD simulations. Data collected from the experimental tests served as boundary conditions for the CFD modelling. Carbon dioxide (CO_2) and oxygen (O_2) emission levels were used as key performance indicators in both the experimental and simulation analyses. The fuel properties are detailed in Table 3.1

Table 3.1: Properties of natural gas and diesel fuels

FUEL PROPERTIES USED IN THE BOILER			
Natural Gas		Diesel	
Fuel Component	Mole (%)	Component	Volume (%)
Methane	95.0518	Alkanes (Parafin)	20 - 40
Ethane	2.8707	Cycloalkanes (Naphthenes)	30 - 50
Propane	0.9457	Aromatic (Hydrocarbons)	10- 30
i-Butane	0.1328	Olefins (Alkenes)	<5%

n-Butane	0.1272	Sulphur compounds	<0.001
i-Pentane	0.0257		
n-Pentane	0.0156		
Hexane	0.0158		
Nitrogen	0.5808		
Carbon dioxide	0.2339		

Figure 3.2: Schematic diagram of the boiler

3.2. Boiler Tube Failure Investigation

The Failure investigation of the industrial 12ton boiler tubes involves a systematic approach to identify the causes of the recurring failure and to recommend corrective actions. The methodology adopted for investigation the r tube failure is shown in the procedure of Figure

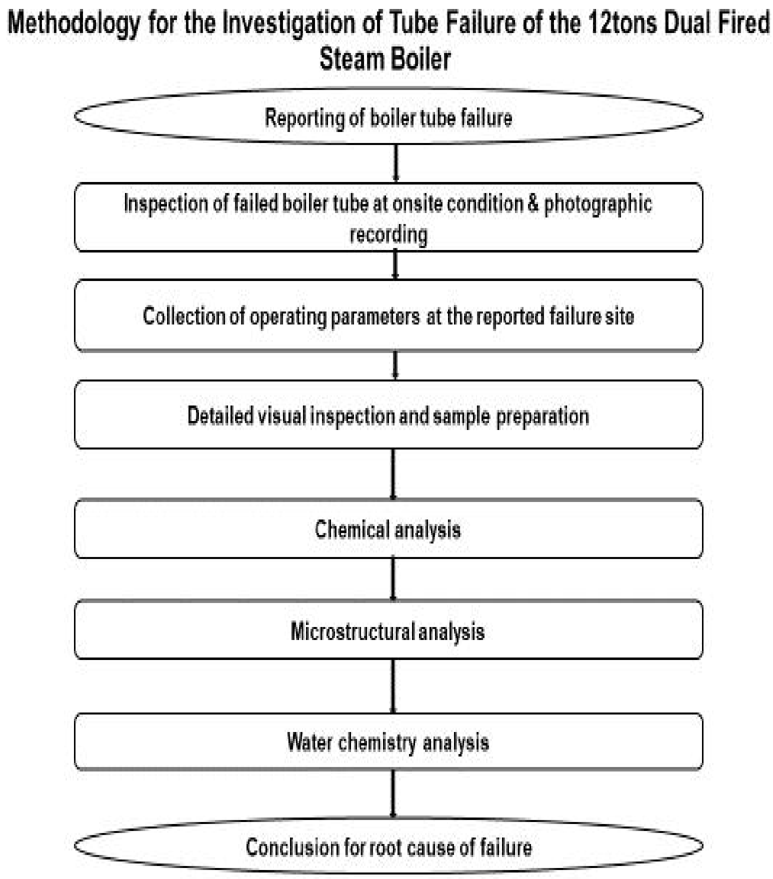

Figure 3.3: Methodology for Investigating the reoccurring tube failure in the 3rd pass

3.2.1 Preliminary Data Collection

The preliminary data collection phase involves gathering all relevant information to understand the context and progression of the boiler tube failures. In this instance, the industrial boiler encountered its initial tube failure two years after installation. Remedial action was taken by sealing off the four affected tubes, as illustrated in Figure 3.4

Table 3.2: Operating Conditions and failure data of Boiler

Fuel Used	Operating Conditions
Operating Pressure	10.54 bars
Operating Temperature	179.97^{o}C

Operation	Running continuously
Type of fluid media	Flue gas found inside tube, water found outside tube
Number of tube passes	Three
Tube size	50mm
Number of Tubes	170
Design boiler flow rate	12,000kg/h
Operation boiler flow rate	6000 kg/h -9000kg/h
Location of Failure	Leakage from the third-pass tubes
Number of blinded tubes	17
Sample Identification	Observed pin hole on area of failure

Despite this intervention, multiple tube failures leading to severe leakage were later detected. As a temporary measure, all thirteen (13) affected tubes were blinded. Significantly, the observed failures in both instances were located in the third pass of the boiler, with pinholes identified in the failure regions. The operational conditions and key failure data of the boiler are shown in Table 3.2

Figure 3.4: Four Physically Blocked Tubes in the 3rd Pass

The critical operating and material parameters were gathered from operational logs to facilitate the investigation of the boiler tube failures. The boiler's operational feed and drum water parameters were analyzed alongside pieces of the failed tube.

3.2.2 Visual Investigation

Visual examination was conducted to assess the conditions of the inner and outer surfaces of the boiler tube surfaces as well as its corrosion profile. This process involves a careful inspection and photographing areas of concern, with images zoomed and magnified to evaluate the extent of damage and impact on the tube.

Visual investigation was performed using both physical inspection and a digital camera to document the failure. This method is one of the most commonly employed in failure analysis elsewhere (Munda *et al.,* (2016); Hosseini and Yareiee (2019); Hanke (2012) where direct investigation is used for observing, comparing and documenting the conditions of the tubes and surrounding media of the boiler tubes. Afterwards, properties of the failed tube area and unfailed tube area were compared.

Major aspects of the visual examination conducted in this study included:

1. Comparison of Failed and Un-failed Areas

The condition of the failed tube areas was compared with the un-failed regions to identify patterns of damage or anomalies.

2. Photographic Documentation

High-resolution images of the failure sites and surrounding areas were captured to support detailed analysis.

3. Corrosion Profile Assessment

The extent and type of corrosion were evaluated visually to gather insights into the degradation mechanisms affecting the tubes.

3.2.3 Chemical Composition Analysis

The chemical composition of the failed boiler tube was analyzed to verify its compliance with the BS 3059 PART 1 GR 320 ERW material specification standard. This examination was carried out in the materials and metallurgical laboratory of African Steel Nigeria Limited, situated in Ikorodu, Lagos State.

Optical Emission Spectroscopy (OES) was employed to determine the elemental composition of the tube, with a focus on the region where failure occurred. The surface of a small portion of the failed boiler tube material is first polished and etched to remove any contaminants, the prepared sample is then mounted on the OES instrument's sample holder. The atoms on the polished surface were then excited by passing an electric charge through it, this was done using a spark in an argon filled environment. The excited atom emits light at a specific wavelength unique to each element, which a detector measures and correlates to the concentration of the particular elements in the sample. The results obtained were compared with a calibration curve developed using standard reference materials containing known elemental concentrations, in accordance with the accredited standards 8811-1998 (RA2018) and JIS G 1253-2013.

3.2.4 Microstructure Analysis

To investigate the potential causes of failure, including microstructural anomalies and material degradation, the surface morphology of the failed boiler tube was analysed in the materials and metallurgical laboratory of African Steel Nigeria Limited, located at Ikorodu, Lagos state.

Specimens were taken from the ruptured portion of the tube as well as from nearby affected portion for comparative analysis. Specimens for microstructural analysis were prepared following ASTM E3 standards. The preparation process involved:

1. Surface Preparation:

   Samples were polished using progressively finer grades of sandpaper to achieve a smooth surface.

2. Etching Process:

   The polished samples were etched with a nital solution of 1.5%, a nitric acid (HNO_3) mixture of 1–5% and an alcohol (CH_3OH) mixture of 95–99%. Etching revealed the microstructural features of the material.

3. Optical Microscopy: The microstructure of the specimen was analyzed under an optical microscope at 100× magnification to assess the material's grain structure, phase distribution, and possible inclusions.

3.2.5 Water Chemistry Analysis

Water chemistry analysis is a important aspect in boiler tube failure investigations, as improper water treatment is often a leading cause of degradation mechanisms like scaling, corrosion, and pitting. The process typically involves collecting and analyzing water samples to assess key chemical parameters and their impact on boiler operation.

The water chemistry tests were conducted in Seindo Limited, Ikeja, Lagos. Water samples were collected from the boiler at two different locations- feedwater inlet and boiler drum water. The collected water samples were then subjected to the following analytical tests and measurements:

1. pH Measurement: pH meters calibrated with standard solutions. To indicate the acidity or alkalinity of the water
2. Total Dissolved Solids (TDS): Gravimetric methods to determine TDS. High TDS can lead to scaling and deposit formation on tube surfaces
3. Conductivity Testing: Conductivity meters were employed to determine ionic concentration.
4. Titration: For parameters like alkalinity, hardness, and chloride content were adopted for titration
5. Spectrophotometry: For measuring silica, phosphate, and iron levels.

6. Dissolved Oxygen Analysis: Winkler titration or electrochemical sensors

3.3 Numerical Simulation of the 12ton Dual Fired Steam Boiler

Numerical simulation provides a useful tool for analysing and optimizing the performance of the 12-ton dual-fired steam boiler. This section presents the computational modelling techniques used to assess the boiler's thermodynamic behaviour and temperature distribution induced by scale formation especially in the area surrounding tube failure in the third pass of the fire tube. Two major simulation approaches were adopted in this study: combustion modelling using Aspen Plus and thermal flow and structural analysis using Computational Fluid Dynamics (CFD) and Finite Element Analysis (FEA).

Combustion analysis was carried out to evaluate the combustion process and characterize the properties of the resulting flue gas. In this study, the combustion analysis was carried out using the following steps:

1. Developing an approximate chemical equation that describes the firing process in the boiler
2. Select a thermodynamics equation of state to accurately predict the state of the fuel, air and combustion product
3. Collect both the thermodynamic and physical properties of the resulting combustion gas realized after the combustion analysis.

CFD analysis was carried out to investigate the area surrounding the tube failure to understand the intensity and heat localization which could cause the failure. In this study, CFD models were developed and simulated. The study included the following steps:

1. Development of appropriate CFD models to replicate features of the boiler tube in the 3rd pass.
2. Investigation of the thermal deformation, focusing on the effect of scale formation thickness and temperature distribution inside the boiler.

3. Study the thermal flow behaviour and heat transfer near the 3rd pass that could describe the reason for the failure.
4. Deduce from the CFD model, the root cause for the boiler tube failure.
5. Validation of the CFD results with the experimental result obtained from the investigation of the actual boiler failure.

3.3.1 Combustion Modelling

(a) Process simulation environment

The combustion analysis was carried out using Aspen Plus, a steady-state process simulation software used to model chemical processes. Aspen allows for rigorous thermodynamic and mass-energy balance modelling of chemical reactions.

(b) **Thermodynamic model selection**

The Peng-Robinson Equation of State (PR EOS) was selected as the property method to handle both the gas phase hydrocarbon flue and combustion products. The Peng-Robinson EOS is particularly suitable for the systems involving non-ideal gas behaviour, especially at elevated pressure and temperatures commonly associated with combustion.

The PR-EOS is expressed with equations (3.1) according to Ota *et al.* (2025) ; Xiong and Yang (2025).

$$P = \frac{RT}{V-b} - \frac{a\propto(T)}{V(V+b)+b(V-b)} \qquad (3.1)$$

Where P,T, V, R are the pressure (bar), temperature (°C), molar volume (K.mol), while ɑ and b are attraction and repulsive parameter, which are functions of critical pressure and temperature. The temperature dependent function for modifying the attraction parameter is expressed with equation (3.2) according to Xiong and Yang (2025) is given as;

$$\propto(T) = \left(1 + k\left(1 - \sqrt{\frac{T}{T_c}}\right)\right)^2 \qquad (3.2)$$

Where T_c and K are the critical temperature (K) and acentric factor respectively

(c) Reactor Setup

A R Stoic reactor block was used to simulate the combustion process. The R Stoic reactor calculates the product composition based on the user-defined reactions and stoichiometric coefficient, without requiring detailed reaction kinetics. For complete combustion, the following generalized reaction was defined in equation (3.3) according to

$$\left((1-a-b)C_xH_y + aCO_2 + bN_2\right) + \Lambda(0.21O_2 + 0.79N_2) \rightarrow mCO_2 + nH_2O + pN_2 + qO_2 \quad (3.3)$$

Where is Λ = mole ratio of air to fuel while a, b, m, n, p and q are the mole of respective element/compound and $(1-a-b)C_xH_y$ = the total hydrocarbon in the fuel.

(d) Reactor Output

After the reaction is defined, the material and energy balance, along with PR EOS is used to compute the stream properties of the combustion product. The adiabatic reactor's energy balance is expressed as with equation (3.4)

$$\sum\dot{n}_{in}\left(\widetilde{H}_{in} + \widetilde{U}_{in}\right) + \dot{Q} = \sum\dot{n}_{out}\left(\widetilde{H}_{out} + \widetilde{U}_{out}\right) \quad (3.4)$$

Where $in\ and\ out$ represents reactants and products while $\widetilde{H}\ and\ \widetilde{U}$ imply molar enthalpy (kJ/mol) and molar internal (kJ/mol) energy respectively

$\dot{Q}$ represent the added Work

Assumptions

1. Reactions were assumed to be instantaneous and complete.

2. The system was treated as adiabatic.

3. No pressure drop across the reactor was considered.

4. Nitrogen was treated as an inert component in the reaction.

Table 3.3: Mole Fraction and Composition of Fuel and Air Parameters

Mole Fraction and Fuel Composition & Air Parameters		
Fuel parameters	**Unit**	**Value**
Methane	Mole %	95.0518
Ethane	Mole %	2.8707
Propane	Mole %	0.9457
i-Butane	Mole %	0.1328
n-Butane	Mole %	0.1272
i-Pentane	Mole %	0.0257
n-Pentane	Mole %	0.0156
Hexane	Mole %	0.0158
Nitrogen	Mole %	0.5808
Carbon dioxide	Mole %	0.2339
Pressure	bar	24.54
Temperature	℃	40.4
Mole flow	*Kmol/s*	0.2
Air parameter		
O2	Mole %	0.21
N2	Mole %	0.79
pressure	bar	1.013
temperature	℃	27.5
Mole flow	*Kmol/s*	2.43

(e) Heat Transfer Analysis

The heat transfer analysis was conducted using Ansys fluent, a finite volume-based computational fluid dynamics (CFD) software. The general procedure used by ANSYS in analyzing the model is depicted in Figure 3.5

The procedures used for analysis are itemized below:

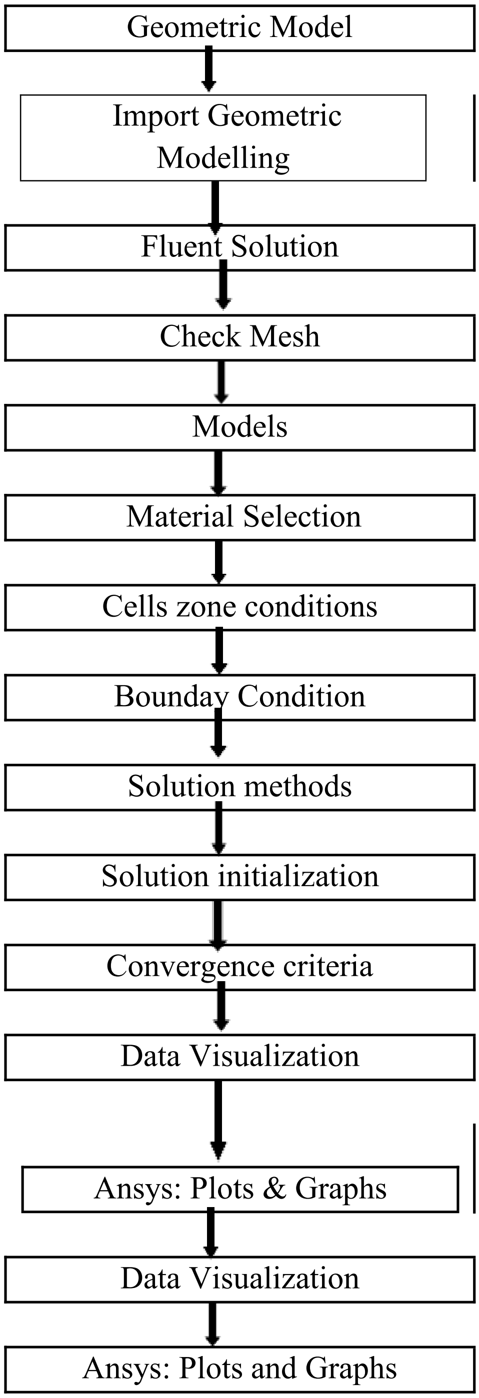

Figure 3.5: General Procedure Used in Ansys Fluent Analysis

(f) Geometrical Model

For the purpose of this CFD simulation, a representative section of the counter-flow, concentric tube heat exchanger within the boiler was modelled using Ansys Design Modeler.

The resulting geometric model, visualized in Figure 3.6 illustrates the three-Dimensional representation of this heat exchanger section.

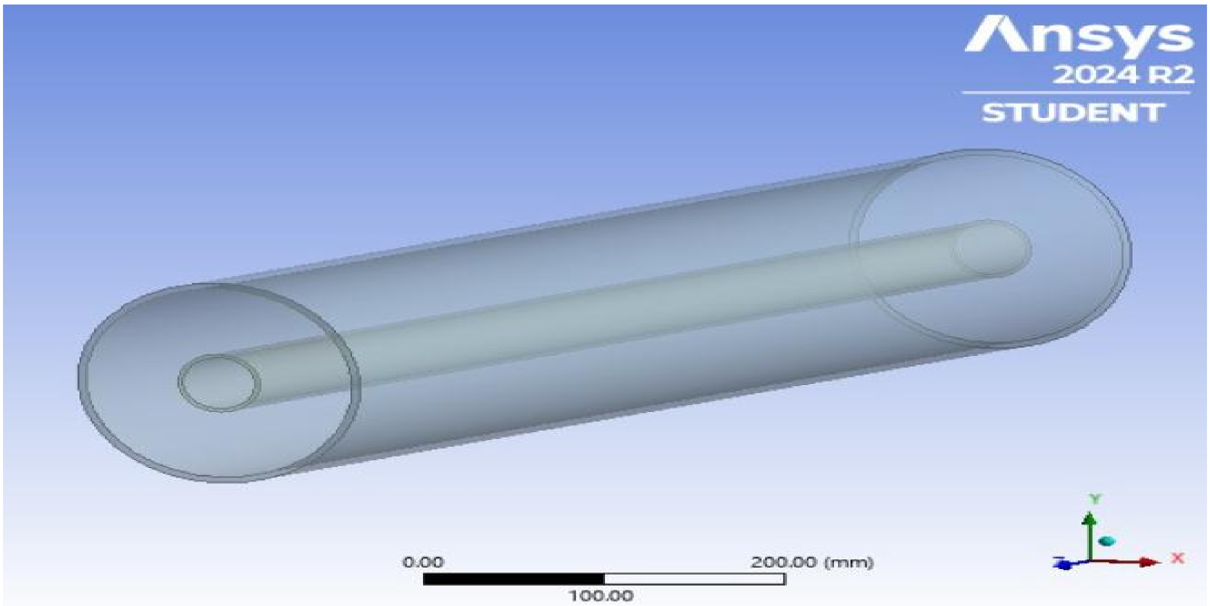

`Figure 3.6: Geometric model of the boiler tube in 3-D View

The geometry consists of two concentric circular tubes, clearly showing the inner tube through which the flue gas flows and the outer tube containing the counter-flowing water in the annular space. The inner tube has a diameter of 50mm and a thickness of 2.9mm, while the outer tube has a diameter of 169mm and a thickness of 5mm. The modeled length of the heat exchanger tube is 1000mm. The representative length is chosen to minimize the influence of inlet and outlet boundary conditions on the regions of interest, allowing for the development of hydrodynamically and thermally developed flow as shown in Figure 3.7.

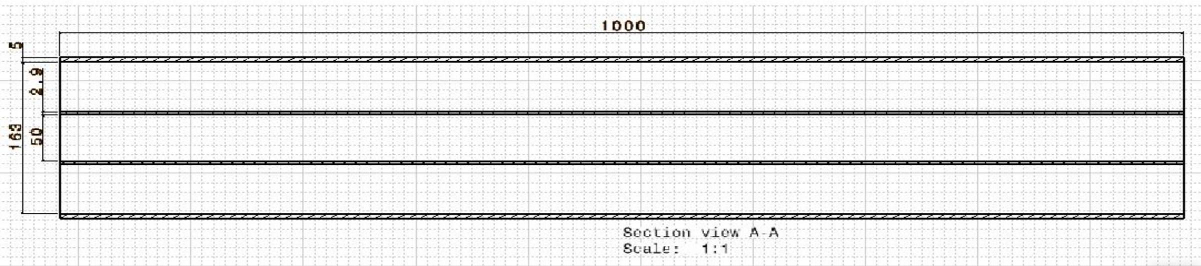

Figure 3.7: Geometric model of the boiler tube

Table 3.4: Geometric parameters of the modelled boiler

Geometry	Inner Diameter (mm)	Outer Diameter (mm)	Length (mm)
Boiler tube	50	52.9	1000
Boiler drum	169	174	1000

(g) Meshing

A fine structured mesh with regular tetrahedral elements was generated for the boiler using the standard settings in the Ansys Mechanical. The element size was varied to produce an equal mesh distribution across the entire geometry. The mesh was refined in the heat transfer boundaries and burner surfaces to allow for resolving of temperature and pressure gradients accurately. Different mesh counts in each domain/material were studied for the mesh sensitivity as seen in Table 3.4 while a mesh independence study was carrying out to ensure accuracy and reduce computational cost. Figure 3.6 shows the 3D image of the meshed boiler tube and drum. The combustion gas domain and water domain are also indicated during the meshing process. The inlet and outlet surface for each domain are also specified in the meshing process.

Table 3.5: Number of elements and nodes in each component of the boiler

Part	No of Elements	No of Nodes
Water	53,738	61,620
Scale	10,065	20,196
Pipe	232,637	105,848
Flue	86,088	92,637

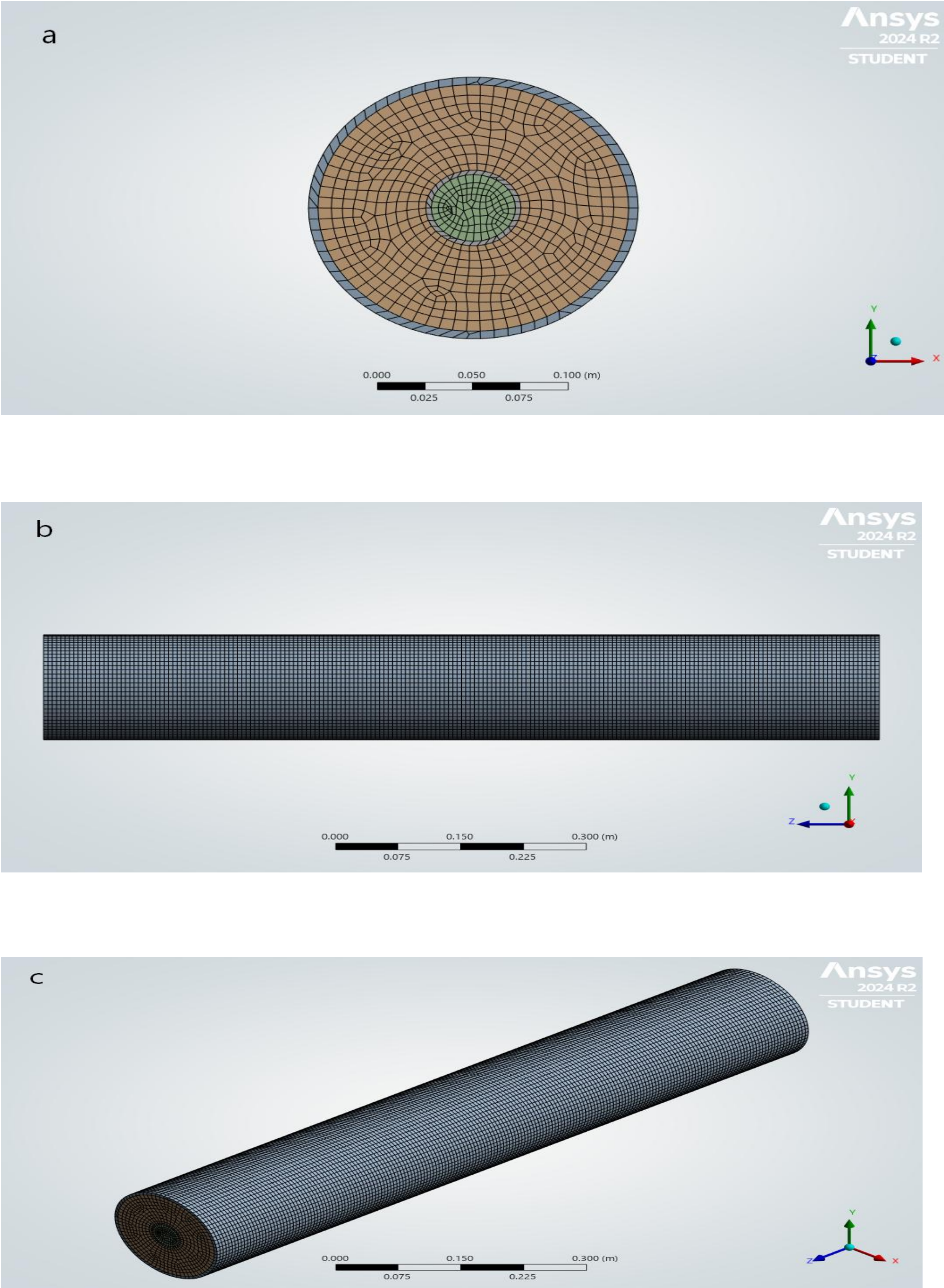

Figure 3.8: Different Views of Boiler Tube and Drum

(h) Numerical Methods

In Ansys fluent, the Reynolds-Average Navier-Stokes (RANS) equations for turbulent flow and heat transfer are represented by the continuity, momentum and energy equations, given in equation 3.5, 3.6, and 3.7, respectively. However, the del operator is expressed using equation 3.8

a. Continuity Equation

$$\frac{\partial \rho}{\partial t} + \nabla \cdot (\rho \vec{v}) = 0 \qquad (3.5)$$

b. Momentum Equation

$$\frac{\partial(\rho \vec{v})}{\partial t} + \nabla \cdot (\rho \vec{v}\vec{v}) = -\nabla \rho + \nabla \cdot \left[\mu_{eff}(\nabla \vec{v} + (\nabla \vec{v})^T)\right] + \rho \vec{g} \qquad (3.6)$$

c. Energy Equation

$$\frac{\partial(\rho E)}{\partial t} + \nabla \cdot \left(\vec{v}(\rho E + p)\right) = -\nabla \rho + \nabla \cdot \left(k_{eff} \nabla \mathrm{T} + \left(\tau_{eff} \cdot \vec{v}\right)\right) + S_h \qquad (3.7)$$

Where ρ, $\vec{v}$, t, and ∇ are the density of the fluid (g/m^3), velocity vector (m/s), time (s), gradient or del operator

$$\nabla = \vec{i}\frac{\partial}{\partial x} + \vec{j}\frac{\partial}{\partial y} + \vec{k}\frac{\partial}{\partial y} \qquad (3.8)$$

Where p, μ_{eff}, $(\nabla \vec{v})^T$, $\vec{g}$, E, k_{eff}, T, τ_{eff}, S_h are static pressure, effective viscosity, transpose of the velocity gradient, gravitational acceleration vector (m/s^2), total energy per unit mass (J/kg), effective thermal conductivity (W/m·K), temperature (K), effective stress tensor (includes turbulent contribution) and volumetric heat source (W/m^3) respectively. Where;

Effective viscosity (μ_{eff}) = μ + μ_t (molecular + turbulent viscosity)

Total energy per unit mass (E) = Internal energy + kinetic energy (J/kg)

(i) **Turbulence Modelling**

Turbulence was modelled using the standard k-ε turbulent model with scalable wall functions suitable for internal flows with moderate pressure gradients. Equations 3.9 and 3.10 represent the turbulent kinetic energy and dissipation rate. However, turbulent viscosity is expressed using energy equation 3.11.

1. Turbulent kinetic energy (k) equation:

$$\frac{\partial(\rho k)}{\partial t} + \nabla \cdot (\rho k\vec{v}) = \nabla \cdot \left[\left(\mu + \frac{\mu_t}{\sigma_k}\right) \nabla k\right] + G_\kappa - \rho\varepsilon \tag{3.9}$$

2. Turbulent dissipation rate (ε) equation:

$$\frac{\partial(\rho\epsilon)}{\partial t} + \nabla \cdot (\rho\epsilon\vec{v}) = \nabla \cdot \left[\left(\mu + \frac{\mu_t}{\sigma_\epsilon}\right) \nabla\epsilon\right] + C_{1\epsilon}\frac{\epsilon}{\kappa}G_\kappa - C_{2\epsilon}\rho\frac{\epsilon^2}{\kappa} \tag{3.10}$$

$$\mu_t = \rho C_\mu \frac{k^2}{\epsilon} \tag{3.11}$$

Where G_κ, σ_k, σ_ϵ, μ_t represents generation of turbulent kinetic energy due to the mean velocity gradients, turbulent Prandtl number for k, turbulent Prandtl number for ε, and turbulent viscosity respectively and C_μ, $C_{1\epsilon}$ *and* $C_{2\epsilon}$ are empirical constants.

(j) Material Selection

In the simulation study, careful material selection was essential to accurately replicate the real-world conditions within the 12-ton dual fire steam boiler. The following material were considered based on the operational environment and failure characteristics observed in the boiler system.

1. Boiler tube material: Steel was selected in conformity to the material analysis of the failed boiler tube. The selected steel material replicates the real-world characteristics of the failed boiler tube segment observed during the material analysis.
2. Scale formation: Calcium sulfate ($CaSO_4$) was chosen to model the scale layer found on the inner surface of the boiler tube.
3. Flue Gas Properties: the properties of the flue gas were imported from the Aspen plus combustion simulation. This ensured that gas composition, thermal conductivity, the specific-heat- capacity and the flow characteristics were consistent with the outputs from the model. The flue gas primarily consisted of CO_2, H_2O, N_2 and residual O_2.

4. Water properties: water, flowing on the shell side of the heat exchanger, was included in the simulation to represent the heat absorption process.

Model Assumptions

1. All material were assumed to be isotropic.
2. The thermal conductivity, the specific-heat-capacity and density of the material were considered constant and independent of temperature variation throughout the simulation domain.
3. It was assumed that none of the materials undergo phase change during the simulation.
4. Each material was considered homogenous, with no impurities or material gradient that could affect thermal or mechanical performance.
5. Ideal thermal contact was assumed between the layers.
6. No chemical reaction or further scale formation was assumed to occur during the simulation process.

Table 3.7: Parametric Properties for the different materials in the boiler

Parameter	Unit	Steel	Scale	Water	Flue Gas
Density	Kg/m^3	8030	2960	998.2	0.155212
Thermal conductivity	W/mK	50	0.5	0.6	0.169094
Specific heat	J/kgK	502.48	856	4182	1483.5
Viscosity	Kg/ms			0.001003	7.8806e-05

(k) Boundary Condition

In other to accurately simulate the thermal and fluid flow behaviour within the boiler tubes, appropriate boundary conditions were defined for both the flue gas and water domains. The boundary conditions specify the inlet parameters required for the numerical solution including mass flow rate, pressure and temperature. The values are carefully chosen based on data obtained from the process simulation environment and real boiler operation conditions.

Table 3.8: Boundary Inlet Conditions to the boiler

Parameter	Unit	Flue gas
Inlet mass flow	Kg/s	0.33
Inlet pressure	bar	1.013
Inlet temperature	K	1900

(l) Solution Method and Convergence Criteria

The system of discretized governing equations was solved iteratively using coupled scheme. This method simultaneously solves the momentum and continuity equations, which is particularly advantageous for problems involving strong pressure-velocity coupling and significant heat transfer effects, such as those encountered in this simulation.

Convergence of the numerical solution was monitored by observing the scaled residuals for each governing equation. The simulation was considered to have converged when all residuals fell below a specified tolerance value ensuring solution accuracy and numerical stability.

Table 3.9: Tolerance Value for Residuals in Governing Equation

Residual	Tolerance
Continuity	1×10^{-3}
Velocity	1×10^{-3}
Energy	1×10^{-6}
K	1×10^{-3}
Epsilon	1×10^{-3}

To further support solution stability and convergence, default under-relaxation factors were applied to the flow and thermal variables. These default values are typically robust for a wide range of fluid flow and heat transfer problems, and manual adjustments were deemed necessary during the simulation.

This setup provided a stable and efficient framework for solving the coupled thermal-fluid dynamics associated with the heat exchanger section of the steam boiler.

(m) Overview of Simulation Task

To comprehensively investigate the thermal behaviour and structural implications of scaling in boiler tubes, the following simulation analyses were conducted.

1. **Parametric study and optimization of water flow rate**

An initial parametric sweep was performed to determine the water mass flow rate that would yield an outlet temperature matching the operational condition of the reference boiler (473.05 K). The water mass flow was varied between 0.2 to 1.0 kg/s and the resulting outlet temperature were analyzed. From this, a narrow region was identified for further optimization, using smaller step sizes to pinpoint the precise flow rate needed to achieve the target temperature. This step established the baseline flow rate for the water side under no-scale condition.

2. **Effect of Scale Thickness on Outlet Temperatures and Its Implication on Tube Failure**

Simulations were performed with internal scale layer of varying thickness (0.5 to 3.5 mm), in 0.5 increment. For each case, the outlet temperature of both the water and the flue gas were monitored. This allowed an assessment of how scale acts as an insulating barrier, trapping thermal energy on the gas side and reducing heat transfer to the water.

3. **Effect of flue gas flow rate on water outlet temperature in scaled tube**

To assess whether increasing the flue gas flow rate could compensate for the heat transfer losses caused by scaling. The flue gas mass flow rate was varied extensively from 0.33 kg/s to 33 kg/s. This was tested for various scale thicknesses to evaluate the extent to which higher energy input can restore the desired outlet water temperature.

3.4 Combustion and Emission Analysis of 12-Ton Dual-Fuel Steam Boiler

To evaluate the combustion efficiency of the steam boiler under its current operating conditions and to ensure complete combustion while minimising emissions, a comprehensive combustion performance and the emission characteristics of the boiler was carried out.

The boiler combustion characteristics was obtained from the flue gas pot at the tail end of the boiler chimney using the combustion manager. Emission data for the natural gas firing of the boiler is captured using a flue gas emission analyzer, Enerac 700 model, which provides an in-situ result of the flue gas analysis. The boiler parameter and specification of the gas analyzer is used in this study is presented in Table 3.10 and 3.11 respectively.

3.4.1a The Combustion Manager

The boiler relies on a combustion manager to regulate key operational parameters such as ignition, burner firing rate, fuel and air supply, exhaust draft, water temperature, and steam pressure. This system ensures safe, efficient, and consistent production of steam or hot water.

The combustion manager automates the burner firing sequences (on/off, high/low/off, and modulation), adjusts fuel and air input rates, and incorporates essential safety controls such as high/low pressure, flame safeguards, and water level regulation. Additionally, it maintains steam pressure by modulating heating elements based on upper and lower set limits. A pressure switch triggers power supply to the heating elements depending on pressure deviations.

Safety features also include:

i. Transparent water level gauges for monitoring water levels.

Ii. Stop valves and air vents to manage air accumulation or vacuum formation during boiler startup and shutdown.

3.4.1b Flue Gas Analyzer (ENERAC 700 Model)

The ENERAC 700 is a portable flue gas analyzer used for in-situ measurement of exhaust gases at the boiler's chimney. The analyzer determines several key combustion parameters:

i. Oxygen (O_2): Ideally, 2.0–3.0% for natural gas and 3.0–3.5% for diesel combustion.

ii. Carbon Monoxide (CO): Indicates incomplete combustion.

iii. Carbon Dioxide (CO_2): A calculated value based on fuel type.

iv. Flue Gas Temperature

v. Ambient Temperature

vi. NO_x ($NO + NO_2$) levels in ppm

vii. Combustion Efficiency (%)

viii. Excess Air (%)

These values are automatically calculated and displayed by the analyzer based on sensor readings as shown in Table 3.10, While the specifications for the boiler and the burner are displayed in Table 3.11.

Table 3.10: Specification for dual-fired boiler and burner

Parameter	Value
Boiler Make	Thermax Limited
Max Operating Pressure	10.54 bar
Boiler Capacity	12 TPH (12,000 kg/hr at F&A 100°C)
Burner Make	Weishaupt (Germany)
Burner Model	WM-GL50/2-A, M-R-NR
Burner Serial Number	40449245
Fuel Type	Natural Gas / Diesel

Table 3.11: Specification for enerac 700 model flue gas analyzer

Parameter	Range	Resolution	Accuracy
Combustion Efficiency (%)	0 – 100	0.1	±1%
CO_2 (%)	0 – 20	1.0	±1%
CO (ppm)	0 – 1500/4500	1.0	±1%
O_2 (%)	0 – 25	0.1	±0.2%M
NO_2 (ppm)	0 – 500/1500	0.1	±2%M
SO_2 (ppm)	0 – 1500/4500	1.0	±2%M
Stack Temp (°C)	0 – 1100	1.0	±2%FM
Ambient Temp (°C)	0 – 65	1.0	±2%FM
Excess Air (%)	0 – 1000	1.0	±0.2%

3.4.2 Experimental Setup for Combustion Analysis

The combustion performance tests were conducted on the 12-ton dual-fired steam boiler equipped with a Weishaupt RGMS70/1-B burner. The flue gas was sampled at a designated port between the boiler and the chimney. Different loading rates on the burner were investigated by varying the fuel flow rate and air excess

The values for the combustion parameters shown in Table 3.12 for the 12,000 kg/hr steam boiler were obtained by varying the boiler loading rate at different test points ranging from set point 1 to set point 10, with corresponding boiler load at 14% for set point 1 down to 100% for set point 10 in the combustion manager.

This controls the boiler combustion with its respective emissions at the different loading rate. The fuel flow rate automatically adjusts in response to the load percentage. Simultaneously, the air damper opens proportionally to meet the combustion air requirements at varying load conditions. The auxiliary actuator modulates accordingly to extend the flame travel within the combustion chamber. As the load increases, corresponding changes occur in the fuel flow rate (measured in standard cubic meters, scm), air damper position, and auxiliary actuator position. These adjustments collectively result in a more intense combustion flame. Additionally, the variable frequency drive (VFD) regulates the speed of the motor driving the forced draught (F.D) fan, ensuring that the air supply aligns with the fuel flow rate and the system's loading rate.

Table 3.12: 12-tons steam boiler combustion parameters with natural gas firing

Set Points	**1**	**2**	**3**	**4**	**5**	**6**	**7**	**8**	**9**	**10**
Load (%)	14	20	30	40	50	60	70	80	90	100
Fuel Flow Rate (scm)	12	16	20	25	28	32	36	42	46	52
Air Damper (%)	14	22	28	37	42	49	55	74	86	90
Auxiliary Actuator (°)	6	16	25	33	37	45	50	67	82	89
Variable Frequency Drive (%)	50	56	60	65	70	75	80	85	90	95

3.4.3 Experimental Setup for Emission Analysis

The flue gas emission sampling was performed at the sampling port located between the boiler and the chimney (stack). The in-situ measurement of gaseous emissions was carried out using a portable gas analyzer (enerac model 700 installed at the flue gas exhaust port.

The flue gas analyzer was used to evaluate the characteristics of exhaust gases exiting the combustion system. The key combustion parameters determined include the following:

1. **Oxygen (O_2)**:

   The oxygen content in the flue gas is measured using an in-built oxygen sensor in the analyzer, which is factory-calibrated with 21% oxygen. For natural gas combustion, the typical oxygen concentration in the exhaust should range between 2.0% and 3.0%.

2. **Carbon Monoxide (CO)**:

   Carbon monoxide, an indicator of incomplete combustion, is detected by the CO sensor integrated into the analyzer.

3. **Carbon Dioxide (CO_2)**:

   The CO_2 concentration is not directly measured but is a calculated value based on the fuel type and the measured O_2 concentration.

4. **Flue Gas and Ambient Temperature**:

   Both the flue gas temperature and the ambient (atmospheric) temperature are measured directly by the analyzer's temperature probes.

5. **Other Calculated Parameters**:

   The analyzer also computes and displays the following values based on real-time sensor data:

   i. Nitrogen oxides (NO_x), given as the combined concentration of NO and NO_2 in parts per million (ppm)
   ii. Carbon dioxide concentration (CO_2 %)
   iii. Oxygen concentration (O_2 %)
   iv. Combustion efficiency (% Efficiency)
   v. Flue gas temperature (°C)
   vi. Excess air percentage (% Excess Air)

These parameters are critical for assessing combustion performance, energy efficiency, and emissions compliance at any given operating condition.

3.5 Combustion Control Optimization in 12-tons dual-fuel boiler : Minitab-18 and Taguchi Method

This section investigates the optimal combination of combustion control parameters for a 12-ton dual-fired steam boiler operating on natural gas. Efficient combustion is critical, as even minor deviations from the ideal air-fuel ratio can lead to increased fuel consumption and environmental harm. Insufficient air results in incomplete combustion and increased carbon monoxide (CO) emissions, while excess air leads to energy losses. Therefore, maintaining the proper air-fuel ratio is essential to optimize performance and reduce emissions. This study applies a statistical design of experiment (DOE) approach using the Taguchi method to determine the optimal parametric settings for a 12-ton dual-fired boiler operating with natural gas aimed at maximizing combustion efficiency.

Key combustion input parameters include:

i. Load (%) – percentage of maximum boiler load

ii. Fuel flow (s.c.m) – standard cubic meters of gas consumed

iii. Air flow (%) – volume of combustion air supplied

iv. VFD (%) – percentage setting of the Variable Frequency Drive (VFD) controlling the forced draft fan

3.5.1 Experimental Procedure

Prior to each run, the gas line was purged to remove dust and debris. The gas pressure was regulated as follows to achieve inlet pressure of 2.9 bar, with a corresponding outlet pressure set at 105 mBar, while the low gas solenoid shut-off pressure, high gas shut-off pressure, and the minimum combustion air pressure switch was set at 50mBar, 150mBar and 10mBar respectively.

The boiler was tested at three load levels: 30%, 60%, and 100%. At each level, fuel consumption, air supply, and VFD speed were measured. Data from these runs were recorded and used to assess parameter impacts.

3.5.2 Taguchi Experimental Design

The design of experiment approach was a 27-run L27 orthogonal array using the Taguchi method. It was employed to systematically analyze the effects of four key parameters:

A: Load (%)

B: Fuel Flow Rate (scm)

C: Air Supply (%)

D: VFD (%)

The signal-to-noise (S/N) model adopted in this study was the "Smaller-the-Better" type, aimed at minimizing combustion inefficiency and emission levels.

(a) Selection of Process Parameters

Four control factors were selected for optimization, each with three levels, as shown in Table 3.14

Table 3.13: Experimental Design for Boiler Burner Under Gas Firing

Code	Factor	Unit	Level 1	Level 2	Level 3
A	Load	%	30	60	100
B	Fuel	s.c.m	20	32	52
C	Air	%	28	49	90
D	Variable Frequency Drive position	%	60	75	95

(b) Experimental Layout

The experimental runs were designed using Minitab-18 software based on the L27 orthogonal array, resulting in 27 combinations. The coded experimental matrix is shown in Table 3.15.

3.5.3 Signal-to-Noise (S/N) Ratio Analysis

The S/N ratio was calculated using the "smaller-is-better" criterion to minimize inefficiencies. The formula used is:

$$S/_N = -10\ log_{10}\left(\frac{1}{n}\sum_{i=1}^{n} y_i^2\right) \qquad (3.11)$$

Where y_i is the observed output, and n is the number of observations. The computations were performed using Microsoft Excel

Table 3.14: Coded L27 Orthogonal Array

Run of Experiment	A	B	C	D
1	1	1	1	1
2	1	1	1	1
3	1	1	1	1
4	3	2	1	3
5	3	2	1	3
6	3	2	1	3
7	2	1	2	3
8	2	1	2	3
9	2	1	2	3
10	3	1	3	2
11	3	1	3	2
12	3	1	3	2
13	1	2	2	2
14	1	2	2	2
15	1	2	2	2
16	2	2	3	1
17	2	2	3	1
18	2	2	3	1
19	2	3	1	2
20	2	3	1	2
21	2	3	1	2
22	3	3	2	1
23	3	3	2	1
24	3	3	2	1
25	1	3	3	3
26	1	3	3	3
27	1	3	3	3

Table 3.15: Table: Transformed Parameters (Real Values)

Load (%)	Fuel (s.c.m)	Air (%)	VFD (%)
30	20	28	60
30	20	28	60
30	20	28	60
30	32	49	75
30	32	49	75
30	32	49	75
30	52	90	95
30	52	90	95
30	52	90	95
60	20	49	95
60	20	49	95
60	20	49	95
60	32	90	60
60	32	90	60
60	32	90	60
60	52	28	75
60	52	28	75
60	52	28	75
100	20	90	75
100	20	90	75
100	20	90	75
100	32	28	95
100	32	28	95
100	32	28	95
100	52	49	60
100	52	49	60
100	52	49	60

CHAPTER FOUR

RESULTS AND DISCUSSION

This chapter, presents the results of the boiler tube failure analysis conducted on a 12-ton dual-fired boiler, along with results from both experimental investigations and computational fluid dynamics (CFD) simulations.

4.1 Failure Investigation of the Boiler Tube

Below are the investigation report:

4.1.1 Analysis of Chemical Composition

Chemical composition analysis was conducted in accordance with the accredited standards 8811-1998 (RA2018) and JIS G 1253-2013. Spectrometric evaluation confirmed that the boiler tube material was carbon steel, meeting the chemical requirements specified in BS 3059 Part 1 Grade 320 ERW. A compilation of the results is highlighted in Table 4.1.The results indicate that the chemical composition of the failed boiler tube falls within the acceptable range specified by the relevant standard, confirming that material selection did not contribute to the failure.

Table 4.1: Chemical Composition of the Failed Boiler Tube (% wt.)

Sn	Element	Result (%)	Specification (BS 3059 Gr 320)	Remark
1	Carbon	0.01	Max 0.16	Satisfactory
2	Sulphur	0.004	Max 0.04	Satisfactory
3	Phosphorus	0.012	Max 0.04	Satisfactory
4	Silicon	0.14	Max 0.35	Satisfactory
5	Manganese	0.49	0.30–0.70	Satisfactory

4.1.2 Microstructural Analysis

Microstructural evaluation was carried out at 100X magnification. The unaffected (reference) tube sections displayed a typical normalized ferrite-pearlite microstructure, as shown in Figures 4.7 and 4.8. In contrast, Figure 4.9 shows the affected region (~400 mm before rupture), with more prominent pearlite grains and visible precipitation—evidence of elevated thermal exposure. Further micrographs revealed additional degradation mechanisms as seen in Figures 4.3 and 4.5

4.1.3 Visual Inspection

A physical check of the boiler revealed a rupture on the third-pass tube, as shown in Figure 4.1. Closer visual examination highlighted multiple pinholes around the rupture area. Additionally, particulate matter was found deposited along the path of the flue gas, on the water and also the fire sides of the tube.

Figure 4.1: Blocked boiler tubes in the third pass.

Further examination revealed significant pitting corrosion on the outer diameter (OD) and inner diameter (ID) of other tube sections, as illustrated in Figures 4.2 to 4.4. Scale formation was also observed on the tube's external surface (Figures 4.5 and 4.6)

Figure 4.2: Pitting Corrosion in the OD of tube

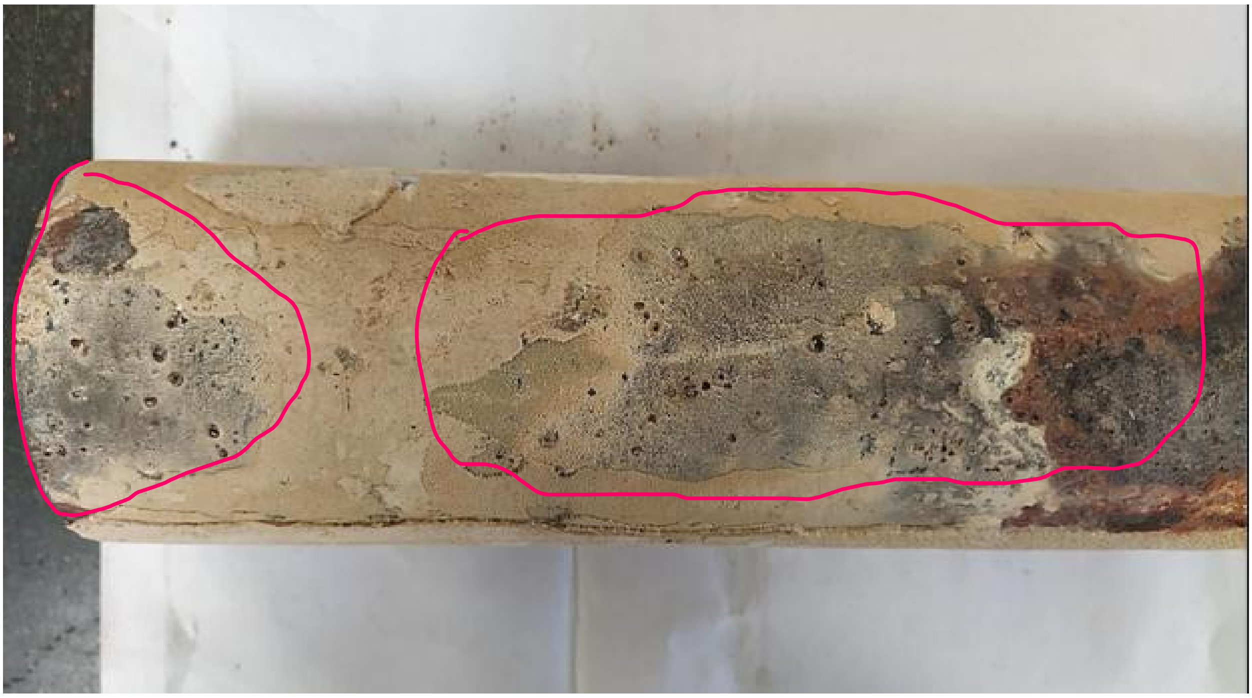

Figure 4.3: Longitudinal sample showing pitting corrosion along the OD

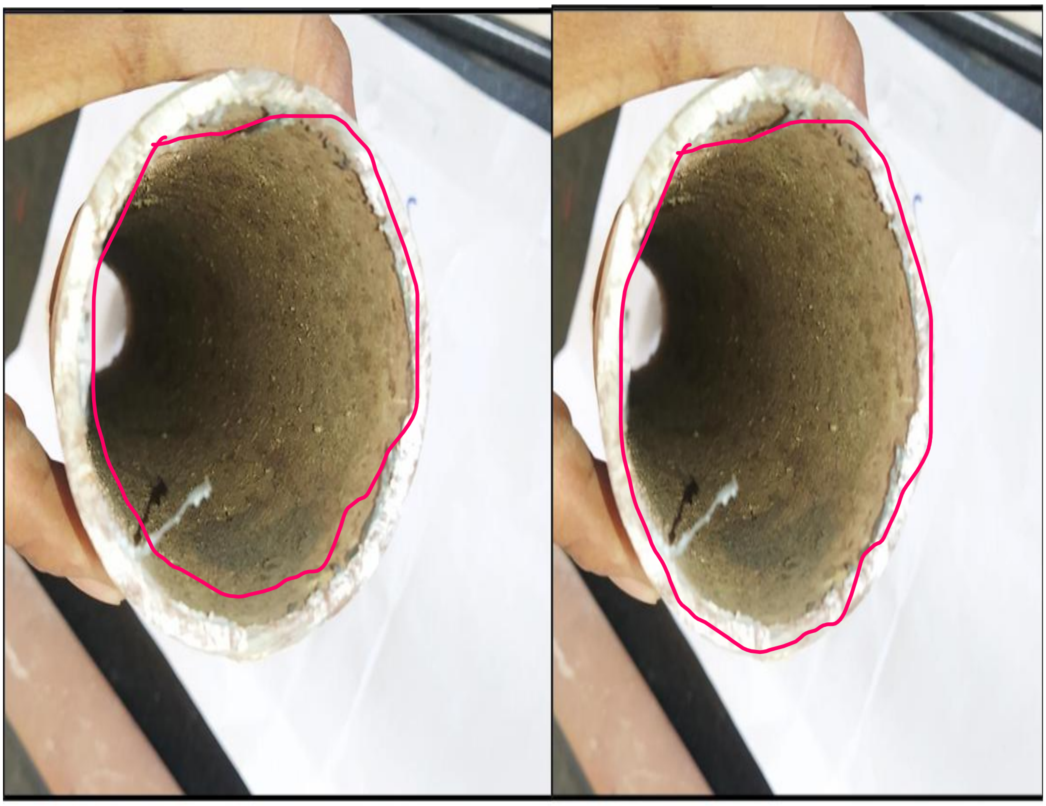

Figure 4.4: Pitting corrosion observed on the inner diameter (ID) of the boiler tube.

Figure 4.5: Layered deposits observed on the boiler tube surface.

Figure 4.6: Fractured Sample collected for further analysis

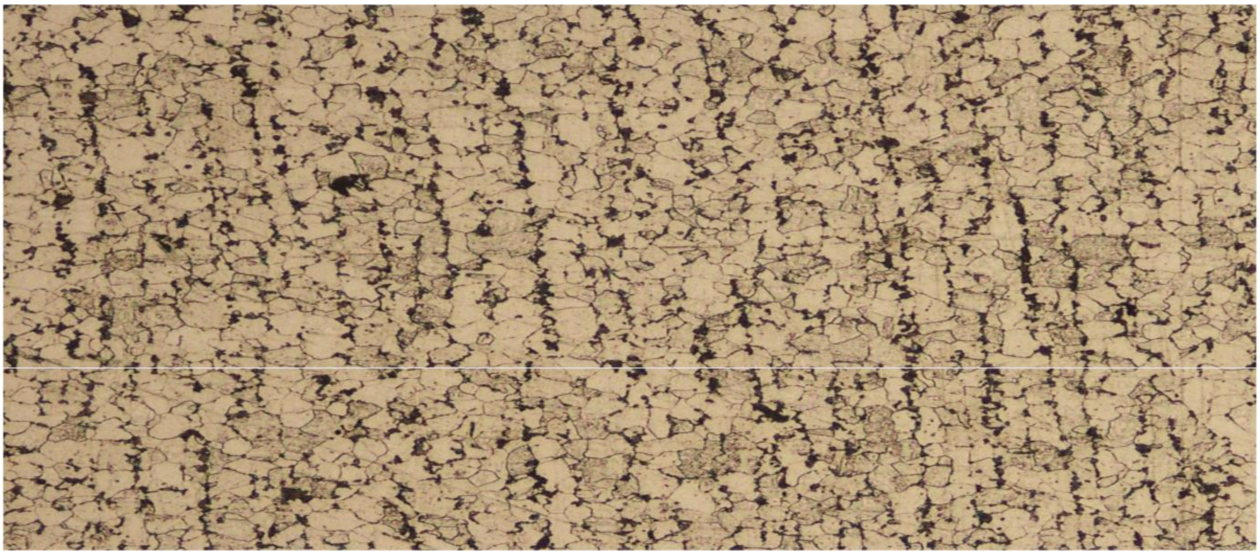

Figure 4.7. Microstructure of referenced tube - Normalize ferrite + Pearlite structure observed

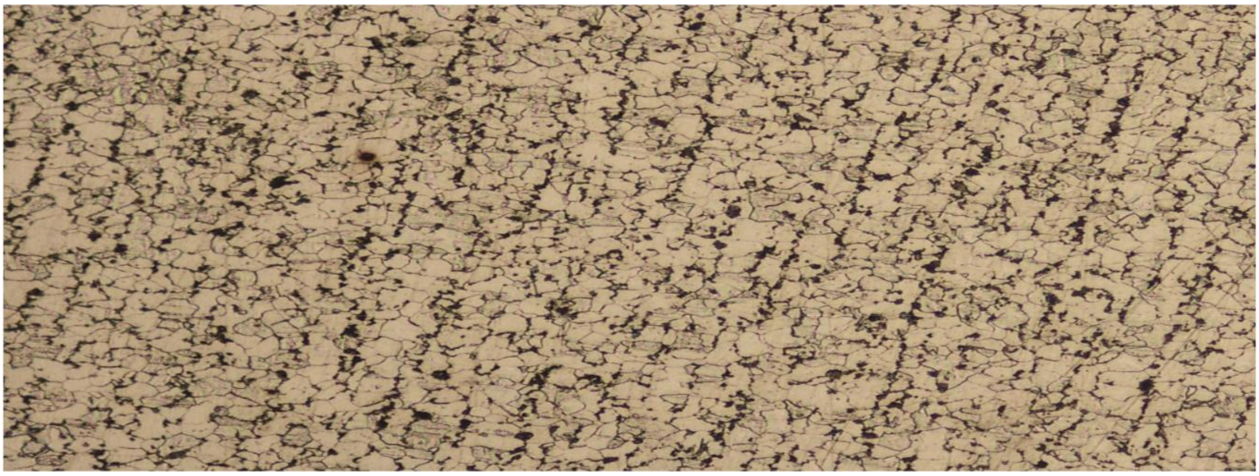

Figure 4.8. Referenced tube with minor precipitation – Indicative of slight thermal exposure

Figure 4.9: Pitting corrosion on the OD of the affected area.

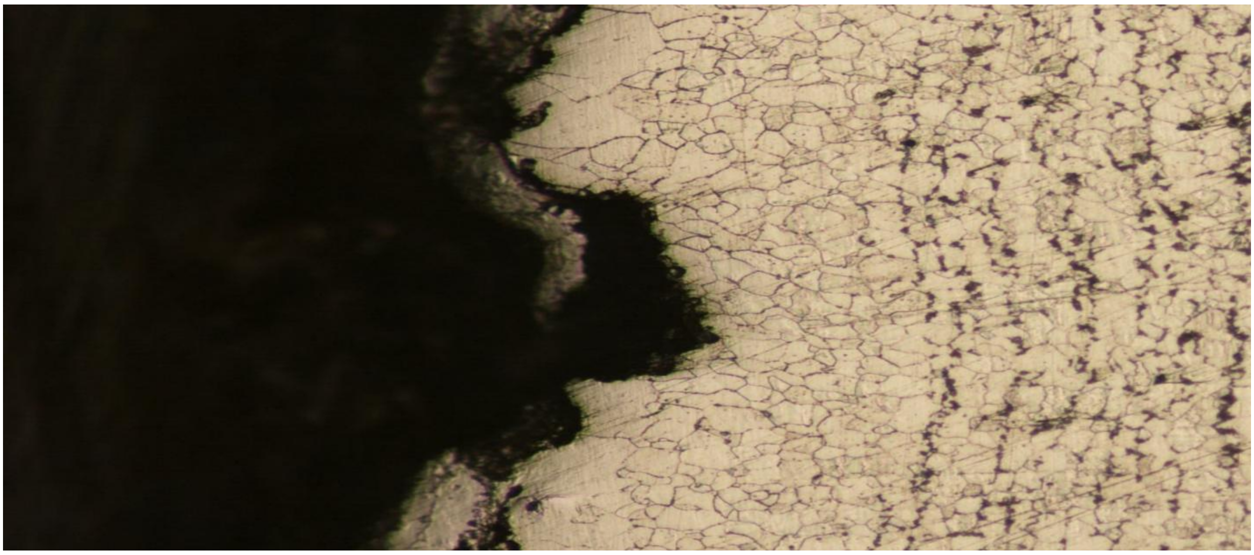

Figure 4.10: Decarburization and oxidation observed on the ID.

Microstructural analysis confirmed thermal degradation of the tube, including decarburization, grain growth, and oxidation at the ID, along with pitting corrosion at the OD. These findings support the conclusion that the failure was thermally induced and aggravated by water-side corrosion.

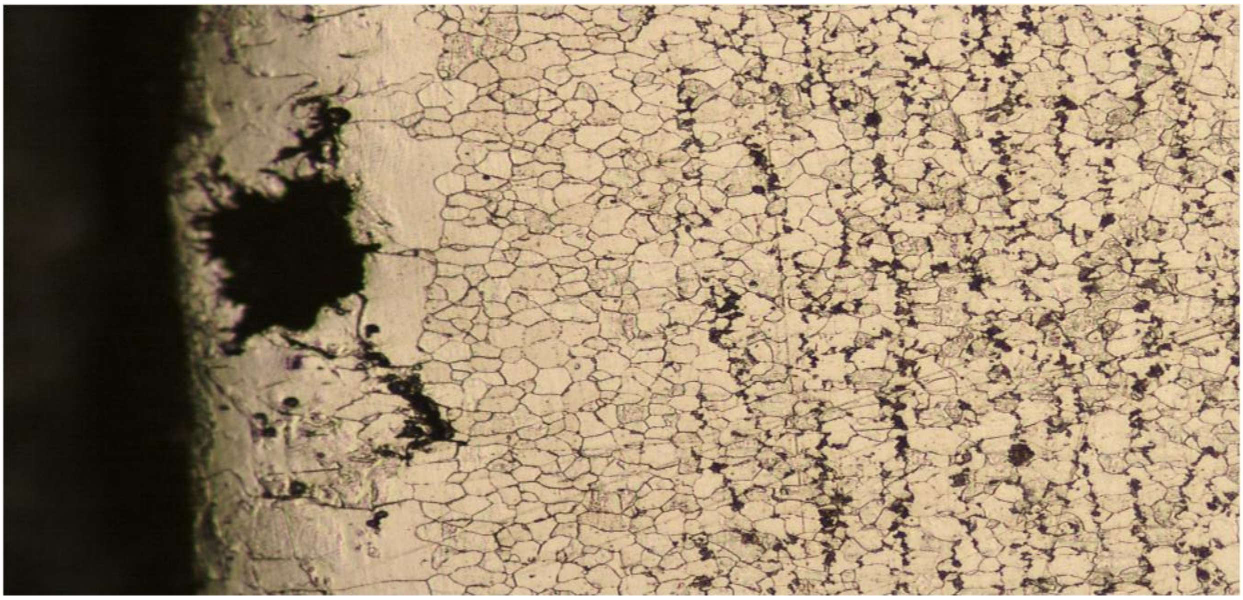

Figure 4.11: Evidence of thermal oxidation on the tube ID.

4.1.4 Water Chemistry Analysis

Both feedwater and boiler drum water were analyzed to assess their compliance with standard water quality parameters. The results, are presented in Tables 4.2 and 4.3.The analysis revealed excessive levels of total dissolved solids (TDS), P-alkalinity, silica and chloride in the boiler drum water—well above the acceptable limits. These elevated concentrations promote deposition, localized overheating and scaling, which likely contributed to tube failure. Feedwater quality also showed suboptimal silica and phosphate concentrations, further supporting this conclusion.

Table 4.2: Feedwater Quality Compared with Standards

Comparison of Feed Water with Specification			
Parameter	**Measured Value**	**Standard Range**	**Evaluation**
Ph	8.21	8.0-9.5	Acceptable
Total Dissolved Solids	127 ppm	75-85 ppm (Max)	Not Acceptable
Total Hardness	5 ppm	< 5 ppm	Acceptable
Chloride	40 ppm	< 150 ppm	Acceptable
Phosphate	15 ppm	20-40 ppm	Not Acceptable
Silica	15 ppm	< 5 ppm	Not Acceptable

Table 4.3: Boiler Drum Water Quality Compared with Standards

Parameter	**Measured Value**	**Standard Limit**	**Evaluation**
pH	11.26	10.5-11.5	Acceptable
Total Solids Dissolved	6855	3500 (Max)	Not-Acceptable
Total Hardness	3	< 5	Acceptable
P-Alkalinity	590	350 (Max)	Not-Acceptable
M-Alkalinity	420	700 (Max)	Acceptable
Sulphite	30	30-40	Acceptable
Chloride	273	<150	Not-Acceptable
Phosphate	25	20-40	Acceptable
Silica	15	5	Not-Acceptable

4.2 Simulated Combustion Analysis Results

The combustion simulation produced key thermophysical properties of the resulting flue gas stream, as summarized in Table 4.4. The gas exhibited a high temperature approximately equal to 1864 °C and a pressure of 1.013 bar, characteristic of an intense exothermic reaction. This is further substantiated by the negative enthalpy flow rate of -16.18 MW, which underscores the significant release of thermal energy during combustion.

The gas density was found to be 0.158 kg/m^3, while its thermal conductivity was relatively low at 0.167 W/m-K, indicating poor heat conduction. The dynamic viscosity was measured at 7.81×10^{-5} $N \cdot s/m^2$, and specific heat capacity was 1.475 kJ/kg-K. These properties suggest a combustion gas mixture that, while energetically rich, is limited in its ability to transfer heat conductively.

A stoichiometric combustion reaction was confirmed by the mole fractions of the gas constituents. Oxygen was nearly depleted, with a residual mole fraction of just 0.00018, indicating near-complete combustion. The mole fractions of the remaining major components are detailed in Table 4.4.

Table 4.4: Thermophysical Properties of the Combustion Gases

	Combustion Gas	
Parameter	**Unit**	**Value**
Temperature	C	1864.39079
Pressure	bar	1.013
Enthalpy Flow	kW	-16181.4325
Mass Density	kg/m^3	0.15836558
Thermal Conductivity	kW/m-K	0.00016661
Viscosity	N-sec/sqm	7.8053E-05
Mass Heat Capacity	kJ/kg-K	1.4754792
	Mole Fractions	
O_2	0.00018	
N_2	0.74702	
H_2O	0.16709	
CO	0.08524	

4.3 Parametric Study for Water Flow Rate Determination

A key aspect of the thermal performance assessment was determining the optimal water mass flow rate to achieve a target outlet temperature of 473.05 K, aligning with real boiler operating conditions. This was approached through a two-step methodology: a broad parametric study followed by a targeted optimization.

4.3.1 Parametric Study

In this initial phase, water mass flow rates were varied systematically, and the corresponding outlet temperatures were recorded. The results, highlighted in Table 4.5 and Figure 4.12, reveal an inverse relationship between the mass-flow-rate and outlet temperature.

At higher flow rates (e.g., 1.0 kg/s), the short residence time of water within the heat exchanger resulted in lower heat absorption and cooler outlet temperatures. Conversely, lower flow rates (e.g., 0.2 kg/s) allowed longer heat exchange durations, resulting in higher outlet temperatures.

Table 4.5: Parametric Study Results

Water Mass Flow (kg/s)	Outlet Temperature (K)
1.0	428.37
0.8	434.07
0.6	442.93
0.4	458.15
0.2	493.33

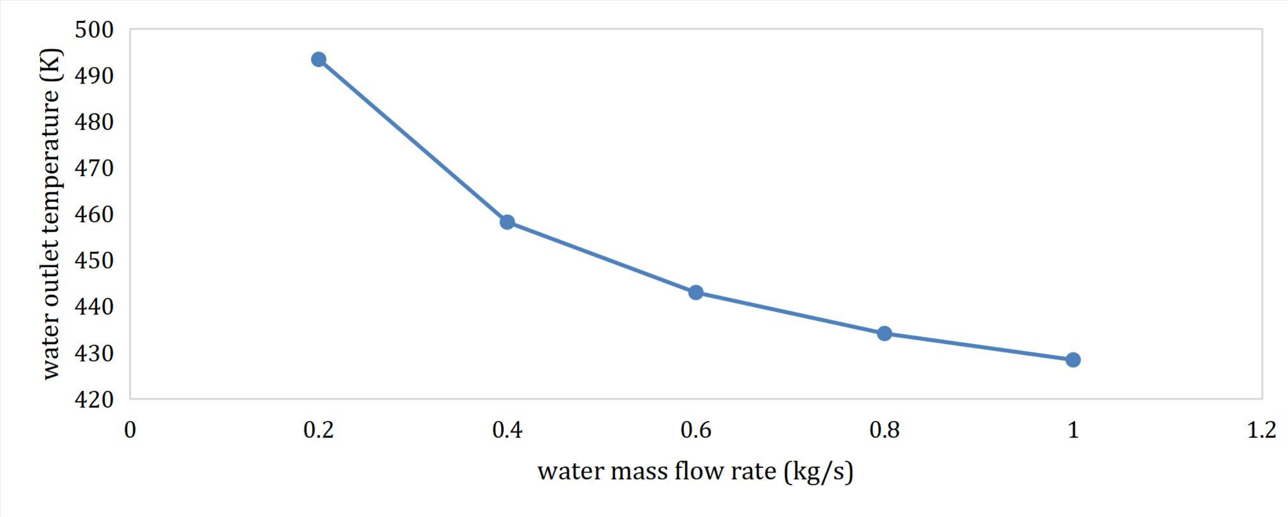

Figure 4.12: Water mass flow vs outlet temperature with (no scaling)

4.3.2 Optimization Study

To narrow down the optimal flow rate, additional simulations were conducted with intermediate values between 0.4 and 0.6 kg/s. The objective was to identify the value that most closely matched the desired outlet temperature of 473.05 K. The optimization results are highlighted in Table .4.3 and Figure 4.12 The optimal flow rate was determined to be approximately 0.454 kg/s, which yielded an outlet temperature closest to the target, within acceptable engineering tolerance.

Table 4.3.: Optimization Results for Water Mass Flow vs Outlet temperature

Water Mass Flow (kg/s)	Outlet Temperature (K)
0.5	449.36
0.58	444.08
0.42	456.14
0.54	446.57
0.46	452.52
0.453895	**453.04**

4.4 Effect of Scale Thickness on Outlet Temperature and Tube Integrity

Simulations conducted in ANSYS FLUENT revealed a strong correlation between scale thickness on boiler tubes and thermal performance degradation. In the scale-free condition (0 mm) as seen in Figure 4.13 and 4.14 for natural gas and diesel firing respectively, water outlet temperature was 454.74 K, and the flue gas exited at 1922.97 K for natural gas and and water outlet temperature and flue outlet temperature of 453.15 K and 1959.73 K for This indicates that a significant portion of the flue gas's thermal energy was successfully transferred to the water, thereby achieving effective heat exchange. However, from Figure 4.15 and 4.16, even a minimal scale thickness of 0.5 mm significantly disrupted this balance, lowering the water outlet temperature to 431.74 K and increasing the flue gas outlet temperature to 2014.31 K. This 23 K drop in water temperature for natural gas and a 16K drop for diesel highlighting the insulating effect of the scale layer, predominantly composed of $CaSO_4$.

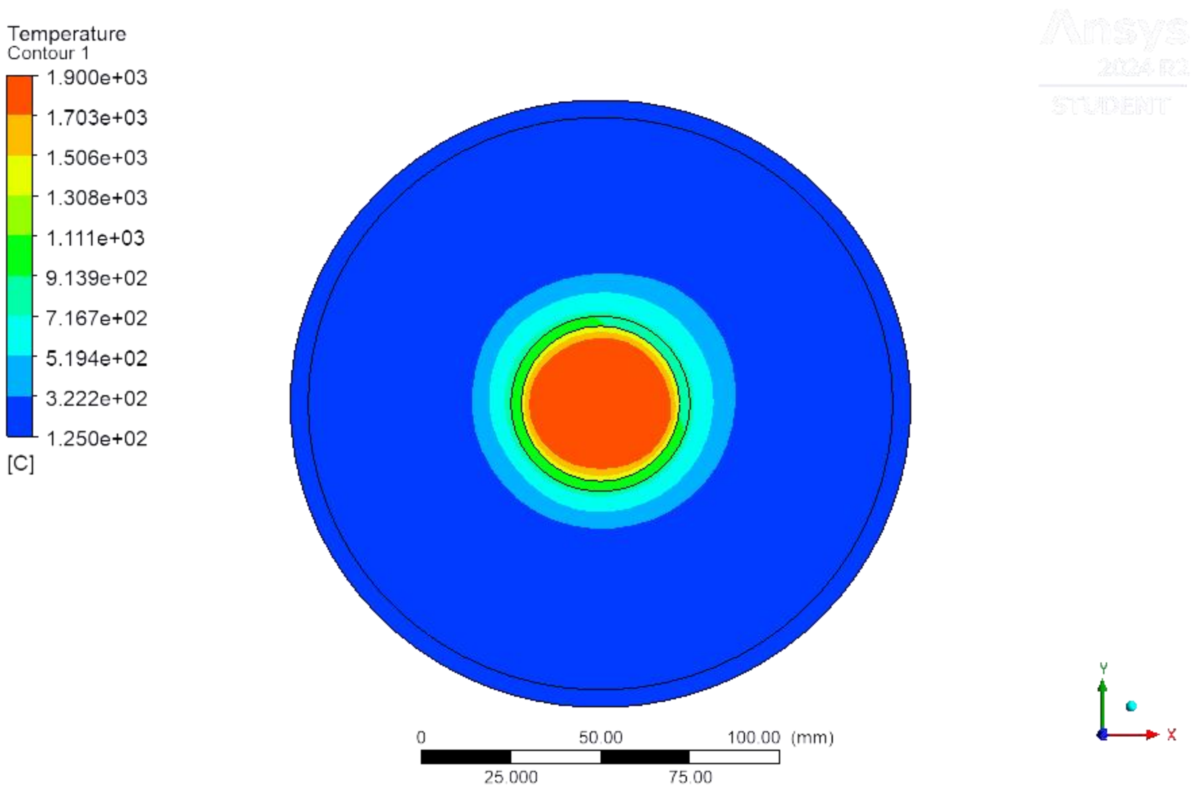

Figure 4.13: Distribution of Temperature for Scale Free Condition for Natural Gas Firing

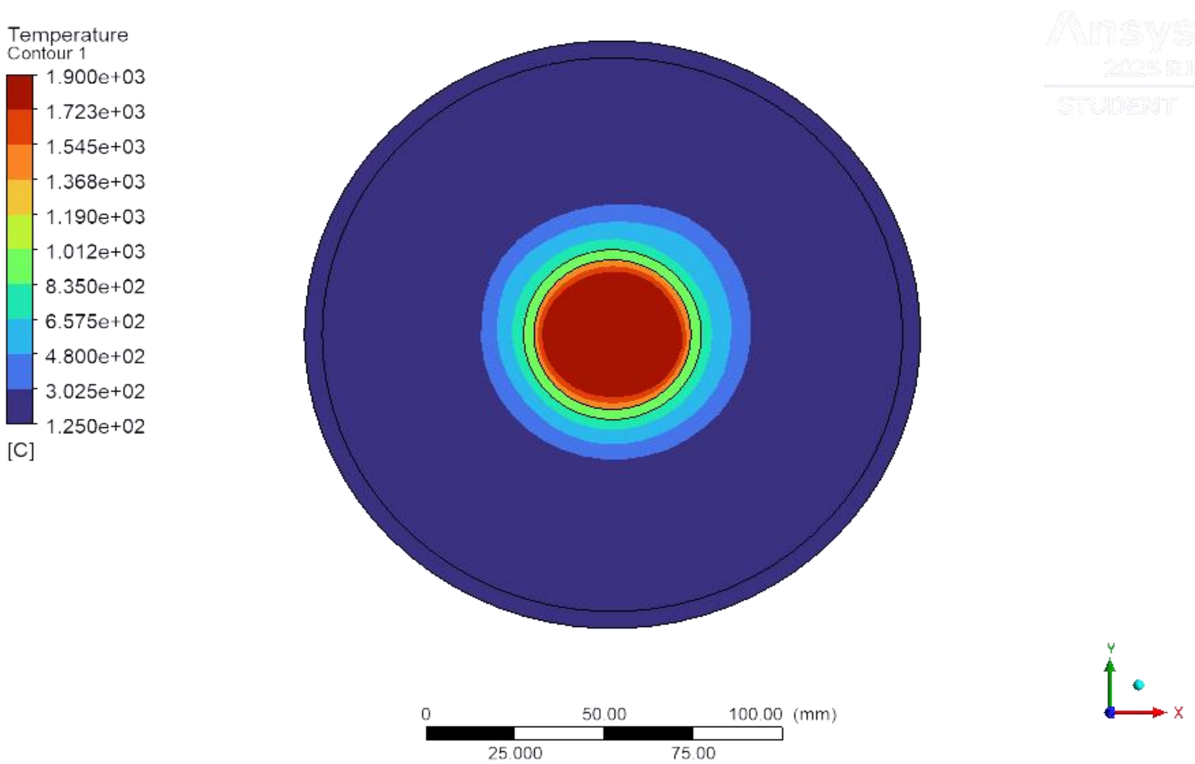

Figure 4.14: Distribution of Temperature for Scale Free Condition for Diesel Firing

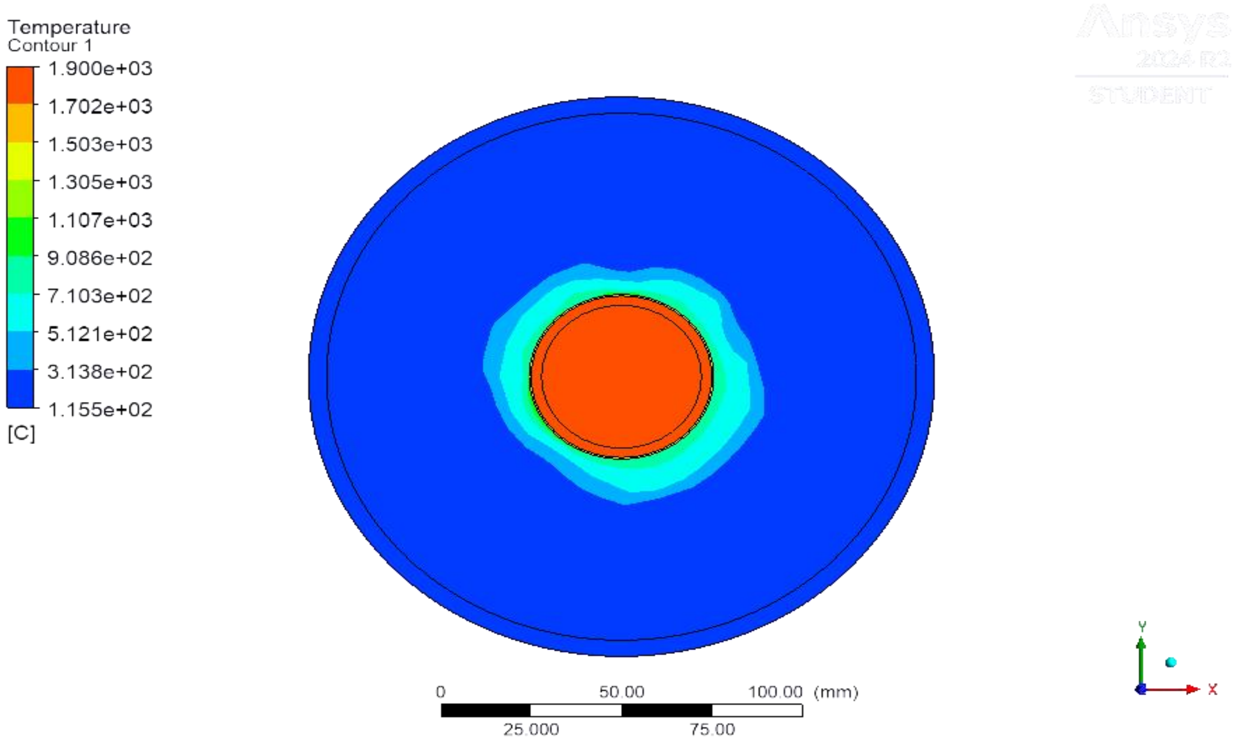

Figure 4.15: Distribution of Temperature for 0.5mm Scale Thickness for Natural Gas

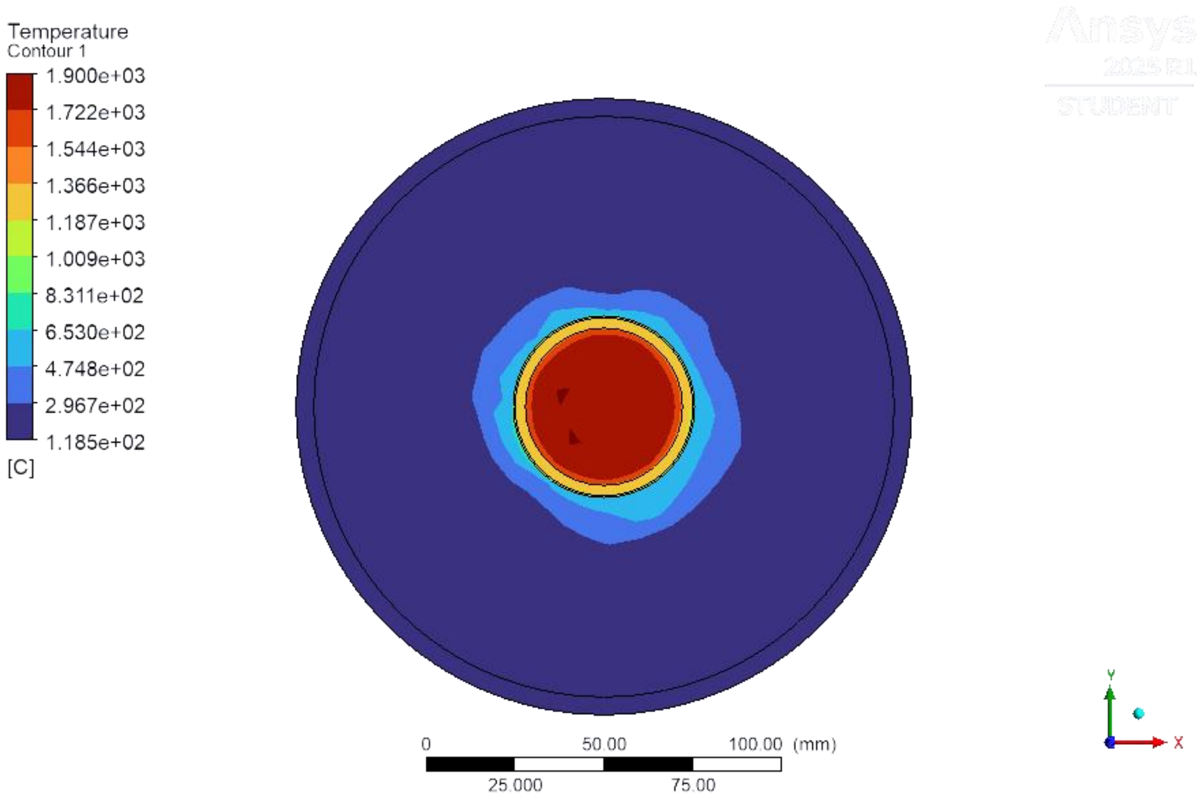

Figure 4.16: Distribution of Temperature for 0.5mm Scale Thickness for Diesel Firing

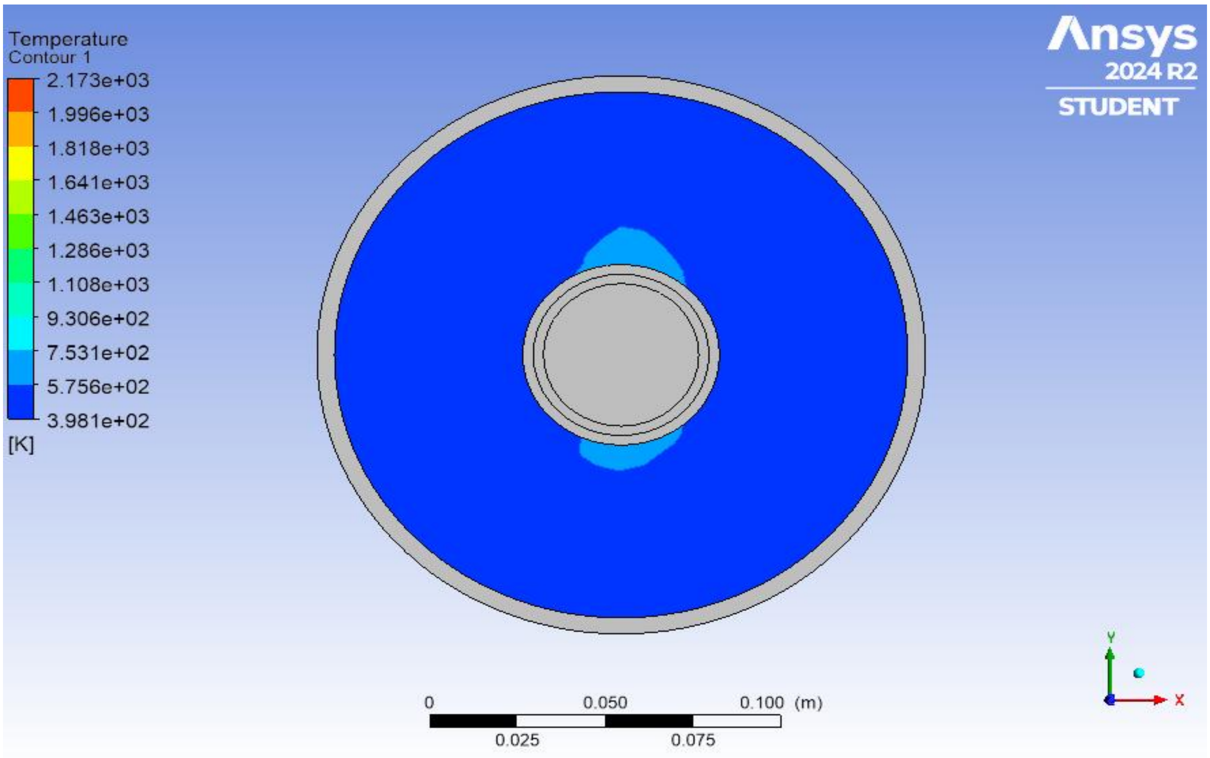

Figure 4.17: Temperature Distribution for 3.5mm scale layer using Natural Gas Firing

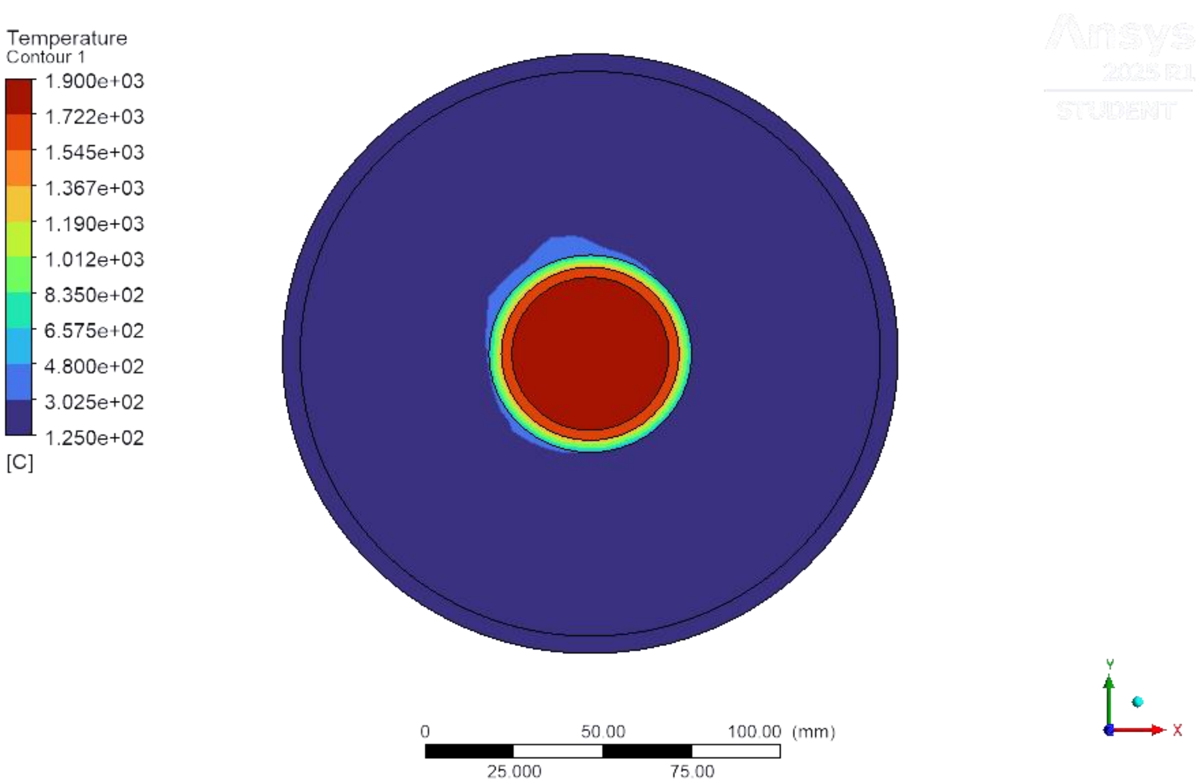

Figure 4.18: Temperature Distribution for 3.5mm scale layer using Diesel Firing

As scale thickness increased, the thermal imbalance between the water and flue gas stream became more pronounced. At a thickness of 3.5mmm the water outlet temperature had dropped further to 413.97K and 415K for natural gas and diesel respectively. This reveals a temperature drop of about 40K in the water outlet temperature when the no-scale and 3.5mm scaled tube is compared. The flue gas outlet temperature gas risen to 2103.43K and 2100.34K indicating a cumulative 180K increase in retained thermal energy within the fuel gas stream compared to the scale-free condition. This flue gas suggests that less heat is being absorbed by the water and more heat is being sustained within the metallic structure of the boiler tube

The Figures 4.13 to 4.18 showing temperature distribution for all other thickness layers (between 0.5mm and 3.5mm) both for natural gas and diesel are displayed in Appendixs A to C. Table 4.4 presents the effect of thickness scale on the water temperatures while Fig 4.19 shows the variations graphically

Table 4.4: Effect of Scale Thickness on Water Outlet Temperatures

Scale thickness (mm)	Natural gas (K) flueg outlet temperature	Diesel (K) flue gOutlet temprature
0	454.74	453.15
0.5	431.74	436.69
1	428.04	429.98
1.5	419.24	425.84
2	417.72	422.09
2.5	414.97	420.48
3	412.41	417.33
3.5	413.97	414.99

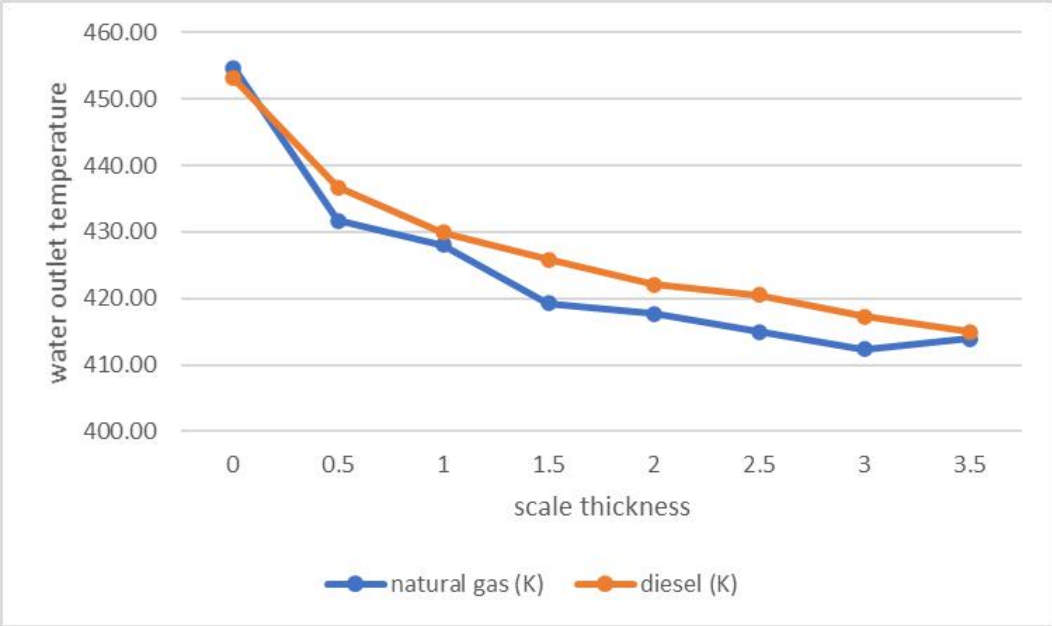

Figure 4.19: Graph of water outlet temperature vs scale thickness

Table 4.5 presents the effect of thickness scale on the flue gas outlet temperatures while Fig 4.20 shows the variations graphically.

Table 4.5: Effect of Scale Thickness on Flue Gas Outlet Temperatures

Scale thickness (mm)	Natural gas (K)	Diesel (K)
0.0	1922.97	1959.732
0.5	2014.31	2011.616
1.0	2041.45	2039.8767
1.5	2057.74	2057.2982
2.0	2072.93	2072.9543
2.5	2086.67	2077.1283
3.0	2094.96	2090.8949
3.5	2103.43	2100.3701

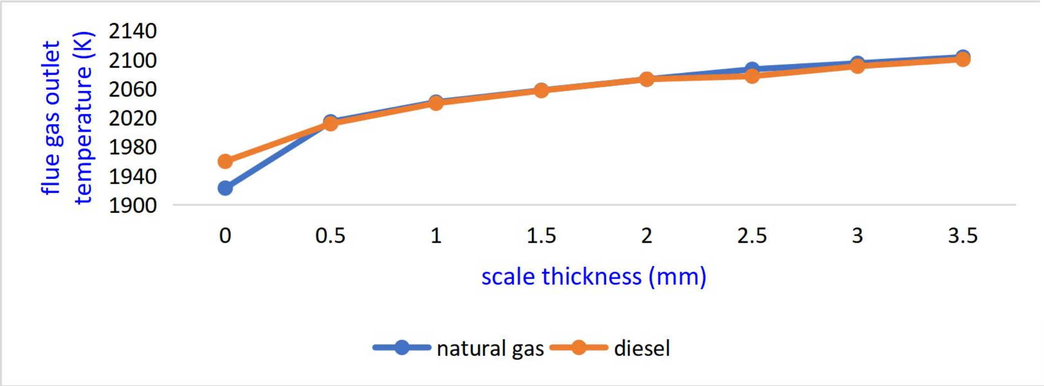

Figure 4.20:Flue gas outlet temperature versus scale thickness

4.5 Effect of Flue Gas Flow Rate on the Temperature of the Water Outlet

A separate simulation was performed to assess the impact of varying mass-flow-rates of the flue gas on the water outlet temperature across different scale thicknesses. The flow rates of the flue gas were incrementally increased from 0.33 kg/s to 33 kg/s. The results of this analysis are presented in Table 4.6 and illustrated in Figure 4.21. While flue gas increases, flow enhances water temperature marginally, it fails to overcome the insulating effect of scale buildup. For instance, at 0.5 mm scale, increasing flow tenfold (from 0.33 to 3.3 kg/s) raises outlet temperature by less than 21 K—still below the required 473.05 K.

Moreover, the system demonstrates diminishing thermal returns: increasing the flow rate from 1.32 to 33 kg/s yields minimal temperature gains, especially for higher scale thicknesses. This diminishing response underscores the inefficacy of simply boosting flue gas mass flow as a remedy for scale-induced resistance.

Apart performance losses, these results carry structural implications. Elevated flue gas outlet temperatures cause increased thermal gradients across the boiler tube wall, especially under uneven or thick scale deposits. This raises the risk of thermal fatigue and eventual failure due to persistent thermal stress.

Table 4.6: Flue Gas Flow Rate for Various Scale Thicknesses

Water Outlet Temperature

Flue Gas Flow Rate (kg/s)	0.5mm	1mm	1.5mm	2mm	2.5mm	3mm
0.33	432.7159	427.1332	423.2498	419.8805	416.8709	415.0265
0.66	439.7618	431.6382	426.6552	422.3733	418.7016	416.5028
1.32	444.9519	435.0206	429.0609	424.1171	419.9404	417.4904
2.31	447.8361	436.863	430.3675	425.0345	420.5742	417.9894
4.62	450.21	438.2812	431.369	425.7326	421.0584	418.3686
5.94	450.8044	438.7266	431.6715	425.9374	421.1994	418.4812
8.25	451.4353	439.1391	431.9559	426.1318	421.3331	418.5861
13.2	452.1186	439.5385	432.2326	426.3216	421.4634	418.6878
26.4	452.7412	439.9172	432.4941	426.5003	421.5858	418.7832
33	452.8729	439.9988	432.5503	426.5386	421.612	418.8037

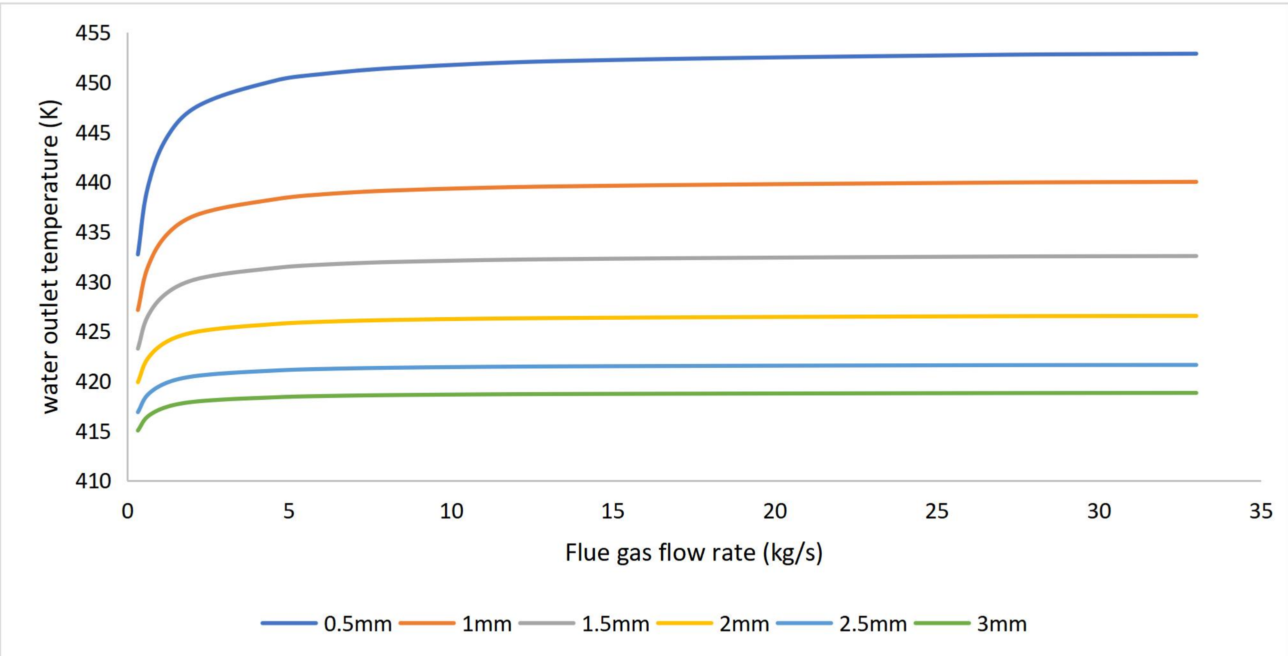

Figure 4.21: Effect of Increasing Flue Gas Mass Flow Rate

4.6 Experimental Combustion and Emission Analysis

Table 4.7 summarizes the flue gas combustion parameters recorded during the operation of the 12,000 kg/hr gas-fired steam-boiler under different load conditions. It includes critical variables such as oxygen (O_2), carbon monoxide (CO), carbon dioxide (CO_2), flue gas temperature (T. Gas), ambient air temperature (T. Air), excess air percentage (% Ex. Air), combustion efficiency (% Effy), pressure readings before and after the pressure reducing valve (PRV), and fuel flow rate measured in standard cubic meters (scm).

Table 4.7: Flue Gas Combustion Parameters for Natural Gas

Load *%*	O2 *%*	CO *ppm*	CO_2 *%*	T. Gas *°c*	T. Air *°c*	Ex. Air *%*	Effy *%*	PRV in Gas *Pr. Bar*	PRV Out Gas *Pr. mBar*	Fuel flowrate *Scm*
14	4.9	0	8.7	183	30	1.35	92.1	2.9	105	12
20	4.6	0	8.8	184	30	1.35	92.1	2.9	105	16
30	3.7	0	8.9	188	30	1.32	92	2.9	105	20
40	3.5	0	9.4	199	30	1.25	91.9	2.9	105	25
50	3.6	0	9.6	212	30	1.23	91.4	2.9	105	28
60	3.1	0	9.7	218	30	1.22	91.1	2.9	105	32
70	2.5	0	10.2	228	30	1.16	91	2.9	105	36
80	2.4	0	10.1	233	31	1.17	90.8	2.9	100	42
90	2	0	10.2	237	31	1.15	90.7	2.9	100	46
100	2	0	10.3	236	31	1.14	90.8	2.9	100	52

4.6.1. Oxygen (O_2) and Combustion Efficiency

As the boiler load increased from 14% to 100%, a decreasing trend in flue gas oxygen content was observed, dropping from 4.9% at 14% load to 2.0% at full load. This trend indicates improved combustion at higher loads due to better mixing of air and fuel. However, this was accompanied by a slight decline in combustion efficiency from 92.1% at 14–20% load to around 90.7–90.8% at 90–100% load.

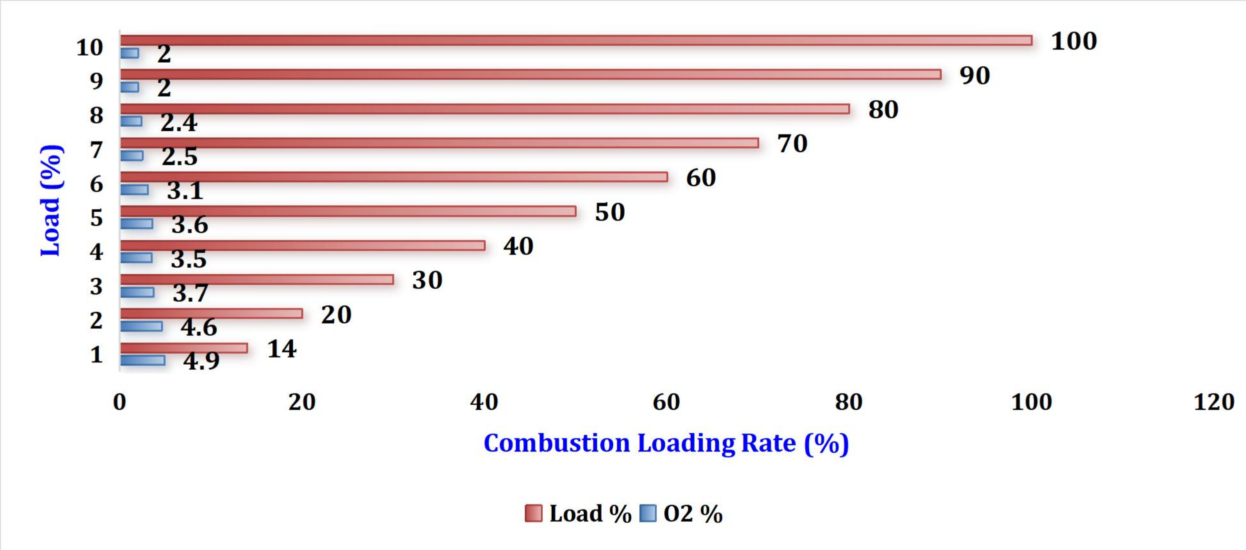

Figure 4.22: Combustion loading rate and amount of excess O_2

This inverse relationship between O_2 content and efficiency is expected; lower oxygen levels imply a leaner excess air supply, which typically enhances combustion efficiency. However, beyond a certain point, excessive reduction in excess air can lead to incomplete combustion.

4.6.2. Flue Gas Temperature and CO_2 Emissions

Flue gas temperature (T. Gas) increased progressively with the boiler load, rising from 183°C at 14% load to a peak of 237°C at 90% load. A similar trend was observed for CO_2 concentration, which rose from 8.7% at 14% load to 10.3% at full load.

This correlation is clearly shown in Figure 4.23, which plots CO_2 concentration against flue gas temperature. The increase in CO_2 with temperature suggests more complete combustion at higher loads. However, as combustion temperature increases, the risk of thermal NO_x formation also rises, though NO_x values are not shown in this dataset.

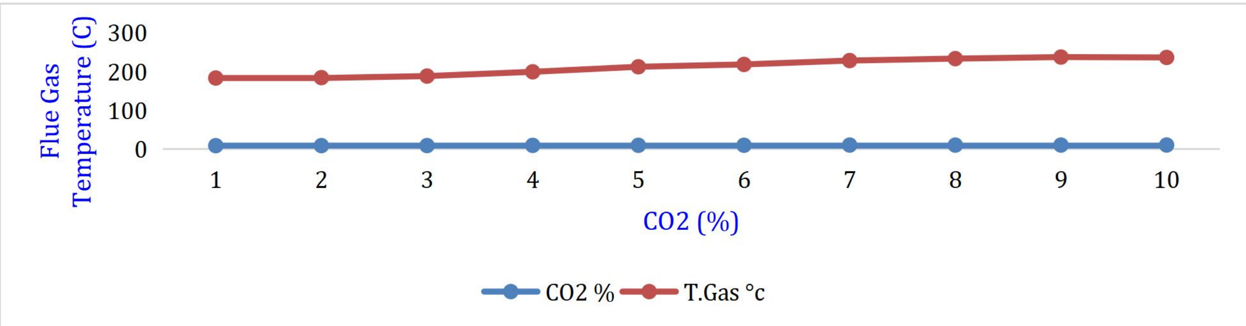

Figure 4.23: CO_2 and exhaust gas temperature versus boiler loading

4.6.3. Fuel Consumption vs Load

Figure 4.24 indicates a linear alignment between boiler load and fuel flow rate. The load increased from 14% to 100%, and fuel consumption rose accordingly from 12 scm to 52 scm. This trend is expected, as higher loads demand more fuel input to sustain steam production. The gradual increase in fuel flow confirms the responsiveness of the fuel control system to varying load conditions.

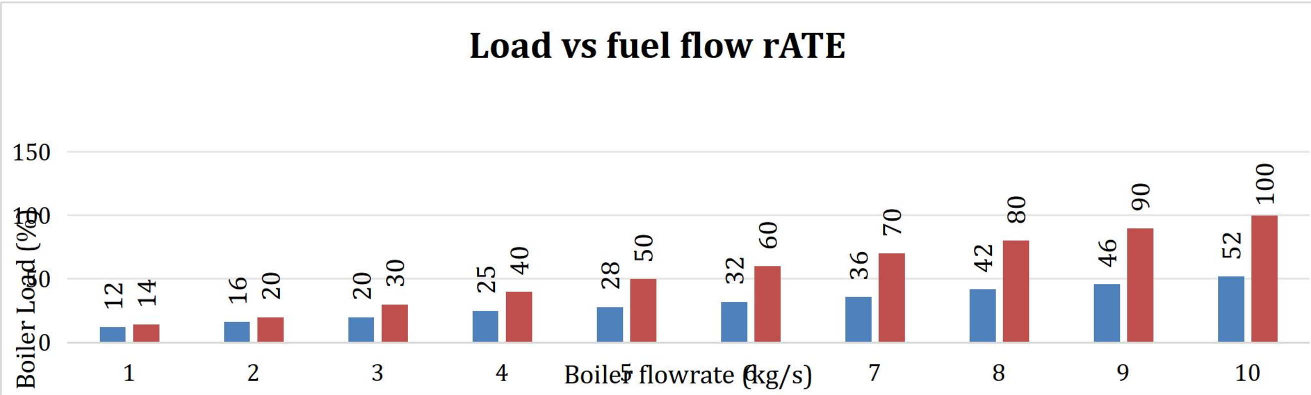

Figure 4.24: Relationship between boiler load and fuel flow rate

4.6.4. CO Emissions

Carbon monoxide (CO) levels remained at 0 ppm across all load conditions as seen in Figure 4.25. This shows efficient combustion with no measurable unburnt carbon, reflecting proper air–fuel mixing and optimal flame stability throughout the operational range.

4.6.5. Excess Air and PRV Pressure Stability

The excess air percentage decreased with increasing load, from 1.35% at minimum load to 1.14% at maximum load, aligning with the reduction in O_2. This suggests the boiler control system effectively manages air intake to minimize heat loss due to unused air. The PRV-in and PRV-out pressures remained constant across the loading range (2.9 bar and 100–105 mbar respectively), indicating stable upstream and downstream gas pressure regulation, crucial for maintaining consistent burner performance.

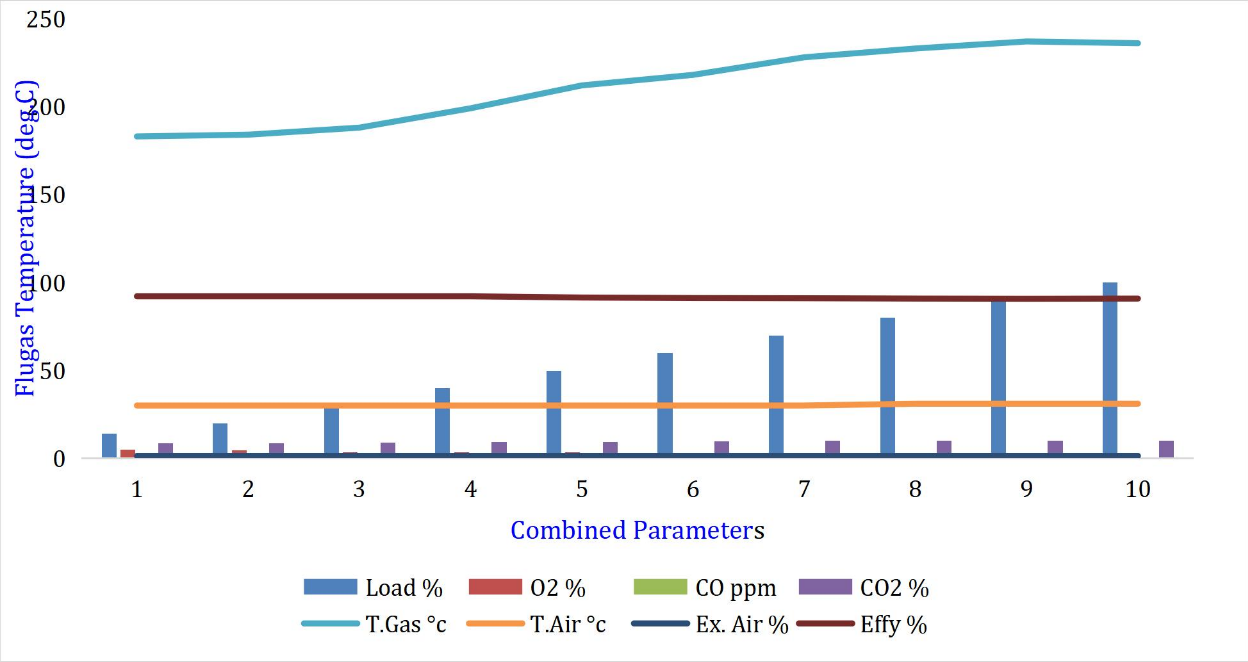

Figure 4.25: Relationship between flue gas parameters and boiler loads

4.6.6. Optimal Load Range

Operating the boiler between 70% and 80% load appears optimal. In this range, combustion efficiency remains high (90.8–91%), CO_2 concentration is elevated (10.1–10.2%), O_2 is within acceptable limits (2.4–2.5%), fuel consumption is efficient and flue gas temperatures supports efficient energy transfer. These values suggest this load range strikes a good balance between thermal efficiency and emissions compliance.

4.7. Simulated Natural Gas Emissions

Table 4.8 shows the simulated combustion emissions for various load conditions (14%–100%) using Aspen HYSYS. The results obtained show CO_2 Concentration Increases from 7.3% at 14% of the load to 8.7% at full load, indicating more complete combustion as the fuel input increases. O_2 Concentration was noticed to decreases from 4.8% to 1.7%, which reflects improved combustion efficiency at higher loads due to reduced excess air while, excess Air Drops significantly from 33% at 14% load to 10% at full load, further confirming more stoichiometric combustion at higher loading.

Table 4.8: Simulated combustion emissions at various boiler loads

Simulated Natural Gas Combustion Emission Characteristics						
Load (%)	**CO2 (%)**	**O2 (%)**	**CO (%)**	**% Excess Air**	**Flue Gas Temp (°C)**	**Efficiency**
14	7.3	4.8	0.0	33	264.56	N/A
20	7.5	4.5	0.0	30	268.53	N/A
30	7.9	3.6	0.0	23	278.45	N/A
40	7.9	3.5	0.0	22	279.94	N/A
50	8.0	3.4	0.0	21	281.46	N/A
60	8.1	3.1	0.0	19	284.55	N/A
70	8.2	2.8	0.0	17	287.74	N/A
80	8.4	2.5	0.0	15	291.02	N/A
90	8.5	2.2	0.0	13	294.39	N/A
100	8.7	1.7	0.0	10	299.65	N/A

4.8 Validation of Simulated Results with Experimental Results for Natural Gas Emissions

4.8.1 Flue gas temperature difference

Table 4.9: Comparison of Actual and Simulated Temperatures of the Flue Gas

Load (%)	Actual Flue Gas Temp (°C)	Simulated Flue Gas Temp (°C)	Flue Gas Temperature Difference (°C)	% Temp Deviation
14	183.0	264.56	-81.56	-44.57
20	184.0	268.53	-84.53	-45.94
30	188.0	278.45	-90.45	-48.11
40	199.0	279.94	-80.94	-40.67
50	212.0	281.46	-69.46	-32.76
60	218.0	284.55	-66.55	-30.53
70	228.0	287.74	-59.74	-26.20
80	233.0	291.02	-58.02	-24.90
90	237.0	294.39	-57.39	-24.22
100	236.0	299.65	-63.65	-26.97

A consistent overprediction of flue gas temperature by the simulation is noticed, with deviations ranging from -24% to -49%, with the largest discrepancy noticed at 30% loading and the smallest at 90%. The difference is attributed to some of the simulation assumptions including idealized combustion, not considering heat losses and possible instrumentation lag. From the table, it can be observed that the simulated temperatures are higher because actual operating conditions includes heat losses, imperfect mixing and variable burner performance that could reduce flue gas temperatures

4.8.2 CO_2 and O_2 Difference

This section compares for values of CO_2 and O_2 for the actual flue gas composition with simulated data for the burner operating on natural gas across varying loading conditions (14% - 100%).

Table 4.10: Comparison of CO2 and O2 values of actual fuel gas composition with simulated values

Validation of Simulated Results with Actual Emission from Weishaupt WM-GL50/2-A, ZM-R-NR								
Load (%)	**Actual CO2 (%)**	**Simulated CO2 (%)**	**Actual O2 (%)**	**Simulated O2 (%)**	**Diff CO2**	**Diff O2**	**CO2 Error %**	**O2 Error %**
14	8.7	7.3	4.9	4.8	1.4	0.1	16.10	2.00
20	8.8	7.5	4.6	4.5	1.3	0.1	14.77	2.17
30	8.9	7.9	3.7	3.6	1.0	0.1	11.23	2.70
40	9.4	7.9	3.5	3.5	1.5	0.0	15.96	0.00
50	9.6	8.0	3.6	3.4	1.6	0.3	16.67	8.3
60	9.7	8.1	3.1	3.1	1.6	0.0	16.50	0.00
70	10.2	8.2	2.5	2.8	2.0	-0.3	19.6	12.00
80	10.1	8.4	2.4	2.5	1.7	-0.1	16.83	4.17
90	10.2	8.5	2.0	2.2	1.7	-0.2	16.67	10.00
100	10.3	8.7	2.0	1.7	1.6	0.3	15.53	17.65

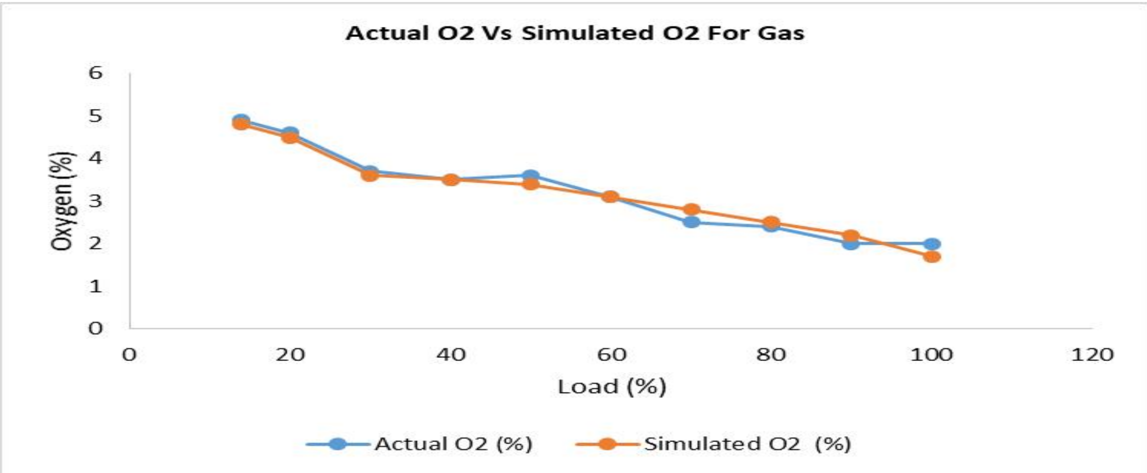

Figure 4.26: Actual O_2 vs Simulated O_2 values

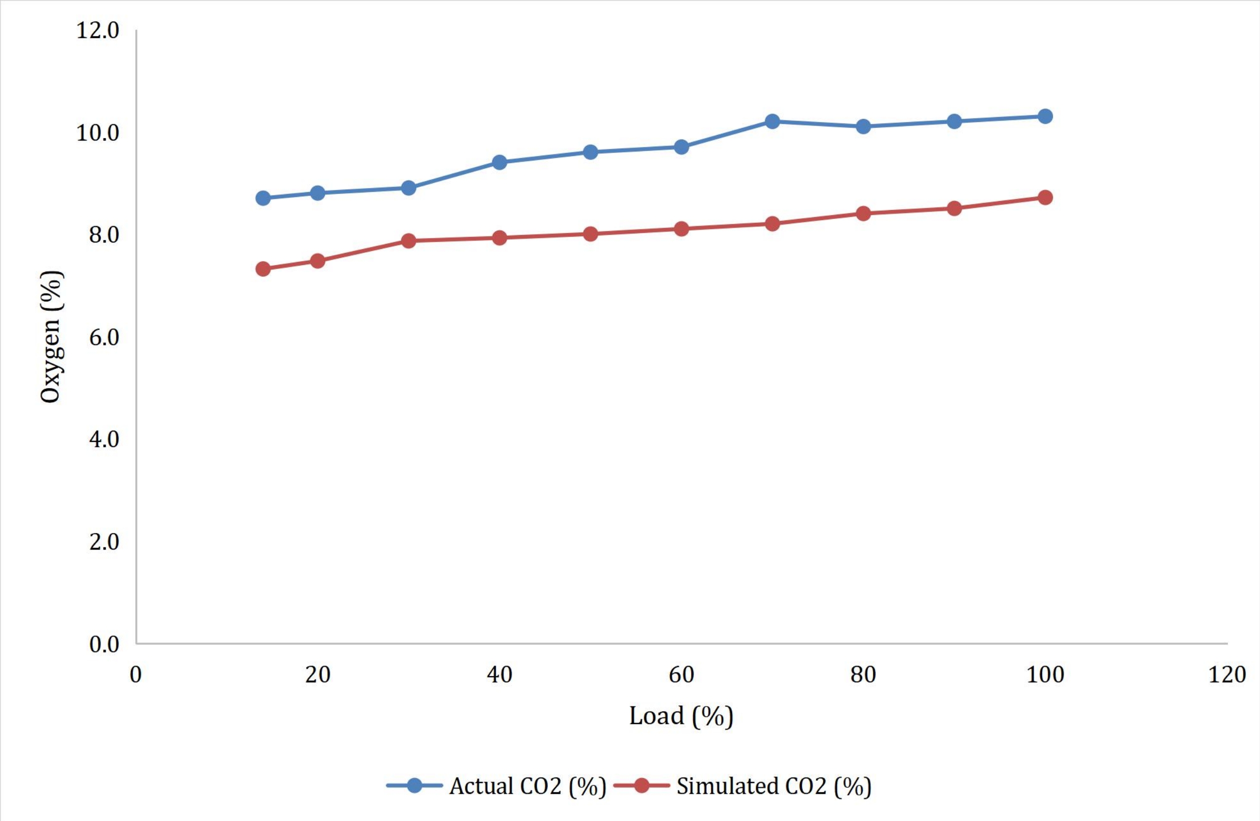

Figure 4.27: Actual CO_2 vs Simulated CO_2

The actual CO_2 levels from 8.7% at 14% loading up to 10.3% at 100% loading shows a steady increase as load increases for both actual and simulated. However, the simulated values are consistently lower than the actual due to overestimation of the ratio of air fuel and the inability of the simulation to account for real-world combustion kinetics. With CO_2 percentage error ranging from 11.23% to 19.6%, with more significant errors at higher loads, this might be due to increased combustion dynamics under higher burner firing conditions which are not well captured in the simulation

For the O_2 values, the actual values decline from 4.9% at 14% loading down to 2.0% at 100% reflecting excess air and improved combustion, the simulated values of O2 follows a similar trend with some deviations. The error percentages are relatively low mostly less than 10% except at 100% loading when it spikes to 17.65%. The increasing deviation of simulated from actual values at high loads above 70% suggests the model's limitation in representing burner air dynamics and load induced turbulence.

As seen from Figures 4.26 and 4.27, there is a strong correlation between the actual O_2 and CO_2 measurements and the corresponding simulated values, indicating good agreement between experimental and simulation results. The divergence noticed especially at higher loads is attributed to the simplified assumption of constant excess air and failure of the simulation to reflect correct carbon-to-air reaction extent.

4.9 Validation of Simulated Results with Experimental Results for Diesel Fired Emissions

4.9.1 Actual Diesel Emission and Simulated Diesel Emissions for Diesel Firing

Table 4.11 shows the emission values of CO, O2 and CO2 in the flue gas in the actual experimental studies while table 4.11 shows the flue gas values for the simulated studies.

Table 4.11: Results of Actual Diesel Emission of Boiler on Diesel Firing

12 Tons Dual Fired Boiler Actual Diesel Combustion Emission Characteristics Parameter							
Load (%)	**CO2 (%)**	**O2 (%)**	**CO (%)**	**% Excess Air**	**Flue Gas Temperature (deg C)**	**Efficiency**	**Fuel Pump Pressure**
20	11.6	5.2	0	1.33	189	92.1	29
33	11.8	4.9	0	1.30	199	91.7	29
45	11.7	5.0	0	1.31	207	91.3	29
53	12.0	4.6	0	1.28	217	91.0	29
60	12.4	4.1	1	1.24	226	90.7	29
67	12.8	3.6	2	1.20	230	90.7	29
75	13.1	3.1	3	1.17	235	90.8	29
83	13.4	2.7	3	1.15	235	90.9	29
92	13.9	2.1	2	1.11	241	91.0	29
100	13.9	2.1	4	1.11	245	90.8	29

Table 4.12: Results of Simulated Flue Gas Emission of Boiler on Natural Gas Firing

12tons Dual Fired Simulated Diesel Combustion Emission Characteristics Parameter							
Load (%)	**CO2 (%)**	**O2 (%)**	**CO (%)**	**% Excess Air**	**Flue Gas Temperature (deg C)**	**Pressure Bar**	**Efficiency**
20	9.4	5.5	0	38	315	1.013	NA
33	9.5	5.3	0	36	318	1.013	NA
45	9.7	4.9	0	33	323	1.013	NA
53	9.9	4.6	0	30	328	1.013	NA
60	10.1	4.2	0	27	333	1.013	NA
67	10.4	3.7	0	23	341	1.013	NA
75	10.7	3.3	0	20	347	1.013	NA
83	11.1	2.6	0	15	357	1.013	NA
92	12.0	2.0	0	11	366	1.013	NA
100	11.6	1.8	0	10	369	1.013	NA

4.9.2 CO_2 Comparison for Simulated and Actual Values for Diesel Firing

Figure 4.28 shows the comparison between the CO2 values for natural gas firing and diesel fuel firing. Figure 4.28 demonstrates a good correlation between actual and simulated values; however, the actual values were consistently higher than the simulated ones, particularly at higher loads. This indicates that the simulation may be underestimating combustion efficiency.

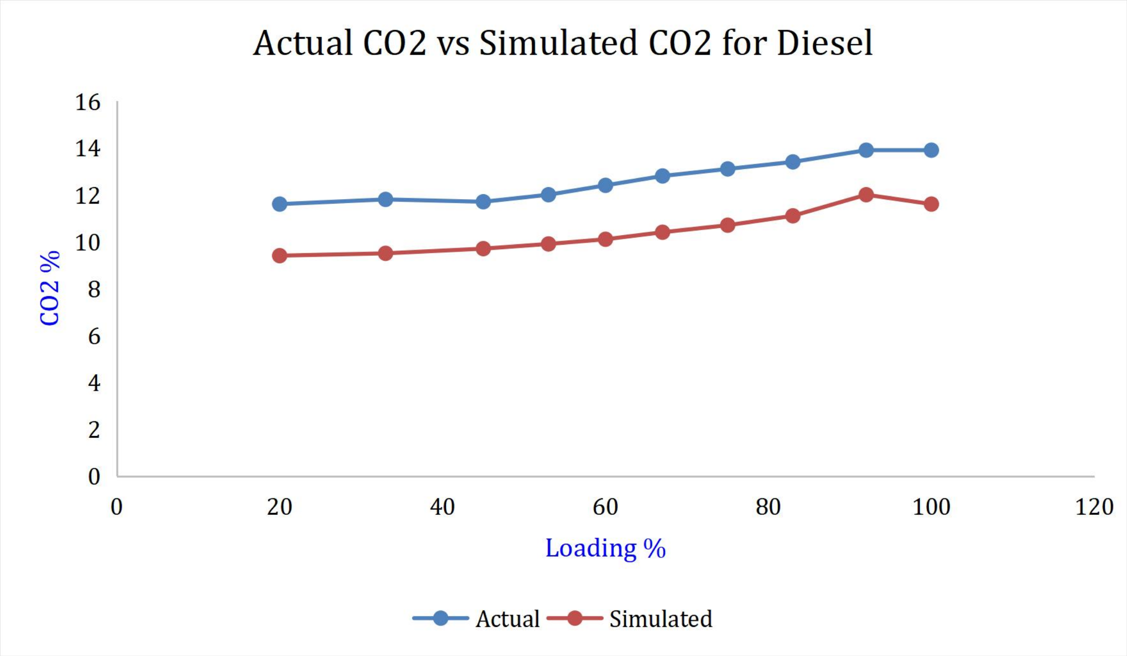

Figure 4.27: Actual CO2 vs simulated CO2 for diesel firing

4.9.2 O_2 Comparison for Simulated and Actual Values for Diesel Firing

Figure 4.29 shows a much better agreement between the actual and the simulated with the simulated slightly higher at low loading conditions than the actual, indicating that the model assumes a leaner combustion.

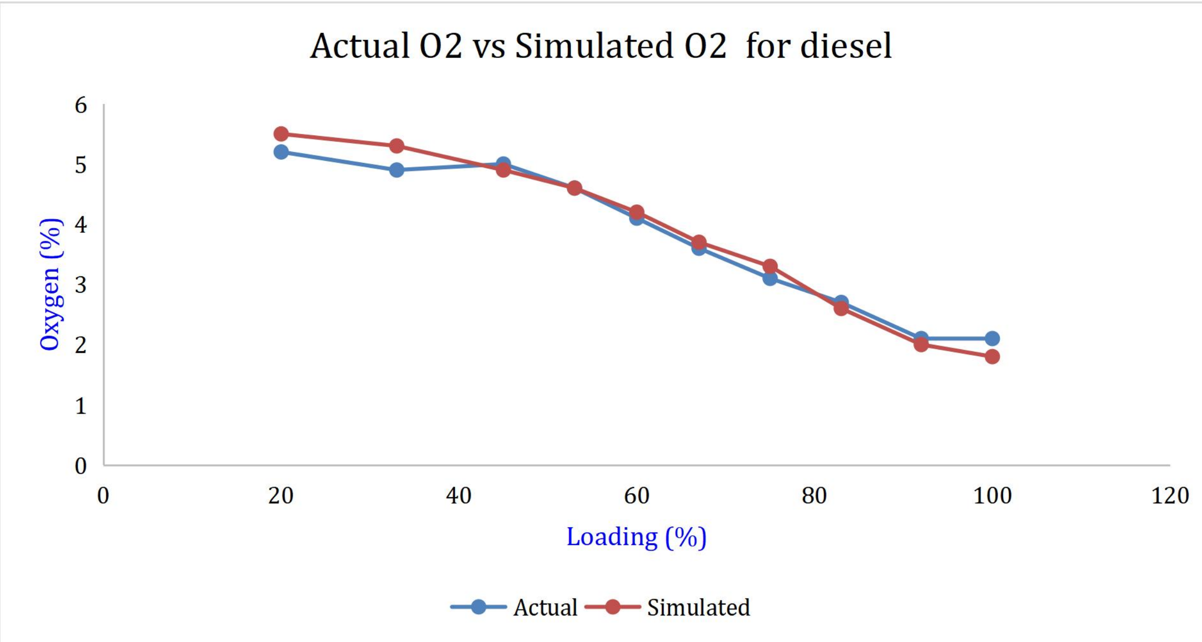

Figure 4.29: Actual O2 vs simulated O2 for diesel firing

4.9.3 CO Comparison for Simulated and Actual Values for Diesel Firing

Figure 4.30 shows perfect agreement for the actual and simulated values up to 60% loading, after which the actual values begin to rise peaking at 100%, simulated values remain at zero throughout, signifying that the simulation does not account for incomplete combustion dynamics

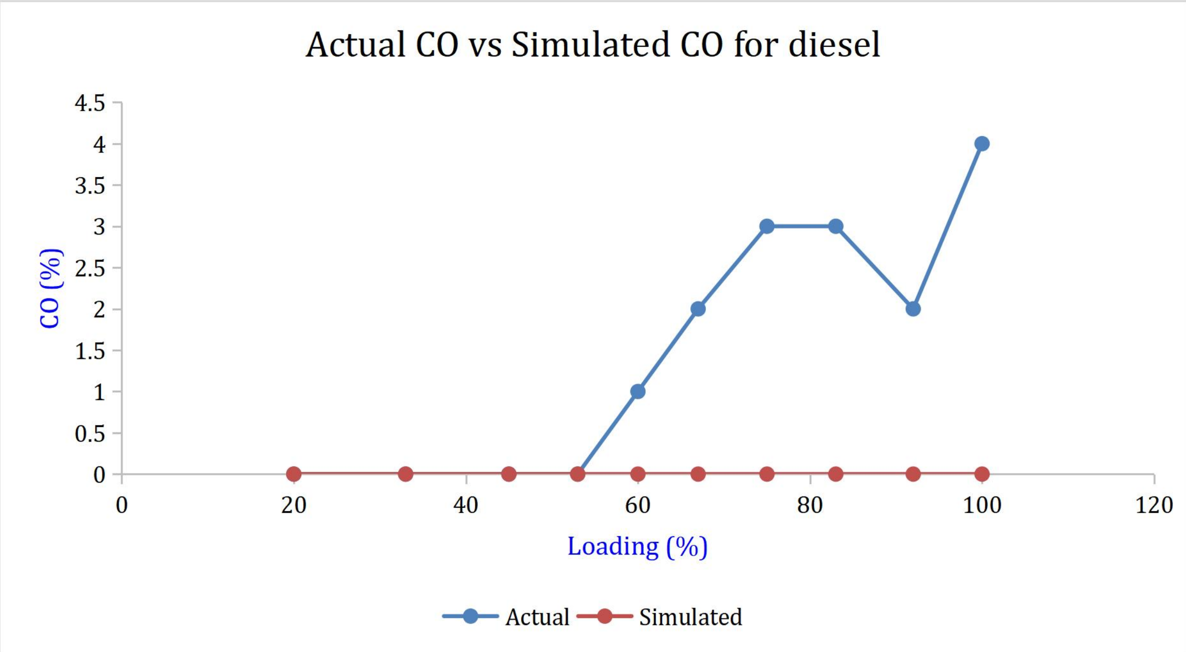

Figure 4.30: Actual CO vs simulated CO for diesel firing

4.9.4 Exhaust Gas Temperature Comparison for Simulated and Actual Values for Diesel Firing

Figure 4.32 highlights the comparison between actual and simulated flue gas temperatures shows that the simulated values were consistently higher across all load conditions. This discrepancy suggests a possible overestimation of combustion heat release or the absence of heat loss modelling in the simulation.

4.10 Optimizing the 12Tons Boiler Control Parameter

The "Smaller-the-Better" S/N ratio model was applied since the aim is to minimize undesirable emissions or maximize combustion efficiency, implying that lower output values are better i.e. less CO_2 and less fuel waste implies better boiler efficiency. From the results shown in table 4.13, the S/N ratios ranged from -31.52dB to -37.80Db. The lower S/N values indicate worse performance i.e. signifying more noise and variability in the system, the worst performance was noticed in Run 18 and 19 which had high loads and high air or fuel inputs.

Table 4.13: Signal-to-Noise Ratio Analysis

Signal-to-Noise Ratio Analysis Using Excel Spreadsheet on Lower the Better Model											
-10	Load^2	Fuel^2	Air^2	VFD^2	Y^2	1	n	1/n	1/n(EY^2)	L0G(1/NEY^2)	SNR
-10	900	400	784	3600	5684	1	4	0.25	1421	3.152594078	-31.5259408
-10	900	400	784	3600	5684	1	4	0.25	1421	3.152594078	-31.5259408
-10	900	400	784	3600	5684	1	4	0.25	1421	3.152594078	-31.5259408
-10	900	1024	2401	5625	9950	1	4	0.25	2487.5	3.395763089	-33.9576309
-10	900	1024	2401	5625	9950	1	4	0.25	2487.5	3.395763089	-33.9576309
-10	900	1024	2401	5625	9950	1	4	0.25	2487.5	3.395763089	-33.9576309
-10	900	2704	8100	9025	20729	1	4	0.25	5182.25	3.71451836	-37.1451836
-10	900	2704	8100	9025	20729	1	4	0.25	5182.25	3.71451836	37.1451836
-10	900	2704	8100	9025	20729	1	4	0.25	5182.25	3.71451836	-37.1451836
-10	3600	400	2401	9025	15426	1	4	0.25	3856.5	3.586193336	-35.8619334
-10	3600	400	2401	9025	15426	1	4	0.25	3856.5	3.586193336	-35.8619334
-10	3600	400	2401	9025	15426	1	4	0.25	3856.5	3.586193336	-35.8619334
-10	3600	1024	8100	3600	16324	1	4	0.25	4081	3.610766595	-36.1076659
-10	3600	1024	8100	3600	16324	1	4	0.25	4081	3.610766595	-36.1076659
-10	3600	1024	8100	3600	16324	1	4	0.25	4081	3.610766595	-36.1076659
-10	3600	2704	784	5625	12713	1	4	0.25	3178.25	3.502188056	-35.0218806
-10	3600	2704	784	5625	12713	1	4	0.25	3178.25	3.502188056	-35.0218806
-10	3600	2704	784	5625	12713	1	4	0.25	3178.25	3.502188056	-35.0218806
-10	10000	400	8100	5625	24125	1	4	0.25	6031.25	3.780407331	-37.8040733
-10	10000	400	8100	5625	24125	1	4	0.25	6031.25	3.780407331	-37.8040733
-10	10000	400	8100	5625	24125	1	4	0.25	6031.25	3.780407331	-37.8040733
-10	10000	1024	784	9025	20833	1	4	0.25	5208.25	3.716691823	-37.1669182
-10	10000	1024	784	9025	20833	1	4	0.25	5208.25	3.716691823	-37.1669182
-10	10000	1024	784	9025	20833	1	4	0.25	5208.25	3.716691823	-37.1669182
-10	10000	2704	2401	3600	18705	1	4	0.25	4676.25	3.669897721	-36.6989772
-10	10000	2704	2401	3600	18705	1	4	0.25	4676.25	3.669897721	-36.6989772
-10	10000	2704	2401	3600	18705	1	4	0.25	4676.25	3.669897721	-36.6989772

From the S/N analysis, the response table is presented in Table 4.14. While Table 4.14 shows the aggregate signal to noise ratios at each level for each factor to determine their relative influence on the system.

Table 4.14: Showing the signal-to-noise response table

Signal-to-noise ratio response table				
LEVEL	A. Load (%)	B. Fuel (scm)	C. Air (%)	D. VFD (%)
1	-34.210*	-35.064*	-34.617	-34.778
2	-35.664	-35.744	-35.790	-35.431*
3	-37.223	-36.289	-37.019*	-36.725
DELTA	3.014	1.225	2.402	1.947
RANK	1st	4th	2nd	3rd

Table 4.14: Implication of Ranking from S/N Response

From the Table 4.14 above for the S/N response, load has the highest effect on combustion, this is expected because increasing load directly affects fuel demand, flue gas rate and the heat release rate. Air was ranked second as it is crucial for ensuring complete combustion and managing oxygen in the system. Poor air fuel ratios leads to combustion inefficiencies. The VFD percent opening affects combustion rates as it controls the fan speed which impacts air fuel mixing and flame stability, the fuel flow rate has the least impact due to the burner design which compensates across moderate variations in fuel .

4.14 Implication of Ranking from Sinal to Noise Response

FACTOR	DELTA	RANK	IMPLICATION
A. Load	3.014	1st	Most influential on system performance
C. Air	2.402	2ND	Strong impact on combustion behavior
D. VFD%	1.947	3rd	Influences air delivery and mixing
B. Fuel	1.225	4th	Least impact among the four

4.11 Findings

At the end of the study, the major findings are outlined as follows:

(i) Visual inspection revealed the presence of pinholes and rupture along the third pass, as well as signs of pitting corrosion and scale formation on the outer surface of the boiler tube.

(ii) The chemical composition of the failed boiler tube was found to be within the acceptable limits of the referenced specification, indicating that improper material selection was not a factor contributing to the failure.

(iii) Micro structural analysis revealed evidence of decarburization and grain growth at the inner diameter (ID) of the tube, resulting from thermal oxidation, while pitting corrosion was identified at the outer diameter (OD).

(iv) Micro structural examination showed a normal ferrite–pearlite structure away from the damaged area, gradually developing minor precipitate formations toward the failure zone. This transition indicates progressive thermal exposure and material degradation. Overall, the failure mechanism was predominantly thermally driven and intensified by water-side corrosion.

(v) Water chemistry results showed TDS, P-alkalinity, chloride, and silica in the boiler drum exceeded permissible limits. These conditions favor scaling, deposition, and localized overheating of the tube metal. Feed water silica and phosphate control were also inadequate, contributing to the tube failure mechanism.

(vi) The optimal water flow rate through the boiler which yields the outlet steam temperature of 453K was determined to be 0.454 kg/s

(vii) Without scale, efficient heat transfer was observed (flue gas 1922 K; steam 454.7 K). Increasing scale thickness reduced heat transfer, lowering steam temperature to 413.9

K and raising flue gas temperature to 2103 K at 3.5 mm.Thus, scale acts as an insulating layer, promoting overheating and increasing thermal fatigue risk

(viii) As the boiler load increased, oxygen in the flue gas dropped from 4.9% to 2.0%, showing better air–fuel mixing, although combustion efficiency slightly decreased from 92.1% to about 90.7–90.8%. The model matched experiments well at low loads, showed moderate differences at mid loads, and larger gaps at high loads above 70%.

(ix) As the boiler load increased, flue gas temperature rose from 183 °C to 237 °C and CO_2 increased from 8.7% to 10.3%, showing more complete combustion at higher load. However, the higher temperatures also raise the possibility of thermal NO_x formation. The strong agreement between measured and simulated CO_2 indicates the boiler was operating efficiently and the model predicted its behaviour well.

(x) Optimization of combustion parameters showed that operating at full load (100%) with high air and fuel settings produced the poorest S/N ratios, indicating unstable combustion and increased emissions (unburnt fuel, CO_2 and NO_x). Conversely, a moderate load range (60–70%) with balanced air–fuel ratio and controlled VFD speed achieved optimal combustion stability and improved S/N ratios. Although excess air supports complete combustion, excessive air lowered flame temperature and increased heat losses, thereby reducing overall thermal efficiency.

(xi) Based on the analysis, the optimal parameters were ranked according to their level of significance, as outlined the table 4.15:

Table 4.15: Optimum Parameter Ranking Based on Significance

Rank	Parameter	Delta (Effect Size)	Significance
1st	**Load (%)**	3.014	Most critical to combustion stability and emissions
2nd	**Air (%)**	2.402	Strong influence on fuel efficiency and flame quality
3rd	**VFD (%)**	1.947	Affects fan speed, air mixing, and burner performance
4th	**Fuel Flow**	1.225	Least sensitive due to burner's fuel control tolerance

CHAPTER FIVE

CONCLUSION AND RECOMMENDATION

This research conducted an in-depth investigation into the failure mechanisms, performance behavior, and emission characteristics of a dual-fuel industrial boiler, with the goal of enhancing its reliability, combustion efficiency, and environmental compliance. It explored the crucial interrelationships among material durability, combustion processes, operational parameters, and emission outcomes by integrating experimental analysis with numerical simulations and statistical optimization methods. The main conclusions drawn from the various components of the study are outlined below:

The investigation into the reasons for the continuous tube failure on the third pass revealed that the degradation was a result of complex interactions between thermal stresses, corrosive water chemistry, and fouling-induced heat transfer impairment. The following specific findings were established:

Visual inspection indicated pin holes and rupture on the 3rd pass, also pitting corrosion consistent with long-term overheating and internal scaling.

The Analysis of the Chemical Composition of the failed tube samples verified the base material as low-carbon steel, and is within the acceptable limits confirming material selection is not a contributing factor to failure

Microstructural examination revealed grain growth and decarburization due to thermal oxidation, in addition to pitting corrosion in the inner diameters and outer diameters of the tube confirming that prolonged exposure to high temperatures in combination with scale deposition had weakened the metal matrix.

Water chemistry analysis identified elevated concentrations of calcium and magnesium ions, supporting the hypothesis of scale formation due to poor water treatment practices.

Using CFD simulation tools in conjunction with validated experimental data, the impact of operational parameters on the performance of combustion and heat transfer efficiency was thoroughly examined:

Effect of Scale Layer on Heat Transfer: The presence of a scale layer was found to significantly degrade the effective heat transfer coefficient, resulting in elevated tube wall temperatures and a heightened risk of material failure. Simulation results indicated that even a moderate scale thickness could reduce heat transfer efficiency by up to 20%.

Water Flow Rate Optimization: The study established that increasing water mass flow rate improves convective heat transfer and reduces wall temperatures. An optimum range was identified to balance pump power requirements and thermal stress reduction.

Mass-Flow-Rate of the Flue Gas: Enhancing the mass flow rate of the flue gas increased turbulence and combustion completeness but beyond an optimal point led to higher pressure drops and fan energy consumption.

The combustion behaviour of the boiler under dual-fuel (natural gas and diesel) conditions was experimentally characterized using a combustion manager and exhaust gas analyzer:

Combustion efficiency was observed to be higher during natural gas firing in comparison to diesel, primarily due to cleaner combustion characteristics and more effective air–fuel mixing.

Emission Trends revealed that diesel combustion produced significantly particulate matter levels, while natural gas combustion resulted in higher CO emissions under certain sub-optimal air settings.

Experimental data show that optimal excess air levels were critical for both fuels to ensure combustion completeness and minimize emissions.

Experimental data under natural gas and diesel firing conditions were used to validate CFD predictions, with strong agreement observed in temperature distribution, flue gas composition, and efficiency metrics.

Taguchi Methodology and Signal to Noise (S/N) Analysis were successfully used to identify and optimize critical boiler control parameters in the order of influence. The parameters studied include: load, flue flow, air flow and VFD%.

The optimum operating conditions resulted in reduced emission levels, improved combustion stability, and prolonged component life.

Based on the objectives of this study, the following conclusions were made:

We successfully carried out a detailed failure investigation to determine the causes of the recurring failures in the 3rd pass of the 12-ton dual-fired steam boiler. This involved visual inspection, chemical composition analysis, metallurgical examination, and water chemistry analysis. Through these methods, we gained valuable insights into the root causes of the persistent tube failures and were able to propose appropriate solutions.

We also developed a CFD model of the failed boiler tube and simulated its progressive failure under thermal loading to assess the thermal effects caused by scale formation on the tube surface.

Additionally, we evaluated the actual emission characteristics of the boiler using a flue gas analyzer under various load conditions, firing on both natural gas and diesel.

Finally, we developed a CFD model for the boiler's combustion operating parameters and simulated its combustion performance using both fuels. This enabled us to analyze and understand the heat transfer dynamics under varying load conditions for natural gas and diesel combustion.We proved the validity of the developed models by comparing the actual emission data obtained from flue gas analyzer with the result of the simulated combustion, in most of the cases they were in good agreement, except in a few cases when the model either under predicted or overpredicted the actual data due to certain assumptions made.

We were able to determine the optimal parametric setting required to optimize the boiler combustion performance by employing Taguchi optimization method on the signal-to-noise response, as such we were able to rank the critical parameters in boiler combustion performance in the order of influence on the system performance.

Overall, this research significantly contributes to boiler thermal science by studying and identifying the causes of incessant boiler failure and by developing models that can predict the emission and combustion characteristics of the boiler, thereby predicting the optimum operating conditions for the boiler which would results in reduced emission levels, improved combustion stability and prolonged boiler life.

5.2 Recommendations

Following the findings of this study, the following recommendations are proposed for future work:

i. To mitigate scaling and corrosion, routine maintenance and frequent blowdown of the boiler drum should be prioritized, along with maintaining appropriate water chemistry. It is also advisable to conduct regular water quality analyses for both the feed water and boiler drum water.

ii. Extension of the simulation framework to include transient startup and shutdown conditions to understand thermal fatigue cycles.

iii. Extension of the modelling and simulation framework to include a more robust dynamic combustion model

iv. Application of machine learning models for real-time predictive maintenance using operational sensor data.

v. Exploration of alternative low-carbon fuels (e.g., biogas, hydrogen blends) to further reduce greenhouse gas emissions.

vi. Long-term field validation of optimized control parameters in industrial settings to assess practical robustness and economic impact.

5.3 Contributions to Knowledge

The key contributions of this research to the field of boiler thermal science are as follows:

1. The study has developed a multi-faceted failure diagnosis framework integrating visual investigation, chemical analysis, metallurgical investigation, water chemistry, thermal analysis and boiler tube failure analysis.
2. The study has developed and validated CFD models to simulate heat transfer and combustion behavior in dual fired industrial boilers.
3. The study has established optimum operational strategies using experimental and statistical tools for efficiency and emission control.
4. The study has provided recommendations for boiler water treatment and maintenance protocols to mitigate future failures.

REFERENCES

A.O. Ibrahim, O.O. Ighodaro, S.K. Fasogbon, E.F. Orumwense, and M.A. Waheed. (2023) Failure investigation of the tube of a dual fired steam boiler in a western Nigerian food and beverage manufacturing plant, Eng. Fail. Anal. 143, 106906, https://doi.org/10.1016/j.engfailanal.2022.106906.

Abroshan, H. (2020*). An integrated model to study the effects of operational parameters on the performance and pollutant emissions in a utility boiler*. Journal of Thermal Engineering, Volume 6, No 4, Pages 474 – 498.

Ahmad, A., Purbolaksono, J., Beng, L. C. 2010. *Failure analysis on high temperature superheater* alloy inconel-800 *tube.* Engineering Failure Analysis.17.1: 328-333.

Ahmad, J., Purbolaksono, J., Beng, L.C., Rashid, A.Z., Khinani A., and Ali A.A. (2009). *Failure investigation on rear water wall tube of boiler*. Engineering Failure Analysis. Volume 16. Pages:2325 - 2332.

Ahmad. J and Purbolaksono. J (2010). *Hydrogen damage in a rear riser water wall tube of a power plant*. Engineering Failure Analysis. Volume 17, Pages 1239 – 1245.

Alvarez, A., Pizarro, C., Lavin, A.G., and Bueno J.L. (2018). Size up, monitorization, performance optimization and waste study. A case study, Renewable Energy Focus. Vol 27, pp33-43.

Aminmahalati, A., Fazlali, A., and Safikhani, H. (2022). *Study on the performance and optimization of CO boiler in the oil refinery*, Applied Thermal Engineering, Volume 201, Part B, 117790, ISSN 1359-4311, https://doi.org/10.1016/j.applthermaleng.2021.117790. https://www.sciencedirect.com/science/article/pii/S135943112101214X.

An, H., Yang, W.M., Maghbouli, A., Li, J., Chou, S.K., and Chua, K.J. (2013). *Performance, combustion and emission characteristics of biodiesel derived from waste cooking oils*, Applied Energy, Volume 112, Pages 493-499, ISSN:h7tr 0306-2619.

Arezoo Firouzeh, Khalil Ranjbar, S. M. Lari Baghal, A. Heidari Kaidan, and Enayatolah Mohemi (2018*). Failure assessment of ASTM A213-T12 superheater boiler tubes in a natural gas liquid plant.* Engineering Failure Analysis, Volume 89, Pages 15-27.

Arezoo Firouzeh, Khalil Ranjbar, S. M. Lari Baghal, A. Heidari Kaidan, and Enayatolah Mohemi (2018*). Failure assessment of ASTM A213-T12 superheater boiler tubes in a natural gas liquid plant.* Engineering Failure Analysis, Volume 89, Pages 15-27.

Arhosazani, A., Mohamed, W., and Najmi, W. A. (2006). *Comparison of combustion Performance between natural gas and medium fuel oil at different firing settings for industrial boilers*, International Conference on Energy and Environment (ICEE).

Bena, D.J. (2009). *Failure avoidance brief: estimating heater tube life*. Journal Failure Analysis Prevention. Volume 9. Pages :5–7.

Bettge, D., Klinger, C., Klingbeil, D., and Eberle, A. 2014. *Investigations on the breakdown of a heat recovery steam generator during the initial operation run*. Engineering Failure Analysis 43: 253-270.

Bianco, N., Szubel, M., Fillipowcz, M., Papis, K., and Podlask, S. (2021). CFD analysis of an air manifold for biomass boiler, Renewable Energy, Vol 163, pp2018-2028.

Brooks, C.R, Choudhury, A. (1993). *Metallurgical Failure Analysis*. McGraw-Hill, New York.

Casey Julich-Trojan and Shane Turctt (2019). *Failure Analysis of Cracked boiler tube.*

Centeno-González, F.O., Lora, E.E.S, Nova, H.F.V., Neto L.J.M., Reyes, A.M.M., Ratner, A., and Ghamari, M (2017). *CFD modeling of combustion of sugarcane bagasse in an industrial boiler*. Fuel, Elsevier, Volume 193, Pages 31-38.

Centeno-González, F.O., Lora, E.E.S, Nova, H.F.V., Neto L.J.M., Reyes, A.M.M., Ratner, A., and Ghamari, M (2017). *CFD modeling of combustion of sugarcane bagasse in an industrial boiler*. Fuel, Elsevier, Volume 193, Pages 31-38.

Chaney, J., Liu, H., and Li, J. (2012). An *overview of C.F.D. Modified small-scale fixed-bed biomass pellet boilers were modeled with preliminary results from a simplified approach,* Energy Conversion and Management, Volume 63, Pages 149–156. 10.1016/j.enconman.2012.01.036.

Charan, R., and Prasad, P. (1993). *Energy conservation in milk-spray drying*, Journal of Food Engineering, Volume18, Pages 247-258.

Chavan, D. K., & Pathak, G. K. (2015). *Practical boiler operation engineering and power plant*. Standard Book House. Chavan, D. K., & Pathak, G. K. (2015). *Practical boiler operation engineering and power plant*. Standard Book House.

Chepel V.M., and Shur I.A. Combustion of gases in the furnaces of boilers and furnaces and maintenance of the gas economy of enterprises. - 8th ed., Processing and additional - S.-P.: Nedra, 1990. - 591 p.

Cho, H.M., and He, B.Q. (2009). *Combustion and emission of the natural gas engine under different operating conditions.* Korean Society of Environmental Engineers, Environ. Eng. Res. Volume. 14, No. 2, Pages 95-101.

Cho, M.H., and He, B.Q. (2009) *Combustion and emission characteristics of a natural gas engine under different operating conditions*, *Environmental Engineering Research*, Volume 14, No 2, Pages 95-101, doi: https://doi.org/10.4491/eer.2009.14.2.095.

Cvetkovski. S., (2017). *Failure analysis of ruptured pipe in boiler of thermo power plant*, Scientific Proceedings International Scientific Conference "High Technologies Business Society 2017", Year I, Volume I, P.P. 46-48 (2017) WEB ISSN 2535-0013, PRINT ISSN 2535-0005.

Dehvani, F., Eslami, A., and Ashrafizadeh, F. 2017. *A case study on failure of superheater tube in industrial powerplant engineering*. Failure Analysis 80: 368-377.

Dennies, D.P. 2005. *How to organize a failure investigation*. ASM International, Ohio.

Deshmukh, S and Dhamangaonkar, P. (2023). *Coupled CFD-FEA simulation of bulging tube failure in hot temperature zone*, Materials Today: Proceedings, Volume 72, Part 3, Pages 768-774, ISSN 2214-7853, https://doi.org/10.1016/j.matpr.2022.09.014.

Dhua, S.K. (2010). Engineering failure analysis. 17, 1572-1579

Dhua, S.K. (2010). *Metallurgical investigation of failed boiler water-wall tubes received from a thermal power station*. Engineering Failure Analysis. Volume.17, Pages1572 - 1579.

Duarte C. A., Espejo E., and Martinez J.C. (2017). *Failure analysis of the wall tubes of a water-tube boiler*. Engineering Failure Analysis, Volume 79, Pages 704-713.

Duarte C. A., Espejo E., and Martinez J.C. (2017). *Failure analysis of the wall tubes of a water-tube boiler*. Engineering Failure Analysis, Volume 79, Pages 704-713.

Duarte, C, A., Espejo, E., and Martinez, J.C. 2017. *Failure analysis of the wall tubes of a water tube boiler,* Engineering Failure Analysis, 79: 704-713.

Elkalawy, M., Bastawissi, H.A., Esmaeil, K.K., Radwan, A.M., Panchal, H., Sadasivuni, K.K., Ponnamma, D., and Walvekar, R. (2019) *Experimental studies on the biodiesel production parameters optimization of sunflower and soybean oil mixture and DI engine combustion, performance, and emission analysis fueled with diesel/biodiesel blends*, Fuel, Volume 255, 115791, ISSN 0016-2361.

Er. R.K Rajput. *Thermal Engineering*. 9th Edition. Laxmi publications (P) Ltd. New Delhi. 954p.
Example Report Modified from Original Report-Electronic.

Fagbolagun I.O, and Oke, S.A (2021) *The Optimization of Packaging System Process Parameters Using Taguchi Method.* Engineering Research Journal, Engineering & Technology Research Journal Volume 6, Issue No 2, Pages 48-59.

Fleming, R.D., and Allsup, J.R. (1971). *Emission characteristics of natural gas as an automotive fuel*, Nat Comb Fuels & Lubricants Powerplant & Truck Mtgs St Louis Missouri, S.A.E. Paper 710833, 1971 Oct; 1-7.

Franke, R., Rode, M., and Krüger, K., (2003) *On-line optimization of drum boiler startup*, Proceedings of the 3rd International Modelica Conference, Linköping, November 3-4, Pages 287-296, Peter Fritzson (editor)

.
Graham, R. 2004. *Strategies for failure analysis*. ASM Advanced Materials & Processes. 172.11: 45-50.

Guedes, A.D.M., Braga, S.L., and Pradelle, F. (2018). *Performance and combustion characteristics of a compression ignition engine running on diesel-biodiesel-ethanol (D.B.E.) blends – Part 2: Optimization of injection timing*, Fuel, Volume 225, Pages 174-183, ISSN 0016-2361.

Gupta, G.K., and Chattopadhyaya, S. 2017. Critical Failure Analysis of Superheater Tubes of Coal-Based Boiler, Journal of Mechanical Engineering. 63.5: 287-299.

H. Rusinowski, W. Stanek, Neural modelling of steam boilers, Energy Convers. Manage. 48 (2007) 2802–2809.

H. Rusinowski, W. Stanek, Neural modelling of steam boilers, Energy Convers. Manage. 48 (2007) 2802–2809.

Haase, R. J., Hanke, L. D. 2013. *Boiler stack economizer tube failure. Journal of Failure Analysis and Prevention*. 13.5: 513-520.

Handi Santoso M.H., Nazaruddin, Y.Y., and Muchtadi, F.I. (2005*). Boiler performance optimization using fuzzy logic controller,* IFAC Publication, Elsevier, 16th Triennial World Congress, Prague, Czech Republic.

Hanke, N. 2012. *Evaluation of a failed water wall boiler tube*. Journal of Failure Analysis and Prevention, 12.1: 11-15.

Hewison, F. and Christian, H. (1983). Locomotive boiler explosion, (First Edition). London: David and Charles.

Heyes, A.M. 2001. *Oxygen pitting failure of a bagasse boiler tube,* Engineering Failure Analysis. 8: 123-13.

Heyes, A.M., (2001) *Oxygen pitting failure of a bagasse boiler tube,* Engineering Failure Analysis, Volume 8, Pages 123-131.

Himarosa, R.A., Hariyanto, S.D., Hassan, W.H., Muflikhun, M.A. 2022. *Failure analysis of platen super heater tube and seal pot plate*: A case study from electricity power plant. Failure Analysis. 135. https://10.1016/j.engfailanal.2022.

Hosseini K.R., and Yareiee, Sh. 2019. *Failure analysis of Boiler Tube at a Petrochemical Plant*, Engineering Failure Analysis. 106. DOI: 10.1016/j.engfailanal.2019.104146.

https://Steelimage.com/wp-Content/uploads/2019/02/Thermal-Fatue-of-Boiler-Tube.pdf. Accessed 2023-09-13.

Hu, Z.F., He, D.H., and Wu, X.M. 2014. *Failure analysis of T12 boiler re-heater tubes during short-term service*. Journal of Failure Analysis and Prevention 14.5 :637-644.

Huang, Z., Huang, J., Luo, J., Hu, D., and Yin, Z (2022) *Performance enhancement and emission reduction of a diesel engine fueled with different biodiesel-diesel blending fuel based on the multi-parameter optimization theory,* Fuel, Volume 314, 122753, ISSN 0016-2361.

Ibrahim, A.O. (2020). *Exergetic analysis of juice, dairy and custard processing operations in southwestern Nigeria plant*. Unpublished M.Sc. Thesis, Faculty of Engineering, Mechanical Engineering Department, LASU, Epe.

Industrial Combustion Technology Roadmap (2002): *A technology Roadmap by and for the Industrial Combustion Community*, United States, https: doi.org/10.21728679.

Ingale, A.N., Pathade, V.C., and Tatwawadi, V.H (2012). *CFD Analysis of superheater in view of boiler tube leakage*, International Journal of Engineering and Innovative Technology (IJEIT) Volume 1, Issue 3, Pages 29-31, ISSN: 2277-3754.

Jadhao, P.K., Charjan, S.N., Khobragade, M.M., Waghmare, S.S., Agashe, R.K and Ramteke, K.B. 2017. *Leakage failure analysis in superheater tubes in sugar industry*. International Journal of Engineering Science and Computing. 7.4: 10826 -10823.

Jadhao, P.K., Charjan, S.N., Khobragade, M.M., Waghmare, S.S., Agashe, R.K and Ramteke, K.B. (2017), Leakage failure analysis in superheater tubes in sugar industry, International Journal of Engineering Science and Computing, Volume 7, Issue No 4, Pages 10826 – 10823.

Jagtap, H., Bewoor, Kumar, R., Ahmadi M.H. and Lorenzini. G. (2019) *Markov-based performance evaluation and availability optimization of the boiler–furnace system in coal-fired thermal power plant using PSO,* Energy Report, Vol 6, Pages 1124-1134.

Javidi, M., Nematollahi, M. R., Lalehparvar, M.M., and Ghassemi, A. 2016. *Failure analysis of AISI 321 austenitic stainless-steel water piping in a power plant.* Journal of Failure Analysis and Prevention 16.2: 209-215.

Jayaprabakar, S.S. Dawn, A. Ranjan, P. Priyadharsini, R.J. George, S. Sadaf, C. Rajeswara Rajha, (2019) *Process optimization for biodiesel production from sheepskin and its performance, emission and combustion characterization in CI engine,* Energy, Volume 174, Pages 54-68, ISSN 0360-5442.

Jayaprakasam, K., and Vino, J.A., (2019). *Analysis of tube failure in economizer and superheater tube in thermal power station.* International Journal of Mechanical and Production Engineering Research and Development (IJMPERD) ISSN (P):2249-6890; ISSN (E): 2249-8001, 9.6: 1235-1244.

Jena, S.P., Mahapatra, S., Acharya, S.K. (2021*) Optimization of performance and emission characteristics of a diesel engine fueled with Karanja biodiesel using Grey-Taguchi method*, Materials Today: Proceedings, Volume 41, Part 2, Pages 180-185, ISSN 2214-7853.

K. Søren, S. Kaer, Numerical modeling of a straw-fired grate boiler, Fuel 83 (2004) 1183–1190.

Kain, V., Chandra, K., and Sharma B.P. 2008 *Failure of carbon steel tubes in a fluidized bed combustor* Engineering Failure Analysis. 15: 182–7.

Kalu, I.E; Inglis, E.M and Kok, S (2020). Failure assessment methodology for boiler tubes with localized external erosion defects. International Journal of Pressure Vessels and Piping, Volume 188, 104190, ISSN 0308-0161, https://doi.org/10.1016/j.ijpvp.2020.104190.

Karran, S.A. 2017. *A Case Study on Caustic Corrosion in Refinery Piping*, International Journal of Engineering and Information Technology (IIT).

Katre, B.C., and Murari, K. (2007). *Product technology: A crucial aspect of effective management*, Beverage and food world, April Edition, Pages 43-45.

Khalil Ranjbar, (2007). Failure analysis of boiler cold and hot reheater tubes. Journal of Engineering Failure Analysis, 14,620-625.

Khoirul. A., and Firman L.O.M. (2019). *Design and optimization of boiler economizer for laundry industry using Taguchi.*

Kim, Y.S., Kim, W.C., and Kim, J.G. 2019. *Bulging Rupture and Caustic Corrosion of a Boiler Tube in a Thermal Power Plant*, Engineering Failure Analysis. 104: 560-567.

Kumar, A., and Sapra, P.K. 2013. *Boiler tubes failure: Causes and remedies a case study of a fertilizer plant*. International Journal on Emerging Technologies, 4. 2: 132-135.

Lee, N.H., Kim, S., Choe, B.H., Yoon, K.B., and Kwan, D.I. 2009. *Failure analysis of boiler tube in USC coal power plant.* Engineering Failure Analysis. 16.7: 2031-2035.

Lee, N.H., Kim, S., Choe, B.H., Yoon, K.B., and Kwon, D.I. (2009). *Failure analysis of a boiler tube in USC coal power plant.* Engineering Failure Analysis. Volume 16. Pages:2031–2035.

Lin, C.Y., and Hsieh, M.J (2008). *Emissions of industrial furnaces burning diesel fuel oils of various sulfur contents with nacl- contained atmospheric air*, Journal of Environmental Science and Health. Part A: Environmental science and engineering and toxicology, 31:4, 859-868, Volume 31, Issue 4, Pages 859-868, https://doi.org/10.1080/10934529609376393.

Liu, S.W., Wang, W.Z., and Liu, C.J. 2017. *Failure analysis of boiler water wall tube*. Case Studies in Engineering Failure Analysis, 9: 35-39.

Liu. Z, Jiang, Q., Ning. F., Kim, H., Gong, W., Xu, C., and Zhang, H.O. (2018). *Investigation of energy requirements and environmental Performance*, Sustainability, MPDI doi: 10.3390/su10103606.

Luo, X., and Zhang, Z. 2013. *Leakage failure analysis in a power plant boiler*. IERI Procedia, 5: 107-111. DOI:10.1016/j. ieri.2013.11.078.

Xu, J.L.T. Azevedo, M.G. Carvalho, Modeling of the combustion process and NOx emission in a utility boiler, Fuel 79 (2000) 1611– 1619.

Ma, X., Niu, P., and Zhang, X. (2021). Three-objective optimization of boiler combustion process based on ameliorated extreme learning machine and modified teaching–learning-based optimization. *Machine Learning with Applications*, *5*, Article 100082. doi.org

Makhlouf, S.H., and Aliofkhazraei, M. Butterworth-Heinemann, Chapter 3, Page 49-68, ISBN 9780081001165, https://doi.org/10.1016/B978-0-08-100116-5.00003-X.

Melillo, J.M., T.C. Richmond, and G.W. Yohe (eds.). (2014). *Climate change impacts in the United States: The Third National Climate Assessment*. U.S. Global Change Research Program.

Mnizeskewi, K., Lyson, H., and Hales, C. (2004). *The 1999 Ford Power Plant Explosion: A study of problems encountered during large-loss fire investigation*. Power Loss NPFA Journal, July/August Edition. www.nfpa journal.org.

Modi P.N., Modi, S., and Modi, R. (2012) *PERT and C.P.M. Program Evolution & Review Techniques & Critical Path method.* Fifth Edition, Standard book house. Rajon publications Pvt. Ltd. ISBN978-81-89401-25-2.

Modi, M.A., Patel, T.M., and Patel, S.C. (2012*). Parametric optimization of single-cylinder diesel engine for pyrolysis oil and diesel blend for specific fuel consumption using Taguchi method*, IOSR J Mech Civil Eng, Volume 6, No.1, Pages 83-88.

Morakinyo, T.A., and Bamgboye A.I. (2017). *The optimization of operational parameters of a biomass fire in tube boiler using Taguchi design method*, Volume 5, Pages 167-175.

Movahedi-Rada, A., Plasseyed, S.S., and Attarianb, M. (2014), *Failure Analysis of Superheater Tube, Engineering failure analysis*, Volume 48, Pages 94 – 104, doi: http://dx.doi.org/10.1016/j.engfailanal.2014.11.012.

Munda, P., Kumar, S., Prakash, A. Husain M.M., Rajnikanth, V., and Chowdhury S.G. 2016. *Failure Investigation of Boiler Water Wall Tubes of a Thermal Power Station*. J. Fail. Anal. and Preven. 16: 9-18.

Munda, P., Kumar, S., Prakash, A., Husain, M.M., Rajnikanth, V., and Chowdhury, S. G. (2016). *Failure investigation of boiler water wall tubes of a thermal power station*. Journal of Failure Analysis Prevention. Volume 16 Pages :1–10.

Nagpal, G. R. (2000). *Power Plant Engineering*. Khanna Publishers.

Nikhil, B., Sandeep, J., and Mahendra, G. (2022). *Combustion, performance, and emission characteristics of diesel engine using oxyhydrogen gas as a fuel additive*. Environmental Science and Pollution Research. 3. 10.1007/s11356-021-17975-5.

Nimmanterdwong, P., Chalermmsinsuwan, B., and Piumsomboon, P. (2022). Application of neural network modelling and constrained particle swarm optimization of steam production from biomass power plant. Energy Reports, Vol 8, pp1060-1072.

Nwachukwu, O.A., and Woyengi, E. B. (2017). Failure Investigation of an In-service Steam Boiler, *American Journal of Mechanical and Materials Engineering*. Volume 1, Issue 3, Pages. 69-77. doi: 10.11648/j.ajmme.20170103.12.

O.O Ighodaro (2016). *Modelling and Simulation of Intermediate Temperature Solid Oxide Fuel Cells and their Integration in Hybrid Gas Turbine Plants*. (PhD Thesis). School of Chemical Engineering and Advanced Materials. Newcastle University, Ochoa, V.O., Rojas, J.P., and Avella, J.C. (2019). *Optimization of industrial steam boiler using performance energy indicator,* International Journal of Energy Economy and Policy.

Ohijeagbon, I.O., Jekayinfa, S.O., and Waheed, M.A. (2012). *Assessing the emission factors of low-pour-fuel-oil and diesel in steam boilers*, International Journal of Development and Sustainability, Volume. 1 No. 3, Pages. 688-700.

Ota, M., Yang, N., Komatsu, H., Inomata, H., and Smith, R. L., Jr. (2025). Entropy-Based Solubility Parameter-Translated Peng–Robinson Equation of State (*e*SPT-PR EoS). *Liquids*, *5*(3), 21. https://doi.org/10.3390/liquids5030021

Othman, H., Purbolaksono, J., and Ahmad, B. 2009. *Failure investigation on deformed superheater tubes. Engineering Failure Analysis*. 16.1: 329-339, DOI:10.1016/j.engfailanal.2008.05.023.

Pandey, A.K., Kumaraswamidhas, L.A., and Kathirvelu, C. (2012). *Analysis of Flow Induced Vibration in Superheater Tube Bundles in Utility Boilers Using Computational Method,* International Journal of Computational Engineering Research, Volume 2, Issue No 2, Pages 481-486, ISSN: 2250–3005.

Patil, R.B (1977). *Water, steam, and refrigeration in a multi dairy plant*. Unpublished M. Tech Thesis, Agricultural Engineering Department I.I.T., Kharagpur.

Perdomo, J.J., and Spry, T. D. (2005). *An overheat boiler tube failure*. Journal of Failure Analysis Prevention. Volume 5. Pages: 25 - 28.

Prabhakar, P.K., Srivastar, P. P., and Murari, K. (2015). *Energy consumption during manufacturing of different dairy products*. Asian journal Dairy and Food Res, Volume 32, No. 2, Pages 98 – 103.

Prof. D.K Chavan and Prof. G.K. (2010). Pathak. *Applied Thermodynamics. 1st Edition.* Standard Book House, Rajsons Publications. Pvt. Ltd. Delhi, 728p.

Purbolaksono, J., Ahmad, J., Beng, L. C., Rashid, A.Z., Khinani, A., Ali, A.A. 2010. *Failure analysis on a primary superheater tube of a power plant*. Engineering Failure Analysis.17.1: 158-167.

Purbolaksono, J., Khinani A, Ali A.A., Rashid A.Z., and Nordin N.F (2009) Iterative technique and finite element simulation for supplemental condition monitoring of water tube boiler. Journal of Simulation Modeling Practice and Theory, 17, 897-910.

Qyyum, M.A., Junaid Haider, J., Qadeer, K., and Lee. M. (2009). *Performance enhancement of offshore LNG processes by introducing optimal mixed refrigerant self-cooling recuperator*, International Conference on Applied Energy, Aug 12-15, 2019, Vasteras, Sweden Paper ID: 0588.

Rahimi M., Khoshhal A., Shariati S.M. (2006). *CFD modeling of a boiler's tubes rupture*, *Applied Thermal Engineering*, Volume 26, Issue 17-18, Pages. 2192-2200, ISSN 1359-4311, https://doi.org/10.1016/j.applthermaleng.2006.03.017.

Rahmana, M. M., Purbolaksono, J., Ahmad, J. 2010. *Root cause failure analysis of a division wall superheater tube of a coal-fired power station*. Engineering Failure Analysis.17. 6: 1490-1494.

Rajput, R.K (2007). *A textbook of power plant emgineering (4^{th} ed.)*. Laxmi Productions.

Ranjbar, K. 2007. *Failure analysis of boiler cold and hot reheater tubes*. Engineering Failure Analysis. 14.4: 620-625.

Rao, M.A., and Narayanan, T.S.N.S. 2012. *Failure investigation of a boiler bank tube from a 77 × 2 MW coal based thermal power plant in the northwest region of India*. Engineering Failure Analysis. 26: 325-331.

Rao, R.V., and Patel., (2011). *Optimization of mechanical draft counter flow wet- cooling tower using artificial bee colony algorithm*, Energy Conversion, and Management, Volume 52, No.7, Pages 2611- 2622.

Ritchie, R., and Roser, M. (2020). *Energy Published* online at ourworldinData.org. Retrieved from: https://ourworldindata.org/energy (Online Resource).

Ryder, D.A., Davies, T.J., Brough, I., and Hutchings, F.R.1986). *General practice in failure analysis. Failure analysis and prevention.* Metals handbook, American Society for Metal, Ohio.

Saha, A. (2016). Boiler tube failures: Some case studies, Handbook of Failure Analysis with Case Studies from Chemicals, Concretes, and Power Industries, Editor: Editor(s): Abdel.

Saha, A. 2016. *Boiler tube failures: Some case studies*, Handbook of Failure Analysis with Case Studies from Chemicals, Concretes, and Power Industries, Editor: Editor(s): Abdel.

Sakthivel, P., Kalaimani, S., and Sasikumar, R. (2017). *Analysis of tube failure in water tube boiler*, International Journal of Innovative Research in Science, Engineering and Technology, Volume 6, Special Issue 8, Pages 91-106, ISSN (Online): 2319 - 8753 ISSN (Print): 2347-6710.

Sanjay, P.S., and Mandloi, R. K. 2016. *A Failure Analysis and Remaining Life Assessment of Boiler Water Wall tube*. International Journal of Advanced Engineering Research and Science (IJAERS).

Santhoshkumar, G., Ramanichandran, R., and Eazhil, K.M (2019) Reheater Failure Analysis Using ANSYS, Journal of Xidian University, Pages 41 – 45, Volume 13, Issue 5, ISSN No: 1001-2400, http://xadzkjdx.cn/

Santhoshkumar, G., Ramanichandran, R., and Eazhil, K.M. 2019. *Reheater Failure Analysis Using ANSYS*, Journal of Xidian University 13.5: 41- 45.

Satyabrata Chaudhuri, (2006). Some aspects of metallurgical assessment of boiler tubes-Basic principles and case studies. Journal of Material science and Engineering, A 432, 90-99

Satyabrata, C. (2006). *Some aspects of metallurgical assessment of boiler tubes—basic principles and case studies*. Material Science Engineering. A. Volume 432. Pages: 90 - 99.

Saxena, M.R., and Maurya, R.K. (2020). *Optimization of engine operating conditions and investigation of nano-particle emissions from a non-road engine fuelled with butanol/diesel blends*, Biofuels, Volume 11, Issue 5, DOI: 10.1080/17597269.2017.1378987.

Sefeedpari, Paria. (2012). *Assessment and Optimization of Energy Consumption in Dairy Farm: Energy Efficiency*. Iranica Journal of Energy & Environment, Volume 3, Pages 213-224. 10.5829/idosi.ijee.2012.03.03.0924.

Sekhar, S.C., Karuppasamy, K., Vedaraman, N., Kabeel, A.E., Sathyamurthy, R., Elkalawy, M., and Bastawissi, H.A.E. (2018) *Biodiesel production process optimization from Pithecellobium dulce seed oil: Performance, combustion, and emission analysis on compression ignition engine fueled with diesel/biodiesel blends,* Energy Conversion and Management, Volume 161, Pages 141-154, ISSN 0196-8904.

Sembiring, D., Widodo, D.S., Adjiantoro, B., Saman, A.B., and Kader, B.A. 2019. *Failure Analysis of the Furnace Scotch Boiler*. International Journal of Engineering and Advanced Technology (IJEAT) 9 .1: 3798-3704.

Sembiring, D., Widodo, D.S., Adjiantoro, B., Saman, A.B., and Kader, B.A. 2019. *Failure Analysis of the Furnace Scotch Boiler*. International Journal of Engineering and Advanced Technology (IJEAT) 9 .1: 3798-3704.

Shaji Kumar, K.R and Tide P.S (2012). *An investigation on tube temperature distribution in a water tube boiler*. IOSR Journal of Mechanical and Civil Engineering (IOSRJMCE), Vol 2, Issue 3, Pages 45-50, ISSN: 2278-1684, www.iosrjournals.org,

Singh, P.M., and Mahmood J. (2007). *Stress assisted corrosion of waterwall tubes in recovery boiler tubes: failure analysis*. Journal of Failure Analysis Prevention. Volume 7. Pages:361 - 370.

Singh, P.M., and Mahmood, J. 2007. *Stress assisted corrosion of water wall tube in recovery boiler tubes.* Failure Analysis, J. fail. Anal. and Preven 7: 361-370.

Song, C., Pan, W., Srimat, S.T., Zheng, J., Li, Y., Wang, Y.H., Xu, B.Q., and Zhu, Q.M., (2004*). Tri-reforming of Methane over Ni catalysts for CO2 conversion to syngas with desired H2/CO ratios using flue gas of power plants without CO2 separation, studies in surface science and catalysis.* Elsevier, Vol 153, Pages 315-322, ISSN 0167-2991, https://doi.org/10.1016/S0167-2991(04)80270-2. https://www.sciencedirect.com/science/article/pii/S0167299104802702.

Souhir. E., Abdallah, B., Zied, D., and Mohamed, A. (2018). *CFD simulation and optimization of industrial boiler*. Energy. 169. 10.1016/j.energy.2018.12.006.

Srikanth S, Ravikumar B, Swapan K. Das, Gopalkrishna K., Nandakumar K., and Vijayan P. (2003) Analysis of failures in boiler tubes due to fireside corrosion in a waste heat recovery boiler -Engineering Failure Analysis., 10, 56-66.

Srikanth, S., Ravikumar, B., Das, S.K., Gopalakrishna, K., Nandakumar, K., Vijayan, P. 2003. *Analysis of failures in boiler tubes due to fireside corrosion in a waste heat recovery boiler. Engineering Failure Analysis* 10.1: 59-66.

Talupula, N.V.M.B., Rao, P.S., and Kumar, B.S.P. (2018*). Taguchi's Method for Optimization of Parameters Involved in Biodiesel Production Using Benne Seed Oil*, International Journal of Advanced Trends in Engineering and Technology, Special Issue, January, Page Number 149-155.

TCR Advanced (2004), *Failure and root cause analysis*, a technical White paper, TCR Engineering, India, P8. http://tcradvanced.com/downloads/tcr-whitepaper-failure-analysis.pdf.

TCR Advanced (2016), *Boiler Tube Failure investigation*, TCR Advanced Engineering publication, India, P4, http://www.tcreng.com/download/Boiler-Tube-Investigation.pdf.

Trojan, M. and Taler, J (2013) *Effect of scale deposits on the internal surfaces of the tubes on the superheater operation*, Archives of thermodynamics, Volume 34, No 4, Pages 73 – 91, DOI: 10.2478/aoter-2013-0030.

Trojan, M. and Taler, J .2013. *Effect of scale deposits on the internal surfaces of the tubes on the superheater operation*. Archives of thermodynamics 34.4: 73-91.

U.S. Environmental Protection Agency. 2016. *Inventory of U.S. greenhouse gas emissions and sinks:* 1990-2014. E.P.A. 430-R-16-002.

Vakkilainen, E.K. (2017). *Construction and design of the large boiler*, Principle of steam generation, Butterworth A-Heinemann, Page 1-17, ISBN 9780128043899.

Vakkilainen, E.K., (2022). *Industrial Applications of Steam Generated from Biomass*, Comprehensive Renewable Energy, Volume 5, Second Edition, Elsevier, Pages 299-329, ISBN 9780128197349,https://doi.org/10.1016/B978-0-12-819727-1.00050 https://www.sciencedirect.com/science/article/pii/B9780128197271000509.

Vander Voort, G.F. (2002). *Conducting the Failure Examination Practice*. ASM Handbook, ASM International, Ohio.

Waheed M.A., Jekayinfa. S.O., Ojediran. J.O., Imeokparia. E.O. (2008). *Energetic analysis of fruit juice processing operations in Nigeria.* Energy, Elsevier, Volume 33, Pages 35-45.

Wulpi, D.J. (2000). *Techniques of failure analysis*. Miller, B. (ed.) Understanding How Components Fail. ASM International, Ohio.

Yatish, K.V., Lalithamba, H.S., Suresh, R., and. Harsha Hebbar, H.R (2018). *Optimization of Bauhinia Variegata biodiesel production and its performance, combustion, and emission study on the diesel engine,* Renewable Energy, Volume 122, Pages 561-575, ISSN 0960-1481.

Xiong, X., and Yang, X. (2025). *Evaluating Cubic Equations of State with Various α Functions for Viscosity Predictions of 124 Industrial Important Fluids Based on Residual Entropy Scaling*. ACS Omega, 10(27), 29021–29036. https://doi.org/10.1021/acsomega.5c01157

Zhang, Bei, Yunhua, Li, Mingsheng, Liu, 2014. Case study: Optimization of an industrial steam boiler system operation. In: ASHRAE Papers CD: 2014 ASHRAE Annual Conference, SE-14-C040.

Zhou, H.; Cen, K.; Fan, J. Modeling and optimization of the NOx emission characteristics of a tangentially fired boiler with artificial neural networks. Energy 2004, 29, 167–183.

Zamanzadeh, Mehrooz, Larkin, Edward S., Bayer, George T., and William J. Linhart. "Failure Analysis and Investigation Methods for Boiler Tube Failures." Paper presented at the CORROSION 2007, Nashville, Tennessee, March 2007.

Zinurov V.E., Galiev, A.A., Nasyrova, I.I., and Kharkov, V. V. (2022). *Simulation of Heat Exchange in Combustion Chamber with Premix Burner*, *2022 4th International Youth Conference on Radio Electronics, Electrical and Power Engineering (REEPE)*, Pages 1-4, doi: 10.1109/REEPE53907.2022.973141.

APPENDIX A: 1mm Scale layer effect for Natural gas and Diesel firing

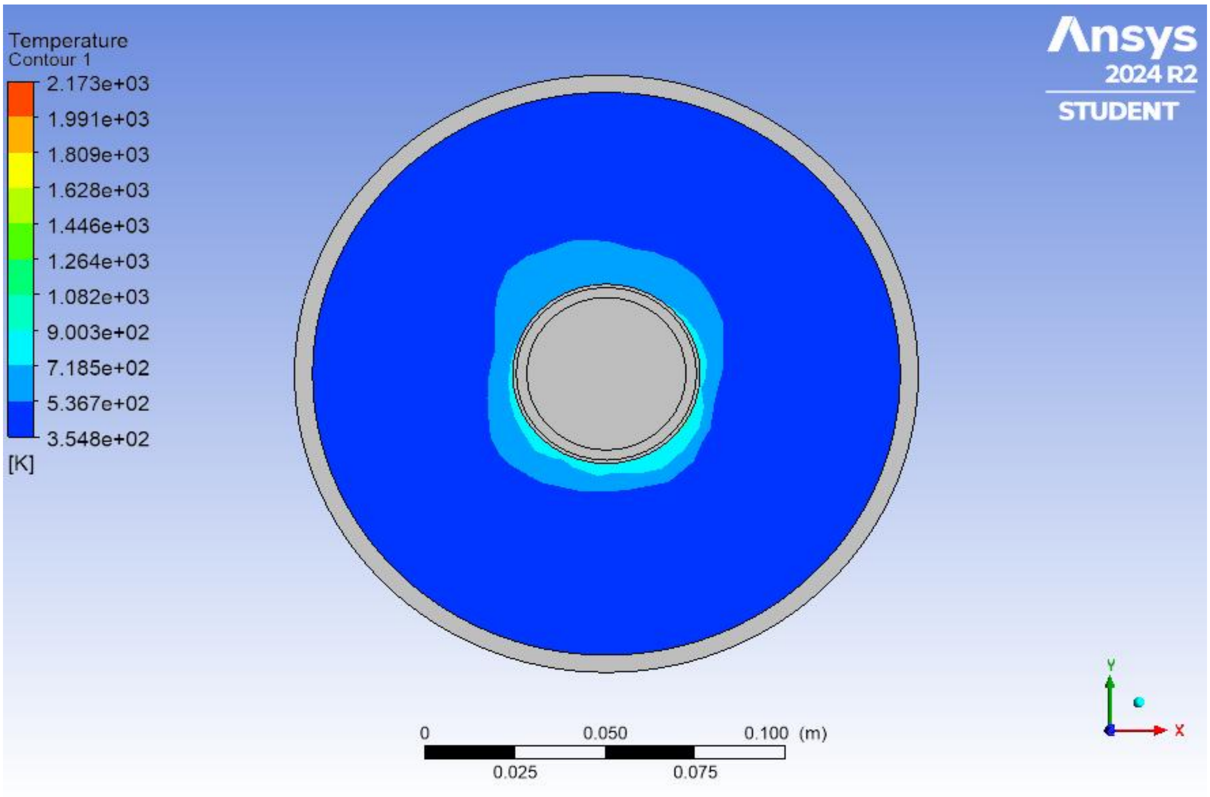

Natural Gas

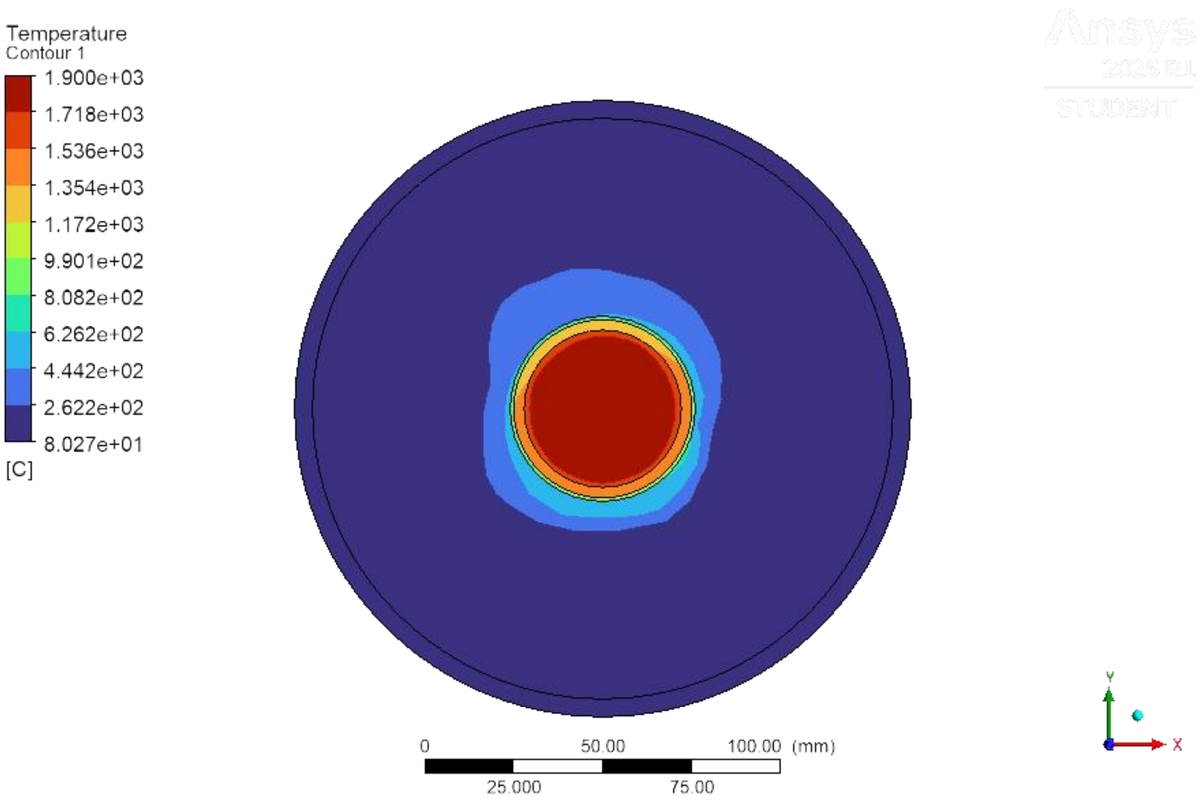

Diesel

APPENDIX B: 1.5mm Scale layer effect for Natural gas and Diesel firing

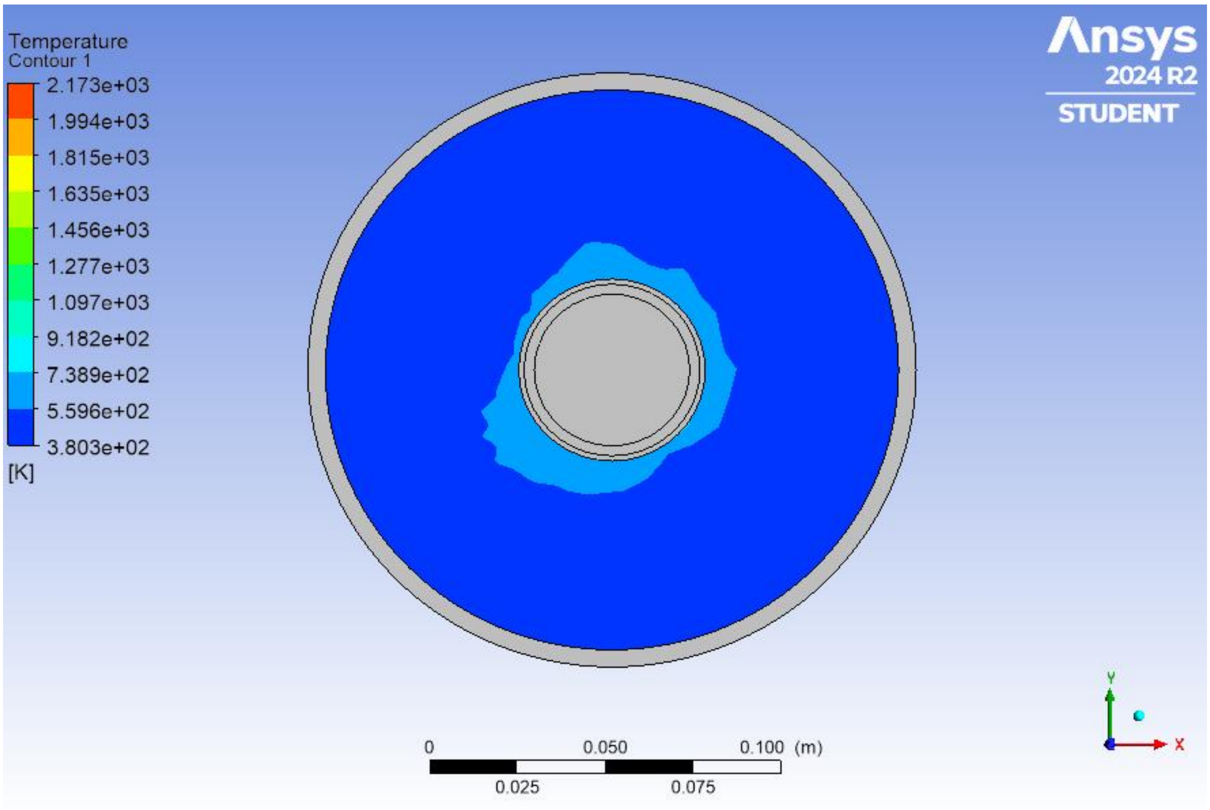

Natural Gas

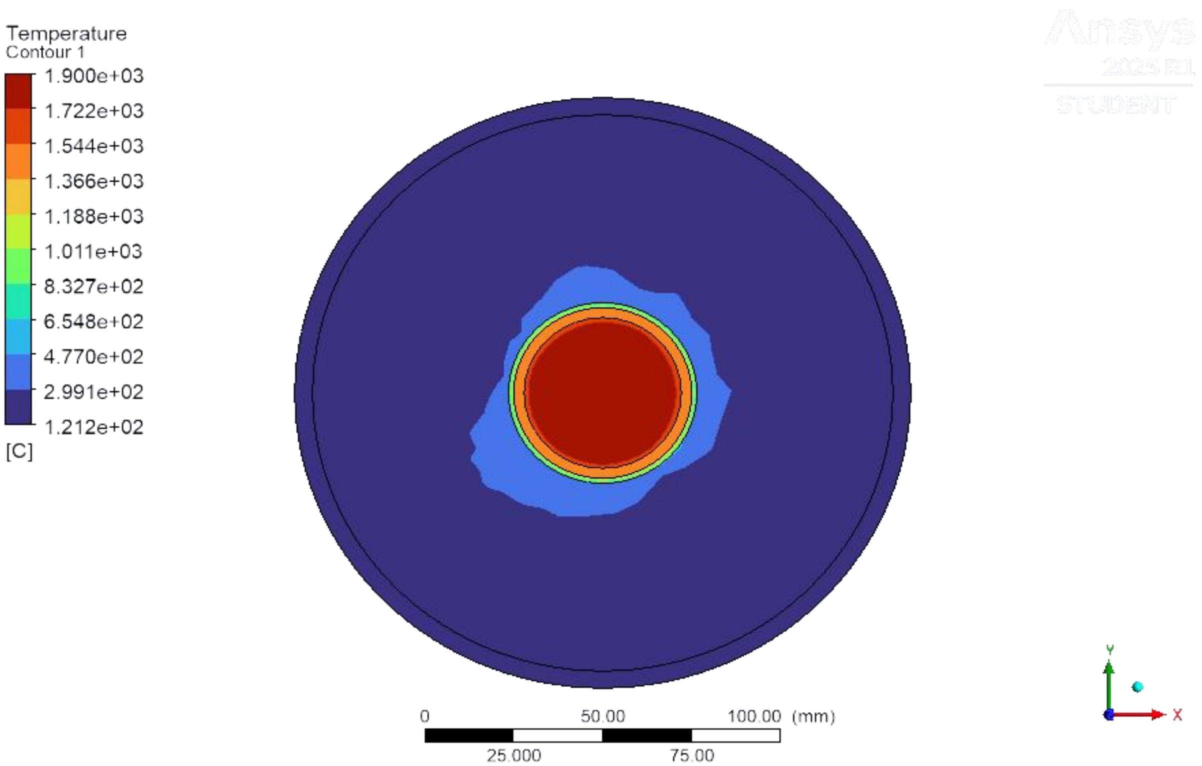

Diesel

APPENDIX C: 2mm Scale layer effect for Natural gas and Diesel firing

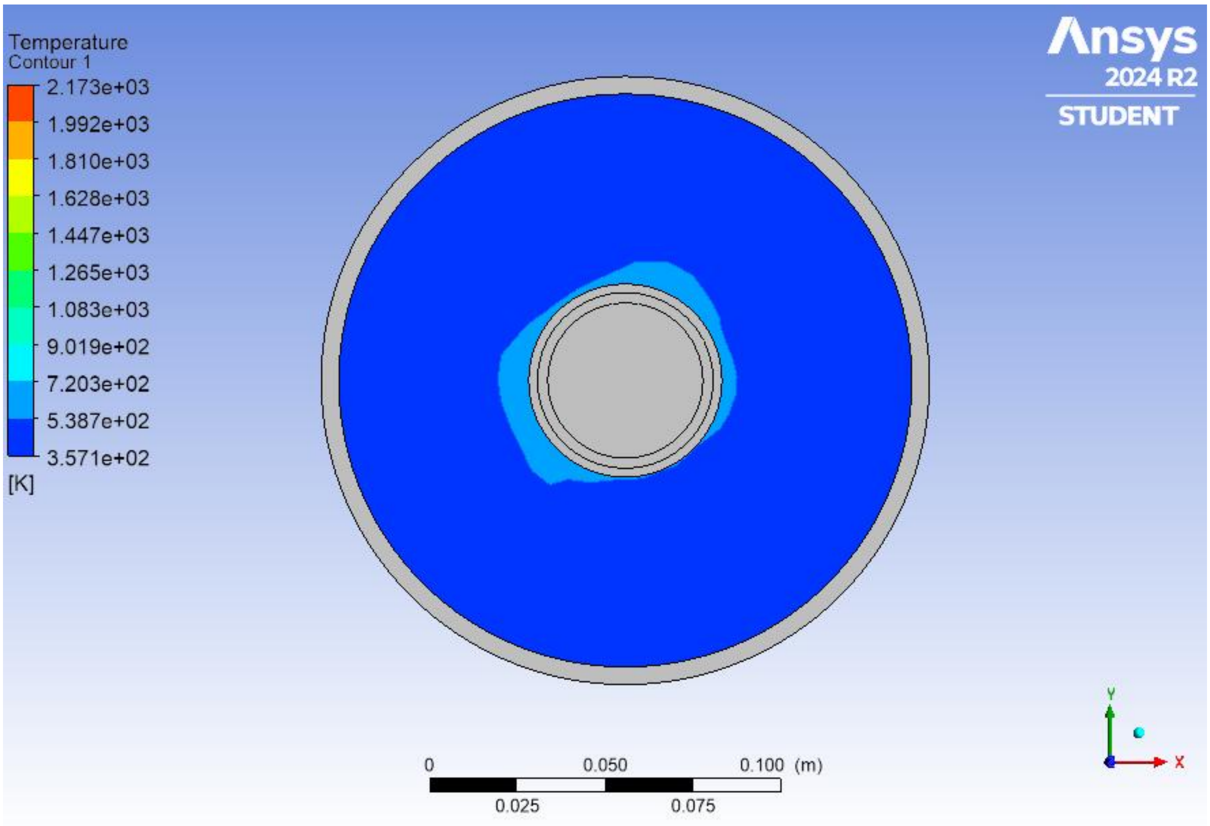

National Gas

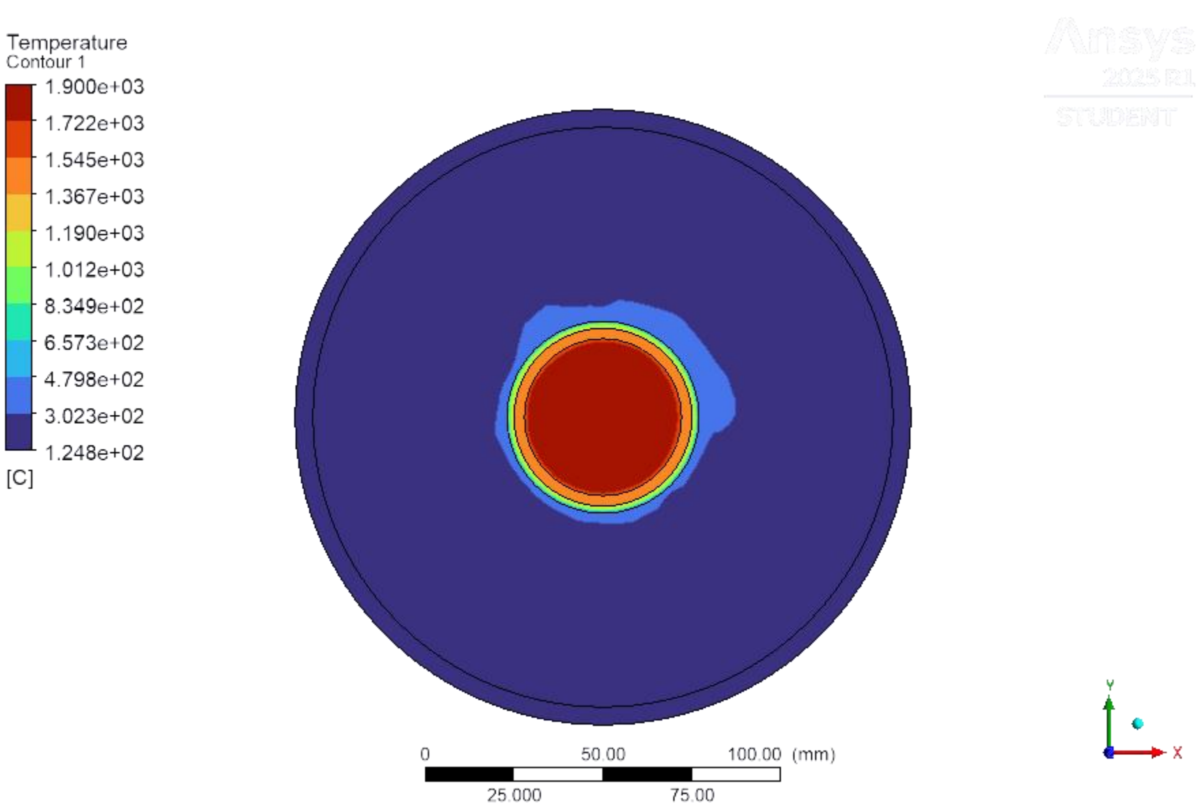

Diesel